

Architectures for molecular electronic computers:

1. Logic structures and an adder designed from molecular electronic diodes

James C. Ellenbogen
J. Christopher Love

Nanosystems Group
The MITRE Corporation

Proceedings of the IEEE,
March 2000, pp. 386-426.

MITRE

Architectures for molecular electronic computers:

1. Logic structures and an adder designed from molecular electronic diodes

James C. Ellenbogen
J. Christopher Love

Proceedings of the IEEE,
March 2000, pp. 386-426.

Nanosystems Group
The MITRE Corporation
McLean, VA 22102

e-mail: nanotech@mitre.org
WWW: <http://www.mitre.org/technology/nanotech>

Copyright © 2000 by The IEEE and The MITRE Corporation.
All rights reserved.

A preliminary version
of this paper was published
in July 1999 as
MITRE Report No.
MP 98W0000183.

MITRE

TABLE OF CONTENTS

LIST OF FIGURES.....	vii
LIST OF TABLES.....	ix
ABSTRACT and KEYWORDS.....	386
I. INTRODUCTION	386
II. BACKGROUND.....	387
A. Polyphenylene-Based Molecular-Scale Electronic Devices	387
1. Conductors or Wires—Conjugated Aromatic Organic Molecules	387
2. Insulators—Aliphatic Organic Molecules	390
3. Diode Switches—Substituted Aromatic Molecules	390
a. Molecular rectifying diodes ("molecular rectifiers")	391
<i>Solid-state rectifying diodes</i>	391
<i>Aviram and Ratner rectifying diodes</i>	
<i>and the origin of molecular electronics</i>	391
b. Molecular resonant tunneling diodes (RTD's)	391
<i>Structure of the molecular RTD</i>	391
<i>Operation of the molecular RTD</i>	393
<i>Current versus voltage behavior of the molecular RTD</i>	393
B. Carbon-Nanotube-Based Molecular-Scale Electronic Devices	394
C. Biomolecules as Possible Molecular Electronic Devices	395
D. An Advantage of Polyphenylene-Based Structures for Logic Design	395
III. APPROACH AND OBJECTIVES.....	396
IV. POLYPHENYLENE-BASED MOLECULAR RECTIFYING DIODE SWITCHES: DESIGN AND THEORETICAL CHARACTERIZATION.....	396
A. Proposed Polyphenylene-Based Designs for A&R-Type Rectifying Diodes	397
1. Basic Structure	397
2. Operational Principles for Polyphenylene-Based and Other A&R-Type Rectifying Diodes	398
a. Energy structure of the donor half...	398
b. Energy structure of the acceptor half...	399
3. Forward-Bias Operation of the Polyphenylene-Based Molecular Rectifier	399
4. Reverse-Bias Operation of the Polyphenylene-Based Molecular Rectifier	400
5. Additional Considerations—Nonresonant Electron Transport Under Reverse Bias	401
B. Results of Quantum Calculations for the Selection of Particular Polyphenylene-Based Rectifier Molecules	401

TABLE OF CONTENTS (CONTINUED)

V. NOVEL DESIGNS FOR DIODE-BASED MOLECULAR ELECTRONIC DIGITAL CIRCUITS.....	402
A. Novel Diode-Based Molecular Electronic Logic Gates	402
1. Molecular AND and OR Gates Using Diode-Diode Logic	403
2. Molecular XOR gates using Molecular RTD's and Molecular Rectifying Diodes	404
a. Structure for the Molecular XOR Gate	404
b. Overview of the Operation of the Molecular XOR Gate	405
B. Molecular Electronic Half Adder	405
C. Molecular Electronic Full Adder	407
VI. DISCUSSION.....	408
A. Further Design Challenges for Molecular Electronic Circuits	408
1. Combining Individual Devices	408
2. Mechanisms of Conductance	409
3. Nonlinear I-V Behavior	409
4. Energy Dissipation	409
5. Necessity for Gain in Molecular Electronic Circuits	409
6. Potentially Slow Speeds	410
B. Architectural Approaches and Architectural Issues for Molecular Electronics	411
VII. SUMMARY AND CONCLUSIONS.....	411
A. The Next Logical Step in Molecular Electronics	411
B. Environment and Interface for Molecular Electronic Circuits	411
1. Grid of Metal Nanowires:	411
2. Molecular Electronic “Breadboard”	412
3. Carbon Nanotubes	412
4. Nanopore	413
C. Circuits One Million Times Denser Than Microelectronics	413
1. Gate and Function-Level Integration to Produce Molecular-Scale Electronic Computers	413
2. Device-Level Integration for More Rapid Prototyping Molecular-Scale Electronic Logic	413
D. Future Prospects	413
1. Key Advantages and Key Applications for Proposed Molecular Electronic Logic	413
2. Matter as Software	413

TABLE OF CONTENTS (CONCLUDED)

APPENDIX I. Ab Initio Quantum Calculations of Rectifying Properties for Polyphenylene-Based Molecular Rectifiers.....	414
A. Calculations Upon Isolated Benzene Rings Monosubstituted with Donor and Acceptor Substituents	415
B. Calculations Upon Bonded Polyphenylene-Based Donor-Acceptor Complexes Built from Monosubstituted Aromatic Rings	416
C. Calculations Upon Bonded Polyphenylene-Based Donor-Acceptor Complexes Built from Disubstituted Aromatic Rings	417
APPENDIX II. Explanation of Diode-Diode Logic.....	418
A. Operation of the Diode-Based AND gate	418
B. Operation of the Diode-Based OR gate	419
C. Operation of the Diode-Based XOR Gate	421
APPENDIX III. Size estimate for CMOS Half Adder and Scaling Estimate for A Molecular Adder	422
A. Motivation	422
B. Naegle's Estimate of the Sizes for CMOS Logic Structures	422
C. Conclusions	422
ACKNOWLEDGEMENT.....	423
REFERENCES	423
AUTHORS' BIOGRAPHIES and PHOTOGRAPHS.....	426

LIST OF FIGURES

Figure 1. Aromatic molecular conductors and aliphatic molecular insulators.....	389
Figure 2. Schematic diagrams of the chemical structures and the molecular orbital structures for benzene and for polyphenylene molecules.....	390
Figure 3. Schematic symbol for a rectifying diode, plus current versus voltage behavior for ideal and Zener diodes.....	391
Figure 4. Molecular structure, schematic of apparatus, behavior in experiment by Metzger et al. demonstrating rectification in a Langmuir–Blodgett (LB) film	392
Figure 5. Experiment by Reed and his collaborators demonstrating molecular rectification (i.e., a molecular rectifying diode) in a monolayer of Tour wires between electrodes of two different metals.....	392
Figure 6. Schematic of the structure and operation for the molecular resonant tunneling diode demonstrated by Reed, Tour, and their collaborators	393
Figure 7. Behavior of the molecular resonant tunneling diode depicted in Fig. 6.....	394
Figure 8. Molecular structure and schematic of electron orbital energy levels for a proposed polyphenylene-based molecular rectifying diode switch.....	397
Figure 9. Schematic describing operation of a proposed polyphenylene-based molecular rectifying diode switch under two opposite externally applied voltages	399
Figure 10. Structure of proposed dimethoxy-dicyano polyphenylene-based rectifying diode for use in the design of molecular electronic diode–diode logic circuits.....	402
Figure 11. Structure of proposed dimethyl-dicyano polyphenylene-based molecular rectifying diode for use in the design of molecular electronic diode–diode logic circuits.....	403
Figure 12. Diode–diode-type molecular electronic AND gate incorporating polyphenylene-based molecular rectifying diodes embedded in Tour wires.....	404
Figure 13. Diode–diode-type molecular electronic OR gate incorporating polyphenylene-based molecular rectifying diodes embedded in Tour wires.....	404
Figure 14. Diode-based molecular electronic XOR gate incorporating molecular rectifying diodes and a molecular resonant tunneling diode.....	405
Figure 15. Design for a molecular electronic half adder built from two diode-based molecular logic gates.....	406
Figure 16. Design for a molecular electronic full adder built from two diode-based molecular half adders and a diode-based molecular OR gate.....	407
Figure 17. Conceptual diagram of a molecular electronic circuit in which carbon nanotube molecules are employed to make electrical contact with and support a polyphenylene-based molecular electronic half adder.....	412
Figure 18. Two modes of operation for ideal rectifying diodes in the component circuits for a diode-based AND gate.....	418
Figure 19. Three cases for operation of a diode-based AND gate	419
Figure 20. Two modes of operation for ideal rectifying diodes in the component circuits for a diode-based OR gate.....	420
Figure 21. Three cases for operation of a diode-based OR gate.....	420
Figure 22. Circuit schematics explaining the operation of the molecular electronic XOR gate.....	421

LIST OF TABLES

Table 1. Approximate Current Densities in Electrons Per Second Per Square Nanometer Calculated from Experimental Data for Selected Molecular Electronic and Macroscopic Metal Devices	389
Table 2. Results of HF STO 3-21G Molecular Orbital Calculations to Determine ΔE_{LUMO} Between Donor and Acceptor Halves of the Dimethoxy-Dicyano Polyphenylene-Based Molecular Rectifying Diode Shown in Fig. 10.....	403
Table 3. Results of HF STO 3-21G Molecular Orbital Calculations to Determine ΔE_{LUMO} Between Donor and Acceptor Halves of Dimethyl-Dicyano Polyphenylene-Based Molecular Rectifying Diode Shown in Fig. 11.....	403
Table 4. HOMO and LUMO Energies Determined from Molecular Orbital Theory Calculations for Benzene and Benzene Rings Monosubstituted with Donor and Acceptor Substituent Groups.....	414
Table 5. Orbital Energies and LUMO Energy Differences Calculated via 3-21G SCF Molecular Orbital Theory for Archetypal Polyphenylene-Based Diodes Assembled from Singly Substituted Benzene Components Separated by an Insulating Dimethylene Group.....	415
Table 6. HOMO and LUMO Energies Determined from Molecular Orbital Theory Calculations for Benzene and Benzene Rings Disubstituted with Donor and Acceptor Substituent Groups.....	416

Architectures for Molecular Electronic Computers: 1. Logic Structures and an Adder Designed from Molecular Electronic Diodes

JAMES C. ELLENBOGEN AND J. CHRISTOPHER LOVE

Recently, there have been significant advances in the fabrication and demonstration of individual molecular electronic wires and diode switches. This paper reviews those developments and shows how demonstrated molecular devices might be combined to design molecular-scale electronic digital computer logic. The design for the demonstrated rectifying molecular diode switches is refined and made more compatible with the demonstrated wires through the introduction of intramolecular dopant groups chemically bonded to modified molecular wires. Quantum mechanical calculations are performed to characterize some of the electrical properties of the proposed molecular diode switches. Explicit structural designs are displayed for AND, OR, and XOR gates that are built from molecular wires and molecular diode switches. The diode-based molecular electronic logic gates are combined to produce a design for a molecular-scale electronic half adder and a molecular-scale electronic full adder. These designs correspond to conductive monomolecular circuit structures that would be one million times smaller in area than the corresponding micron-scale digital logic circuits fabricated on conventional solid-state semiconductor computer chips. It appears likely that these nanometer-scale molecular electronic logic circuits could be fabricated and tested in the foreseeable future. At the very least, such molecular circuit designs constitute an exploration of the ultimate limits of electronic computer circuit miniaturization.

Keywords—Computer architecture, computer design, molecular circuit design, molecular diode–diode logic, molecular electronics, molecular logic circuits, nanoelectronics, quantum-effect circuits, quantum-effect devices.

I. INTRODUCTION

Recently, there have been significant advances in the fabrication and demonstration of molecular electronic wires [1]–[4] and of molecular electronic diodes, two-terminal electrical switches made from single molecules [5]–[14]. There also have been advances in techniques for making reliable electrical contact with such electrically conducting molecules [3], [15]. These promising developments and

others [16]–[19] in the field of nanoelectronics suggest that it might be possible to build and to demonstrate somewhat more complex molecular electronic structures that would include two or three molecular electronic diodes and that would perform as digital logic circuits.

It is the purpose of this paper to provide and to explain novel designs for several such simple molecular electronic digital logic circuits: a complete set of three fundamental logic gates (AND, OR, and XOR gates), plus an adder function built up from the gates via the well-known principles of combinational logic. En route to the design of these molecular electronic logic gates and functions, we also propose and characterize designs for simpler, polyphenylene-based molecular electronic rectifying diode switches that should be easy to integrate in logic circuits with other previously demonstrated [1]–[3], [5]–[7], [10]–[13] polyphenylene-based molecular electronic wires and devices. The design for rectifying molecular diode switches is refined herein to be more compatible with the demonstrated wires through the introduction of intramolecular dopant groups chemically bonded to modified molecular wires.

A key idea of this work is that the implementation of elementary molecular electronic logic gates and elementary molecular electronic computational functions does not necessarily require the use of three-terminal molecular-scale transistors. Only a few two-terminal molecular diode switches are essential to implement simple molecular electronic computer logic circuits.

Moreover, such molecular diode switches already have been demonstrated [5]–[11], [13], [14]. It is only necessary that two or three of them be assembled, either mechanically or chemically, and brought into appropriate electrical contact in order to test and to demonstrate molecular electronic logic.

The molecular electronic logic structures proposed here would occupy an area one million times smaller than analogous logic structures that currently are implemented in micron-scale, solid-state semiconductor integrated circuits. Because of their extremely small sizes, at the very least, these molecular logic designs constitute an exploration

Manuscript received August 19, 1999; revised December 30, 1999. This work was supported by a grant from The MITRE Corporation.

The authors are with the Nanosystems Group, The MITRE Corporation, McLean, VA 22102 USA (e-mail: nanotech@mitre.org).

Publisher Item Identifier S 0018-9219(00)02348-3.

of the limits of electronic computer circuit miniaturization. Further, as detailed below, all these molecular-scale electronic logic structures are built up simply from a few molecular diode switches similar to those already demonstrated experimentally [2], [3], [5], [7], [9]–[12], [15], [20], as well as theoretically [21]–[28]. Thus, it might be possible to fabricate and to test experimentally such ultrasmall, ultradense, molecular electronic digital logic in the relatively near future.

To begin to explain why such dramatic developments now are likely, in Section II of this paper we review and analyze in detail the recent research results that have begun to introduce and demonstrate functioning molecular-scale electronic switches and wires. In Section III, we propose how to integrate these earlier molecular devices with some new compatible diode switches introduced in Section IV. This integration allows the proposal of molecular electronic digital circuit structures for which explicit designs are provided in Section V. Then, Section VI discusses the strengths and weaknesses of these novel molecular circuit designs. They are considered relative to a set of architectural issues that must be addressed in order to design, fabricate, and operate an entire molecular electronic digital computer that might be built from logic structures and functions similar to or evolved from those described in this work.

Finally, Section VII considers possible interface and integration strategies for such molecular circuits, as well as their possible applications and technological impacts. Three appendixes provide more details about important quantitative aspects of the structure, function, and scaling, respectively, for the molecular diode switches and the molecular logic gates.

As outlined above, the work presented here establishes a qualitative framework for molecular circuit architectures and it identifies architectural issues associated with this approach. Therefore, it is an additional purpose of the present work to define an agenda and to provide a direction for future, detailed, systematic, quantitative investigations that the authors and others will perform to explore the validity of this proposed approach to designing molecular electronic computers.

II. BACKGROUND

Recent developments indicate that the physical limits of miniaturization for bulk-effect semiconductor transistors are likely to be encountered sooner and on larger scales than previously had been expected [29], [30]. This eventuality makes it more important than ever to explore alternatives, such as molecular electronics, for the continued miniaturization of electronic devices and circuits down to the nanometer scale.

Presently, there are two primary types of molecules that have been proposed and demonstrated for use as the potential basis or backbone for current-carrying, molecular-scale electronic devices. These two types of molecular backbones are: 1) polyphenylene-based chains and 2) carbon nanotubes.

In addition, there has been much speculation in the literature about still a third possible type of conductive back-

bone involving biomolecules. To provide a sound basis for explaining the molecular circuit designs proposed here, the principal concepts and experimental data concerning each of these three possible conductive molecular-scale backbones is reviewed and discussed separately below.

A. Polyphenylene-Based Molecular-Scale Electronic Devices

Polyphenylene-based molecular wires and switches involve chains of organic aromatic benzene rings. Such chains are shown in Fig. 1(d).

Until recently, it was an open question whether such small molecules, taken individually, had appreciable conductance. However, over the last two or three years, several different groups have shown experimentally that individual polyphenylene molecules can conduct small electrical currents [1]–[3]. Motivated by such experimental advances, several groups of theorists, including Datta *et al.* [26]–[28], Ratner and his collaborators [21]–[23], as well as Reimers *et al.* [31], [32] have begun to establish a set of computational approaches and a qualitative mechanistic framework [24], [25] for the detailed interpretation of electrical conduction in small organic molecules. Calculations using these and related methods have confirmed the experiments by explaining in detail the features of the electrical conduction observed in short polyphenylene wires [28], [33]–[36].

Further, substituted polyphenylenes and similar small organic molecules have been shown experimentally to be capable of switching small currents [5]–[11], [13].

1) *Conductors or Wires—Conjugated Aromatic Organic Molecules:* An individual benzene ring, having the chemical formula C_6H_6 is shown in Fig. 1(a). A benzene ring with one of the hydrogens removed to form C_6H_5 so that it can be bonded as a group to other molecular components is drawn as shown in Fig. 1(b). Such a ring-like substituent group is termed a “phenyl group.” By removing two hydrogens from benzene, one obtains the structure C_6H_4 or “phenylene,” a ring which has two free binding sites as shown in Fig. 1(c).

By binding phenylenes to each other on both sides and terminating the resulting chain-like structures with phenyl groups, one obtains a type of molecule known as a “polyphenylene.” Polyphenylenes, such as the upper molecular structure in Fig. 1(d), may be made in a number of different shapes and lengths. In addition, one may insert into a polyphenylene chain other types of molecular groups (e.g., singly bonded aliphatic groups, doubly bonded ethenyl groups, and triply bonded ethynyl or “acetylenic” groups) to obtain “polyphenylene-based” molecules with very useful structures and properties. An example of such a polyphenylene-based molecule is the lower structure in Fig. 1(d). Molecules such as benzene and polyphenylenes, which incorporate benzene-like ring structures as significant components, are termed “aromatic.”

As discussed briefly above, various investigators recently have performed sensitive experiments in which one or a few polyphenylene-based molecules have been shown to conduct electricity. The results of several of those experimental efforts are summarized in Table 1. In one example

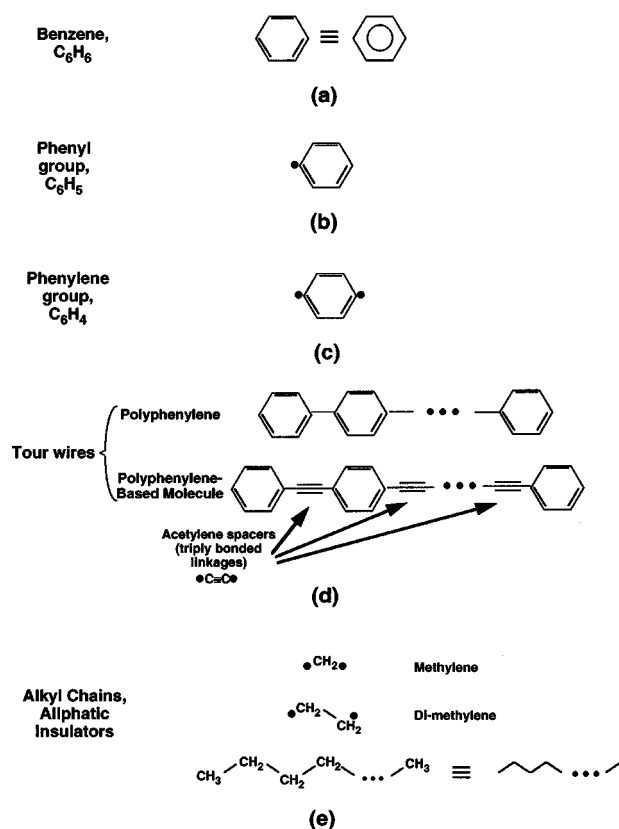


Fig. 1. Aromatic molecular conductors and aliphatic molecular insulators.

of such an experiment, Reed and his collaborators passed an electrical current through a monolayer of approximately 1000 polyphenylene-based molecular wires which were arrayed in a nanometer-scale pore and adsorbed to metal contacts on either end [8]. The system was carefully prepared such that all of the molecules in the "nanopore" were identical three-benzene-ring polyphenylene-based chain molecules. These chain molecules each had a form similar to the molecules diagrammed in Fig. 1(d), including triply bonded, conductive, acetylenic "spacers" bonded between each pair of benzene rings. The total current passed through this assembly of molecules measured 30 μA , which converts to roughly 30 nA of electrical current passing through each molecule. This current, listed in the fourth column of Table 1, corresponds to approximately 200 billion electrons per second being transmitted across each short polyphenylene-based molecular wire.

In tests of molecular electronic devices, such as those cited in Table 1, small lengths of molecular wire are sandwiched between narrow Schottky-type potential barriers, where the molecule joins but is imperfectly bound to the closely spaced metal contacts. Thus, while tunneling can occur through such barriers, the current that can pass through the molecule is greatly reduced and the Schottky barriers have a large impact on the entire molecular electronic system [21], [24], [37]. One can anticipate, however, that further research and development will produce a larger conductive molecule which integrates molecular wires, molecular switches, etc., covalently bonded into a single molecular electronic circuit. In

the operation of the larger molecular electronic circuit, any Schottky barriers would be much farther apart (i.e., at least ten times), and the flow of current between devices within the molecule would be relatively less affected by the Schottky barriers. Therefore, the current or signal could pass among all the devices of a molecular electronic circuit with much less impedance than might be inferred from the experimental results displayed in Table 1.

For comparison with the data in Table 1 in the case of the polyphenylene-based wires and switches, we note that a somewhat larger molecule, a carbon nanotube or "buckytube," has been measured transmitting a current between 10 and 100 times greater than that measured for the simple polyphenylene-based chains. Those measurements, tabulated in Table 1, correspond to a current of approximately 20–500 nanoamps, or approximately 120 billion to 3 trillion electrons per second. Strengths and limitations of these highly conductive carbon nanotube molecules are discussed further in Section II-B.

While polyphenylene-based molecular wires like those depicted in Fig. 1(d) do not carry as much current as carbon nanotubes, polyphenylenes and their derivatives are much smaller molecules. Thus, because of their very small cross-sectional areas, they do have very high current densities. This is seen in Table 1, where approximate current densities are calculated for several selected molecular electronic devices as well as for a typical macroscopic copper wire. We observe that the current density for a polyphenylene-based molecular wire is approximately the same as for a carbon nanotube and as much as half a million times greater than that for the copper wire.

Also, polyphenylene-based molecules have the significant advantages of a very well-defined chemistry and great synthetic flexibility, based upon more than a century of experience accumulated by organic chemists in studying and manipulating such aromatic compounds. Recently, Tour has refined the synthetic techniques for conductive polyphenylene-based chains to produce enormous numbers of these molecules (approximately 10^{23}), every one of which is of exactly the same structure and length [38], [39]. Thus, such polyphenylene-based molecular wires with the chemical structures shown schematically in Fig. 1(d) have come to be known as "Tour wires."

The source of the conductivity for a polyphenylene-based wire is a set of π -type (i.e., "pi"-type) molecular orbitals that lie above and below the plane of the molecule when it is in a planar or near planar conformation [40]–[42]. An example of a π -orbital is illustrated in Fig. 2. In a planar conformation, the π -orbitals associated with each individual atom overlap or "conjugate" in various combinations to create a set of extended π -orbitals that spans the length of the molecule. This occurs because there is a significant energetic advantage that arises from delocalizing valence (and conduction) electrons in orbitals that span or nearly span the length of the entire molecule. The lowest energy π -orbital available in the molecule is depicted in Fig. 2(d). Higher energy π -orbitals differ somewhat in that they do have nodal planes (planes where the orbital vanishes) oriented perpendicularly to the axis of a

Table 1

Approximate Current Densities in Electrons Per Second Per Square Nanometer Calculated from Experimental Data for Selected Molecular Electronic and Macroscopic Metal Devices

<———— Molecular Electronic Device ———>						
Quantity	Units	1,4-Dithiol Benzene	3-Ring Poly-phenylene Wire	Poly-phenylene RTD (5 rings)	Carbon Nanotube	Copper Wire
Applied Voltage	Volts	1	1	1.4 (peak)	1	2×10^{-3} (10 cm wire)
Current Measured in Experiment	Amperes	2×10^{-8}	3.2×10^{-5}	1.4×10^{-11}	1×10^{-7}	1 (approx.)
Current Inferred per Molecule	Amperes	2×10^{-8}	3.2×10^{-8}	1.4×10^{-14}	1×10^{-7}	—
	Electrons per Sec	1.2×10^{11}	2.0×10^{11}	8.7×10^4	6.2×10^{11}	—
Estimated Cross-Sectional Area per Molecule	nm ²	~0.05	~0.05	~0.05	~3.1 (Radius ≈ 1 nm)	~3.1 × 10 ¹² (Radius ≈ 1 mm)
Current Density	Electrons per Sec-nm ²	~2 × 10 ¹²	~4 × 10 ¹²	~2 × 10 ⁶	~2 × 10 ¹¹	~2 × 10 ⁶
Reference		[7]	[8]	[5,6]	[4]	

NOTES:

1. Conversion factor for amperes to electrons per second is:

$$1 \text{ Ampere} \equiv 1 \text{ Coulomb/sec} = (1.6 \times 10^{-19})^{-1} \text{ electrons/sec} = 6.2 \times 10^{18} \text{ electrons/sec}$$

2. In order to estimate the current densities per molecule from the published data on the room temperature nanopore measurements in Refs. [8] and [5,6], it was determined that the samples in the monolayer in the nanopore contained on the order of 1000 molecules per monolayer. This estimate is based on an average nanopore diameter of 30 nm and an estimated molecular diameter on the order of approximately 1 nm.
3. Common copper wire generally is regarded as being highly conductive. Therefore, data for 10 cm of 1mm diameter (18 gauge) copper wire is included only for comparison as a familiar, conductive, macroscopic reference system. A current on the order of 1 ampere is the maximum recommended for such wire to avoid undue heating and danger of fire.

wire-like molecule. The higher the energy of the orbital, the more nodal planes it will contain.

Long π -orbitals are both located out of the plane of the nuclei in the molecule and they are relatively diffuse compared to the in-plane σ -type ("sigma"-type) molecular orbitals. Thus, one or more such long unoccupied or only partially occupied π -orbitals can provide "channels" that permit the transport of additional electrons from one end of the molecule to the other when it is under a voltage bias. The mechanisms of such transport have been discussed in detail by Ratner and Jortner [24], based upon formal considerations explored earlier by Mujica, Ratner and their collaborators [21]–[23] and by Datta [27]. In order to align our discussion and terminology more closely with solid-state electronics, we will refer to the collection or manifold of available molec-

ular channels that is widely spaced in energy—i.e., sparse unoccupied π -orbitals—as a "conduction band" although the term "band" usually is reserved in physics and electrical engineering for an interval of energy where there is a nearly continuous set of allowed quantized energy states.

A delocalized π -orbital usually extends across one or more of the neighboring aromatic rings in the molecule, as well as across other intervening multiply bonded groups. The component π -orbitals from the several substituent aromatic rings and multiply bonded groups can sum or merge to form a number of larger, molecule-spanning π -orbitals, each having a different nodal structure and energy. Several such separate, unoccupied π -orbitals that are low-lying in energy are thought to be primarily responsible for the conduction through polyphenylene-based molecular wires. When such a

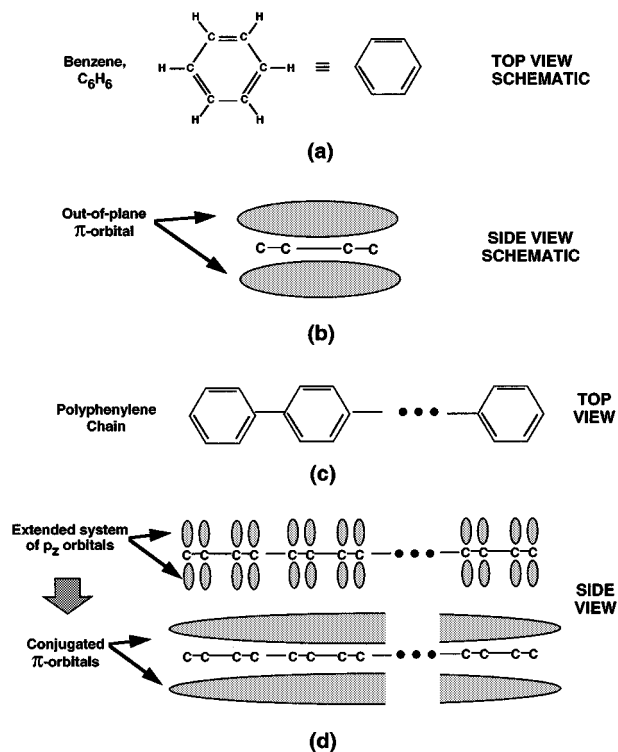


Fig. 2. Schematic diagrams of the chemical structures and the molecular orbital structures for benzene and for polyphenylene molecules.

molecule is placed under an externally applied voltage bias, an unoccupied π -orbital that is lower in energy is likely to be a more effective pathway for electron transport because:

- 1) it can be brought into energetic coincidence more easily with still lower energy occupied orbitals;
- 2) a lower energy unoccupied orbital yields a more stable pathway for a conduction electron.

Generally speaking, it can be expected that conjugated aromatic molecules, such as polyphenylenes, will conduct currents. This also is true of polyphenylene-based molecules with other multiply bonded groups (such as ethenyl, $-\text{HC}=\text{CH}-$, or ethynyl, $-\text{C}\equiv\text{C}-$) inserted between the aromatic rings, so long as conjugation among the π -bonded components is maintained throughout. Thus, in practice, as shown in Fig. 1(d), triply bonded ethynyl or acetylenic linkages often are inserted as spacers between the phenyl rings in a Tour wire [5], [6], [43]–[45]. These spacers eliminate the steric interference between hydrogen atoms bonded to adjacent rings. Otherwise this steric interference would force the component rings in the Tour wire to rotate into a nonplanar conformation. That would reduce the extent of π -orbital overlap between adjacent rings, break up the electron channels, and decrease the conductivity of the molecular wire. The acetylenic linkages themselves permit the conductivity to be maintained throughout the length of the molecule because of their own out-of-plane π -electron density. This is true, despite the fact that acetylenic groups seem to be terminated by single bonds. When the triply bonded structure is inserted into the aromatic chain, the out of plane π -orbitals in the acetylenic triple bond delocalize

and overlap sufficiently with those on neighboring aromatic rings so that the acetylenic linkage maintains and becomes a part of a molecule-spanning electron channel.

2) *Insulators—Aliphatic Organic Molecules:* On the other hand, “aliphatic” organic molecules serve as insulators. Examples are sketched in Fig. 1(e). These are singly bonded molecules that contain only sigma bonds that lie along the axes of the atoms that are joined to form the backbone of the molecule. Such bonds do not form an uninterrupted channel outside the plane of the nuclei in the molecule. The positively charged atomic nuclei are obstacles to negatively charged electrons traveling along the axis or plane of the molecule. Therefore, such singly bonded structures cannot easily transport an unimpeded electron current when they are placed under a voltage bias. For this reason, aliphatic molecules or groups act as insulators.

It follows that when a small aliphatic group is inserted into the middle of a conductive polyphenylene chain, it breaks up the conductive channel and forms a “barrier” to electron transport. This fact plays a significant role in later considerations, as does the notion that such barriers act somewhat like electrical resistors in a molecular circuit.

The data in Table 1 can be used to derive an approximate indication of the effectiveness of aliphatic insulating groups. Note in columns 3 and 4 of the table that a single-ring and a three-ring length of polyphenylene-based wire are measured to conduct approximately the same current. However, in column 5, the data show that the polyphenylene-based RTD, which is simply a five-ring polyphenylene-based molecular wire with two separate one-carbon aliphatic methylene groups inserted into it, conducts approximately 250 000 times less current than the somewhat shorter three-ring wire with no such insulating aliphatic groups inserted into it. (The structure and electrical behavior of the polyphenylene-based RTD is discussed in detail below in Section II-A4.) Assuming, then, that each methylene group reduces the current in the wire by the same factor, these data suggests that each one-carbon insulating group reduces the electron current by a factor of as much as the square root of 250 000—i.e., by a factor of between 100 and 1000 [46].

3) *Diode Switches—Substituted Aromatic Molecules:* A diode is simply a two-terminal switch. It can turn a current on or off as it attempts to pass through the diode from the “in” to the “out” terminal. These terminals usually are termed, respectively, the “source” and the “drain” for the current. Unlike more familiar three-terminal switching devices (e.g., triodes and transistors), diodes lack a third or “gate” terminal via which a small current or voltage can be used to control a larger current or voltage passing from the source to the drain. Thus, unlike a transistor, a single diode switch, by itself, cannot produce current amplification or “power gain.” (See further discussion of this point in Section VI-A5, however.)

Two types of molecular-scale electronic diodes have been demonstrated recently and are discussed here: a) rectifying diodes and b) resonant tunneling diodes. Each of these types of molecular diodes is modeled after more familiar solid-state analogs.

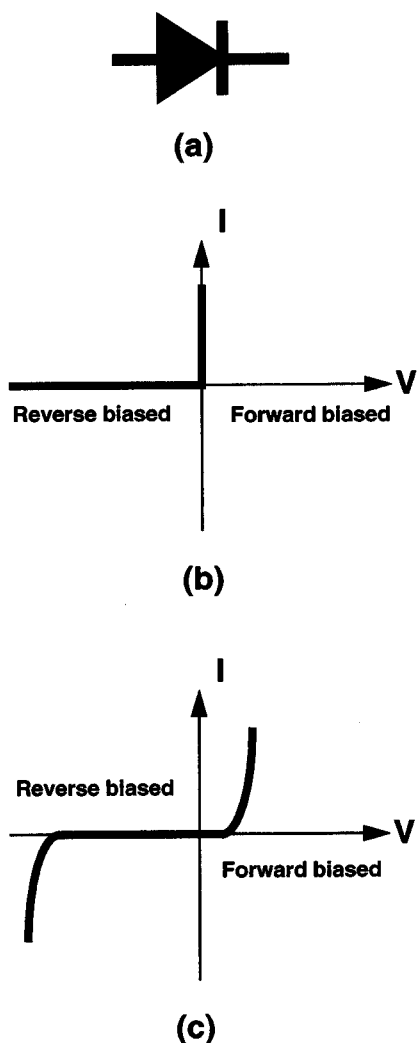


Fig. 3. Schematic symbol for a rectifying diode, plus current versus voltage behavior for ideal and Zener diodes.

a) Molecular rectifying diodes (“molecular rectifiers”): A rectifying diode incorporates structures that make it more difficult to induce electric current to pass through it in one direction, usually termed the “reverse” direction from terminal B to A, than in the opposite “forward” direction from A to B. This “one-way” behavior is suggested by the standard schematic symbol for the rectifying diode, shown in Fig. 3(a), and by the current versus voltage plots for an “ideal” diode and a nonideal Zener diode shown in Fig. 3(b) and (c), respectively. (Note: the reader should be aware that, in accordance with a longstanding convention in electronics, the direction of current flow in a diode or any other circuit element is taken to be the direction of flow of the positive charge, which is the opposite of the direction of flow for the electrons. That is the convention used here.)

Solid-state rectifying diodes: Diode switches implemented using vacuum tubes or bulk-effect solid-state devices (e.g., p–n junction diodes) have been elements of analog and digital circuits since the beginning of the electronics revolution very early in the twentieth century. The behavior of junction diodes was a very important influence in the development of

the transistor [47]. A detailed discussion of the function of such solid-state devices may be found elsewhere [48].

Aviram and Ratner rectifying diodes and the origin of molecular electronics: Diode switches likewise have had a seminal role in the formulation and testing of strategies for miniaturizing electronics down to the molecular scale. Rectifying diode switches were the topic of the first scientific paper about molecular electronics, Aviram and Ratner’s influential 1974 work “Molecular Rectifiers” [49]. Aviram and Ratner based their suggestion for the structure of a molecular diode switch on the operational principles for the solid-state, bulk-effect p–n junction diode.

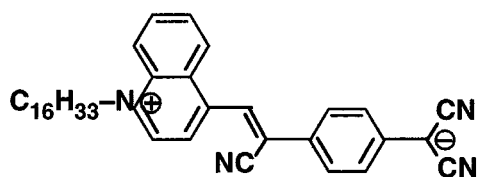
Aviram and Ratner’s proposal and theoretical specification for the structure and function of a molecular rectifying diode was made a quarter century ago, and there have been a number of experimental efforts to demonstrate a molecule with such electrical properties in the intervening years. Building on an earlier experimental demonstration by Martin *et al.* in 1993 [50], two separate groups in 1997, one led by Metzger at the University of Alabama [9] and another led by Reed at Yale University [7] demonstrated molecular rectifiers in independent experiments.

The structures of the molecular rectifiers they demonstrated are shown in Figs. 4 and 5, respectively. Fig. 4(a) shows the molecular structure for Metzger’s molecular diode, Fig. 4(b) shows the experimental setup, and Fig. 4(c) shows the measured electrical properties of the molecular rectifying diode. Fig. 5(a) shows the molecules and the experimental setup for Reed’s molecular rectification experiment, while Fig. 5(b) shows the measured electrical properties of the rectifier. In comparing Figs. 4(c) and 5(b) to Fig. 3, the reader should remain aware that, as noted above, the direction of current flow represented in Fig. 3 is the direction of flow of positive charge or “holes,” which is opposite to the direction of electron flow.

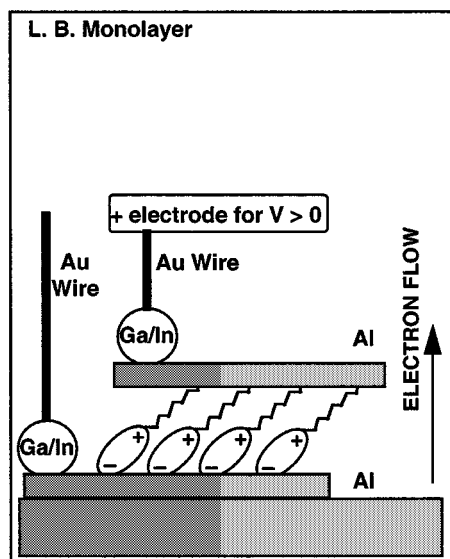
Impressive as is the demonstration of the Metzger’s and Reed’s molecular rectifying diodes, the molecular rectifiers they demonstrated cannot be readily integrated with Tour’s polyphenylene-based wires to produce a compact, purely molecular circuit. Thus, in Section IV of this paper, the authors propose, characterize, and explain the operation of new polyphenylene-based molecular rectifiers. These would operate according to the same principles expounded by Aviram and Ratner, and as were demonstrated by Metzger *et al.* and by Reed *et al.* However, the molecular rectifying diodes proposed in this work should be more appropriate in structure for building molecular-scale digital circuitry.

b) Molecular resonant tunneling diodes (RTD’s): An RTD takes advantage of energy quantization to permit the amount of voltage bias across the source and drain contacts of the diode to switch “on” and “off” an electric current traveling from the source to the drain. Unlike the rectifying diode, current passes equally well in both directions through the RTD.

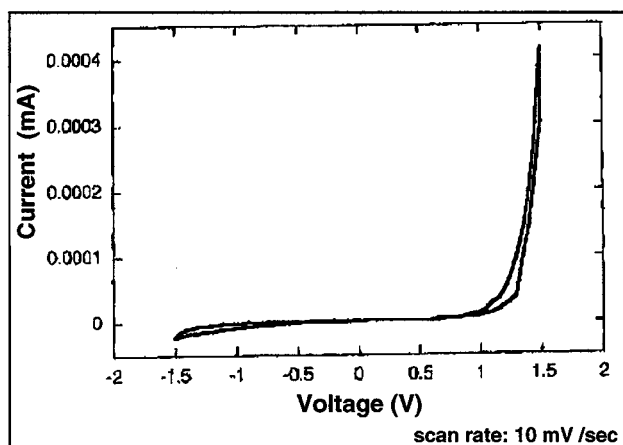
Structure of the molecular RTD: Depicted in Fig. 6(a) is a molecular resonant tunneling diode that has only very recently been synthesized by Tour [45], [51] and demonstrated by Reed [5], [6]. Structurally and functionally, the device



(a)



(b)

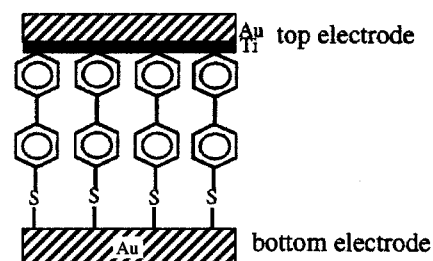


(c)

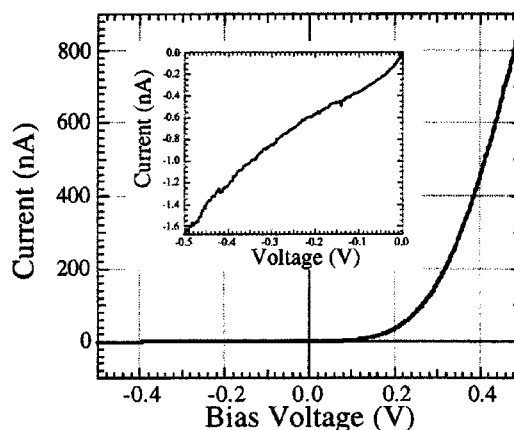
Fig. 4. Molecular structure, schematic of apparatus, and electrical behavior in experiment by Metzger *et al.* demonstrating molecular rectification in a Langmuir-Blodgett (LB) film [9].

is a molecular analog of much larger solid-state RTD's that for the past decade commonly have been fabricated in III-V semiconductors and employed in solid-state, quantum-effect circuitry [17]. However, the Tour-Reed molecular RTD is the first experimental demonstration of a working molecular electronic device of this type.

Based upon a Tour-wire backbone, as shown in Fig. 6(a), Reed's and Tour's polyphenylene-based molecular RTD is



(a)



(b)

Fig. 5. Experiment by Reed and his collaborators demonstrating molecular rectification (i.e., a molecular rectifying diode) in a monolayer of Tour wires between electrodes of two different metals [7]. (a) Schematic of showing Tour-type molecular wires between Ti/Au top electrode and Au bottom electrode. (b) I versus V plot showing characteristic rectifying behavior for molecular diode.

made by inserting two aliphatic methylene groups into the wire on either side of a single aliphatic ring. Because of the insulating properties of the aliphatic groups, as discussed above, they act as potential energy barriers to electron flow. They establish the aromatic ring between them as a narrow (approximately 0.5 nm) "island" of lower potential energy through which electrons must pass in order to traverse the length of the molecular wire. (Note that solid-state RTD's have islands approximately 10 nm wide or approximately 20 times as wide as that in the molecular variant.)

The molecular RTD and the other molecular devices illustrated in this work often are attached at their ends to gold electrodes by thiol ($-SH$) groups that adsorb (i.e., form tight bonds) to the gold lattice. This is seen, for example, in Fig. 6. Groups of this type and others that bind molecules tightly to metals have been termed "molecular alligator clips" by Tour [52]. Ideally, these molecular alligator clips would not only bind the molecules tightly to the metal, as does the thiol, but also promote conduction between metal and molecules.

Thiols on gold are the most common "clips" for attaching molecules to metal substrates, but they may not form the optimal connections for molecular electronic devices. The geometry of the orbitals on the sulfur does not permit the conjugated π -orbitals from the organic chain to interact strongly

with the conduction orbitals of the gold. The mismatch of orbitals creates a potential energy barrier at each end of the wire, raising the resistance of the wire. It has been suggested that other “clip” combinations might make a better electrical contact between the metal and the organic molecule. However, alternative metal contacts may present other experimental difficulties such as surface oxidation and side reactions with the organic molecules.

Operation of the molecular RTD: Whenever electrons are confined between two such closely spaced barriers, quantum mechanics restricts their energies to one of a finite number of discrete “quantized” levels [40], [41], [53]. This energy quantization is the basis for the operation of the RTD [17], [53].

The smaller the region in which the electrons are confined, the farther apart in energy are the allowed quantized energy levels. Thus, on the island between the barriers of the RTD illustrated in Fig. 6, the allowed unoccupied π -type energy levels are relatively far apart. Also shown in the illustration, the unoccupied π -type energy levels are more densely spaced in energy in the less confining low-potential-energy regions of the molecule to the left and right of the barriers surrounding the island. Electrons are injected under a voltage bias into the lowest unoccupied energy levels on the left-hand side of the molecule.

The only way for electrons with these moderate kinetic energies to pass through the device is to “tunnel,” quantum mechanically, through the two barriers surrounding the island. The probability that the electrons can tunnel from the left-hand side onto the island is dependent on the energies of the incoming electrons compared to the widely spaced unoccupied energy levels on the island.

As illustrated in Fig. 6(b), if the bias across the molecule produces incoming electrons with kinetic energies that differ from the unoccupied energy levels available inside the potential well on the island, then current does not flow. The RTD is switched “off.”

However, as illustrated in Fig. 6(c), if the bias voltage is adjusted so that the energy of the incoming electrons aligns with one of the island's energy levels, the energy of the electrons outside the well is “in resonance” with the allowed energy inside the well. In that case an electron can tunnel from the left-hand region onto the island. If this can occur, and, simultaneously, if the bias is such that the energy level inside the well also is in resonance with one of the many unoccupied energy levels in the region to the right of it, then electrons flow through the device from left to right. That is, the RTD is switched “on.”

Current versus voltage behavior of the molecular RTD: To understand the utility of such RTD's in logic circuits, it is essential to be familiar with the characteristic current versus voltage plot that is produced by the operational mechanism described above.

Fig. 7(a) shows the dependence of the transmitted current on the voltage bias in the measurements by Reed and his collaborators for the polyphenylene-based RTD with the structure given in Fig. 6(a) [5], [6]. It shows the transmitted current rising to a characteristic “peak” at the resonance voltage

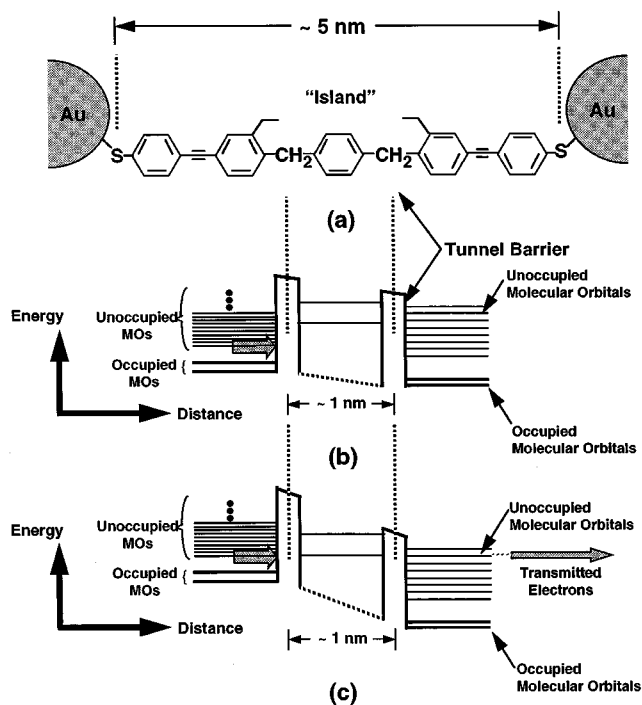
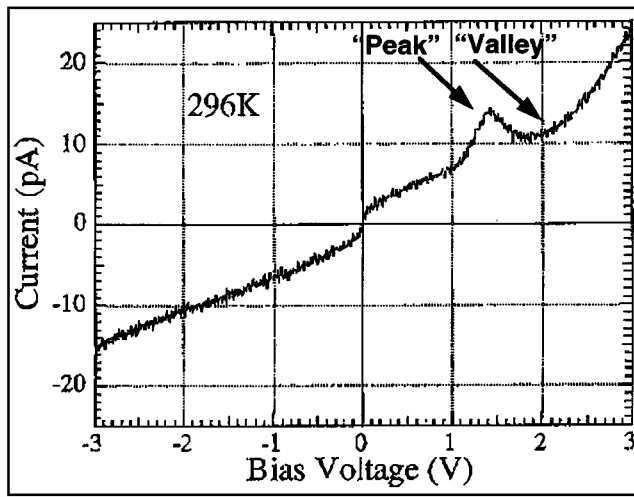


Fig. 6. Schematic of the structure and operation for the molecular resonant tunneling diode demonstrated by Reed, Tour, and their collaborators [5], [6], [45], [51].

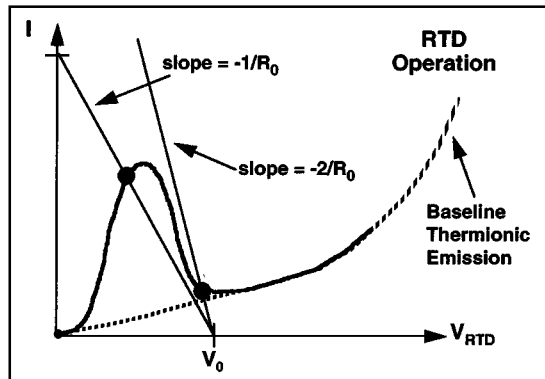
then falling off into a “valley” as the bias sweeps past the resonance voltage. The effectiveness of the operation of a particular RTD often is characterized by how well defined are the peak and valley in the current versus voltage plot. This is measured by the peak-to-valley current ratio. In Fig. 7(a), the measured peak-to-valley ratio is approximately 1.3 : 1.

In very recent work, however, Tour and Reed have modified their molecular RTD using an intramolecular doping strategy based upon the one outlined below in this paper for rectifying diodes. Experimentally, they found that the dopants seemed to enhance greatly the peak to valley ratio (to approximately 1000 : 1), much improving the switching of the molecular RTD [12], [13].

The asymmetry of the current versus voltage plot in Fig. 7(a) about the vertical, zero-bias-voltage axis merits some comment. Generally speaking, one would expect that such a plot for an RTD would be symmetric about the zero voltage axis. However, in the difficult experimental demonstration of this molecular RTD, a number of them (approximately 1000) were aligned vertically in a nanopore, adsorbed in a monolayer between two metal electrodes. To permit the nanofabrication of this system, the electrodes on the top and on the bottom necessarily were of different compositions [5]–[7]. The bottom electrode was gold, while the top electrode consisted of layers of titanium and gold (as is also the case in the earlier experiment illustrated in Fig. 5). It is believed, based upon similar asymmetric performance curves observed in experiments upon both micron-scale and nanometer-scale devices, that the asymmetry in the composition of the nanopore's electrical contacts induced a degree of rectification in the experimental system [7].



(a)



(b)

Fig. 7. Behavior of the molecular resonant tunneling diode depicted in Fig. 6 as (a) measured by Reed [5], [6] and (b) as abstracted by the present authors for the analysis of the logic circuit depicted in Fig. 14.

If so, this would produce the observed asymmetry in the molecular RTD's performance plot. Under a negative bias, the rectifier in which the molecular RTD's were embedded would suppress the negative peak current in the region of the negative resonance voltage. However, under a forward bias, the rectifier would not similarly suppress the peak current that does manifest itself in the positive voltage direction in Fig. 7(a) [43].

For some RTD's (e.g., in III-V semiconductors) the first current peak observed at either positive or negative voltage bias may even be followed by subsequent current peaks observed at higher voltages corresponding to resonances with higher energy unoccupied energy levels that are defined by the potential well on the island. For the purpose of developing the logic circuits described in following sections, however, only one resonance peak is essential. With this in mind, we abstract the current versus voltage plot of the molecular RTD as shown in Fig. 7(b). This current versus voltage behavior is a key contributor to the operation of the molecular XOR gate for which a design is proposed in Section V-A2.

The second type of demonstrated molecular electronic backbone structure is the carbon nanotube, also known as a fullerene tube or "buckytube" [54]. This type of structure can make an extremely conductive wire [4], [55]–[59]. In addition, carbon nanotubes of different diameters and chiralities (characteristic "twists" in their structures) have been predicted and demonstrated to exhibit different semiconducting electrical properties ranging from those of excellent conductors (i.e., semimetals) to those of near insulators [56], [57], [60]–[62]. Taking advantage of these properties, carbon nanotubes that incorporate a junction between two chiral structures of different types have been shown to exhibit electrical rectification, behaving as a diode switch [14], [63]. Also, carbon nanotube wires have been shown to exhibit transistor-like electrical switching properties when employed on a micropatterned semiconductor surface that can be charged to act as a gate [64].

On the other hand, because fullerene structures only have been discovered and characterized within the past two decades, the chemistry for producing them and manipulating them is not as well defined or as flexible as might be desired. Remarkable progress has been made in developing the chemistry of fullerene nanotubes, especially very recently. (For example, this progress in carbon nanotube chemistry is so recent that none of the advances in that direction that are cited in this section were published at the time the design research described in this manuscript was begun; most of those advances were not available in the literature even as late as the time this manuscript was submitted to this journal.) Advances are being made toward establishing rules and methods for substitution of other chemical groups [65]–[70] and also toward extending the range of available structures [71]. Nonetheless, these rules are not well established yet, nor is it known yet how to make with specificity and selectivity a single-walled carbon nanotube structure of a particular desired geometry and chirality, to the exclusion of others.

Further, carbon nanotubes tend to be very stable structures when formed, such that their chemical formation and manipulation in bulk chemical processes occurs only under relatively extreme conditions. Such reactions have tended not to be very selective or precise in the range of carbon nanotube structures they produce at one time. Many carbon nanotube molecules with a range of different structures usually are produced in a synthesis. However, small electronic circuits require components with precisely specified, uniform structures. At this stage, to achieve the requisite precision and uniformity still requires the use of physical inspection and manipulation of the molecules one-by-one in order to segregate and select carbon nanotubes for use in electronic research devices. Bulk chemical methods have not been developed or refined yet for this purpose, although some advances in this direction are being made using finely patterned catalytic surfaces [14], [72]–[74].

One might be able to speculate with some accuracy on the prospective electrical properties of a complex carbon nanotube structure or substructure, such as a chemically bonded "T-junction" or "Y-junction" among two or three carbon nanotube wires [75]–[78] that one might need in order to build carbon nanotube-based molecular electronic circuits [79]. Some such carbon nanotube junction structures have been made (Y-junctions), but only very recently [71]. Others (e.g., T-junctions) still have not been reported. Also, the junction structures that have been made by design are composed of multiwalled carbon nanotubes, not the single-walled junction structures of specific chirality that are likely to be necessary to have sufficiently sensitive control over small electrical currents. Research in the designed synthesis of junction structures is just beginning to exhibit useful results, and it is not yet certain which complex carbon nanotube structures can be made chemically, let alone how to make them easily and with specificity.

Thus, the design and development of carbon nanotube logic architectures is complicated and hampered presently by the fact that carbon nanotubes are relatively inert chemically and also by the fact that the chemistry of carbon nanotubes is relatively immature. This places the molecular electronics community in a situation where the molecular backbone that can be used reliably to make suitably branched structures, polyphenylene, is not the most conductive, while the most conductive molecular backbones, the carbon nanotube, does not yet have a reaction chemistry flexible enough for making the desired branched, chiral structures. Despite some promising new work in this direction [65]–[71], [80]–[83], there does not appear to be a method yet by which one can make reliably and with specificity all the structures that are likely to be needed for purely carbon nanotube-based electronic logic structures. From the point of view of the molecular circuit designer, in particular, the range of accessible carbon nanotube structures has not been clear, although some such carbon-nanotube-based molecular circuit design has proceeded anyway [79].

The fast pace of advances in carbon nanotube chemistry and in the demonstration of carbon-nanotube-based electrical devices, especially very recently, are a cause for optimism, though. With further advances in the chemistry of carbon nanotubes, in the foreseeable future it might be possible to fabricate and to demonstrate purely molecular carbon nanotube logic structures similar to those proposed below for polyphenylene-based molecular circuits. Even sooner, it might be possible to build one-of-a-kind prototype carbon-nanotube-based logic circuits using mechanical nanoprobe to pick and place onto microfabricated contacts the several separate carbon nanotube molecular switches and wires that would be necessary.

C. Biomolecules as Possible Molecular Electronic Devices

For completeness, we also review here the status of investigations toward using biomolecules as the conductive backbone for electronic wires, switches, and circuits. This third possibility for a conductive monomolecular backbone has much appeal, since biomolecules are ubiquitous, come in a

wide range of structures, and advances in biotechnology over the past several decades have provided sensitive methods for their precise chemical manipulation and assembly.

DNA molecules, for example, with their long, wirelike shape, have been suggested as a possible backbone structure. One very early effort considered in some detail a design that used DNA as the basis for an electronic memory cell [84].

Encouragement for the possibility of using DNA in molecular electronics has come from experimental work on the bulk kinetics of electron transfer processes through DNA molecules in solution. Results from such experiments carried out in the mid-1990's suggested that DNA molecules might be conductive enough for use in wires and other electrical devices. This has been a matter of some debate and confusion, though, as is well summarized elsewhere [85]. New experimental and theoretical work seems to be on the verge of resolving this debate in the case of the kinetic experiments, though, by describing how the measured flow of charge results from a combination of mechanisms that produces different results depending on the length, composition, and environment of the DNA [86]–[89]. Disappointingly, from the point of view of using pure DNA as a wire in a molecular circuit, this theoretical work also suggests that DNA's conductance should fall off very rapidly with increasing length of the molecule, unless there is very significant thermal dissipation.

Of great importance, also, Dekker and his collaborators very recently have carried out a remarkable experiment in which they measured directly the conductance of one DNA molecule (or, at most, a few molecules) suspended between two metal electrodes. They found that a DNA molecule can transport charge at high bias voltages, but that it shows negligible conductance at low bias voltages up to a few volts [90].

Despite these discouraging results for DNA, other biomolecules have shown some promise recently for use in molecular-scale electronic systems. Porphyrins and metallo-porphyrins, in particular, are another type of biomolecule [91] that is being considered for use as the conductive backbone of molecular electronic circuits [92]. This is not especially surprising, since well known porphyrins, such as hemoglobin, chlorophyll, and the cytochromes perform their biological roles in processes that chiefly involve them in storing and transferring electrons. Among their useful electrical properties, it has been calculated that porphyrinic molecular substituents will exhibit a relatively high capacitances when considered in comparison to polyphenylene-based molecular components in the same circuit [93].

Nonetheless, experimental progress on using biomolecules as components in molecular electronic devices and circuits lags well behind that in using polyphenylenes and carbon nanotubes.

D. An Advantage of Polyphenylene-Based Structures for Logic Design

Given the primitive state of molecular electronics experiments involving biomolecules and the evolving state of carbon nanotube chemistry, as outlined above, there

are some very significant advantages in considering logic structures that would be built from polyphenylene-based molecules in this first effort to design realizable conductive molecular electronic logic circuits. Using polyphenylenes, it is much easier to propose the more complex molecular electronic structures required for digital logic and to know in advance with some certainty that they can be synthesized. There exists a rational approach to planning the total synthesis of such discrete structures using organic chemistry.

Also, as shown in Table 1, polyphenylene-based molecular electronic devices can be expected to conduct a very appreciable current of electrons for such small structures. The absolute magnitude of the current they conduct may not be as large as that for a carbon nanotube. However, the current density of electrons transported through a polyphenylene-based molecular wire is of the same order of magnitude as for a carbon nanotube, because the polyphenylene-based device is so much smaller and has a smaller cross-sectional area.

The fact that these polyphenylene-based molecules are much smaller than carbon nanotubes provides yet a further reason for basing molecular circuit designs upon Tour wires in this initial effort to design monomolecular electronic digital logic. That is, if electronic logic structures and functions based upon Tour wires can be synthesized chemically (or assembled mechanically) and made to operate, they represent the "ultimate" in miniaturization for digital electronic logic. Virtually any other structure will be as large or larger. If we or others who follow demonstrate that these structures will not operate for any reason, the present effort at least will have established a lower limit on the size and an upper limit on the density for electronic digital logic.

III. APPROACH AND OBJECTIVES

As has been summarized in Sections I and II, previous theoretical and experimental efforts have provided us with a small repertoire of experimentally demonstrated polyphenylene-based molecular electronic devices upon which to build. These devices, which can transport a large current density, are relatively straightforward analogs of well understood existing solid-state micro- and nanoelectronic devices. Moreover, as is discussed in detail above, the design of molecular-scale electronic devices and logic based upon chemically modified or "functionalized" polyphenylene-based Tour wires follows a set of simple structural principles and heuristics.

For these reasons, in the subsequent sections of this paper we shall focus our attention on designing polyphenylene-based structures for building molecular electronic digital logic circuits. In a later paper, building upon this preliminary effort, we shall propose alternative structures for carbon nanotube-based molecular electronic digital logic [79].

With such objectives in mind, we take as our working hypothesis the premise that molecular electronic digital logic circuits can be designed in analogy to microelectronic circuitry using Tour wires as a conductive backbone. Associated with this hypothesis, classically observed and derived prin-

ciples such as Kirchoff's circuit laws and the independent function of discrete circuit elements are assumed to apply on the molecular scale.

In taking that approach to this first effort at molecular circuit design, we have thereby attempted to restrict the consideration of quantum effects to the device level and neglected such effects at the circuit level. At the next higher level of complexity, therefore, one might lift all such simplifying classical assumptions, applying quantum principles at both the circuit and the device level for the molecular electronic logic structures proposed below [94], [95]. For example, since the completion of this research, other investigators have published results that consider some of the likely impacts of quantum effects at the circuit level [96]–[100]. In order to make progress step-by-step, though, for the time being we have adopted a semiclassical approach that restricts the consideration of quantum effects to the switching devices.

Thus, we proceed from the hypothesis above to build in a simple logical manner upon the work of those who have used a polyphenylene-based backbone to make and to demonstrate individual molecular wires and individual molecular-scale electrical switching devices (primarily diode switches). Our approach also attempts to extend to the molecular domain circuit designs and principles of combinational logic well established in the microelectronic domain.

First, in Section IV, we shall propose and explore novel theoretical designs for a set of polyphenylene-based rectifying diodes. These new diode switching devices use the same operational principles as the Aviram and Ratner (A&R)-type molecular rectifiers just recently demonstrated [7], [9], but the ones proposed here should be easier to combine chemically with single molecular polyphenylene-based wires—Tour wires—in molecular-scale electrical circuits.

Second, in Section V, we posit plausible designs for molecular structures that take the next step: they connect via Tour wires first two, then three molecular diode switches to make the three elementary logic gates, AND, OR, and XOR (or NOT). Further, we shall propose a design that combines two of these logic gates to make a molecular electronic adder—i.e., a single molecule that will add two binary numbers.

Third, in Section VI, we consider the strengths and limitations of such diode-based molecular electronic digital circuit structures in the context of a number of architectural issues that must be considered and addressed in order to build a working molecular electronic computer using these or related designs. Finally, in Section VII, we conclude by considering how such small, diode-based molecular logic circuits and functions might be employed in extended circuitry integrated on the nanometer scale.

IV. POLYPHENYLENE-BASED MOLECULAR RECTIFYING DIODE SWITCHES: DESIGN AND THEORETICAL CHARACTERIZATION

In this section, designs are proposed for a set of polyphenylene-based rectifying diodes that use the same

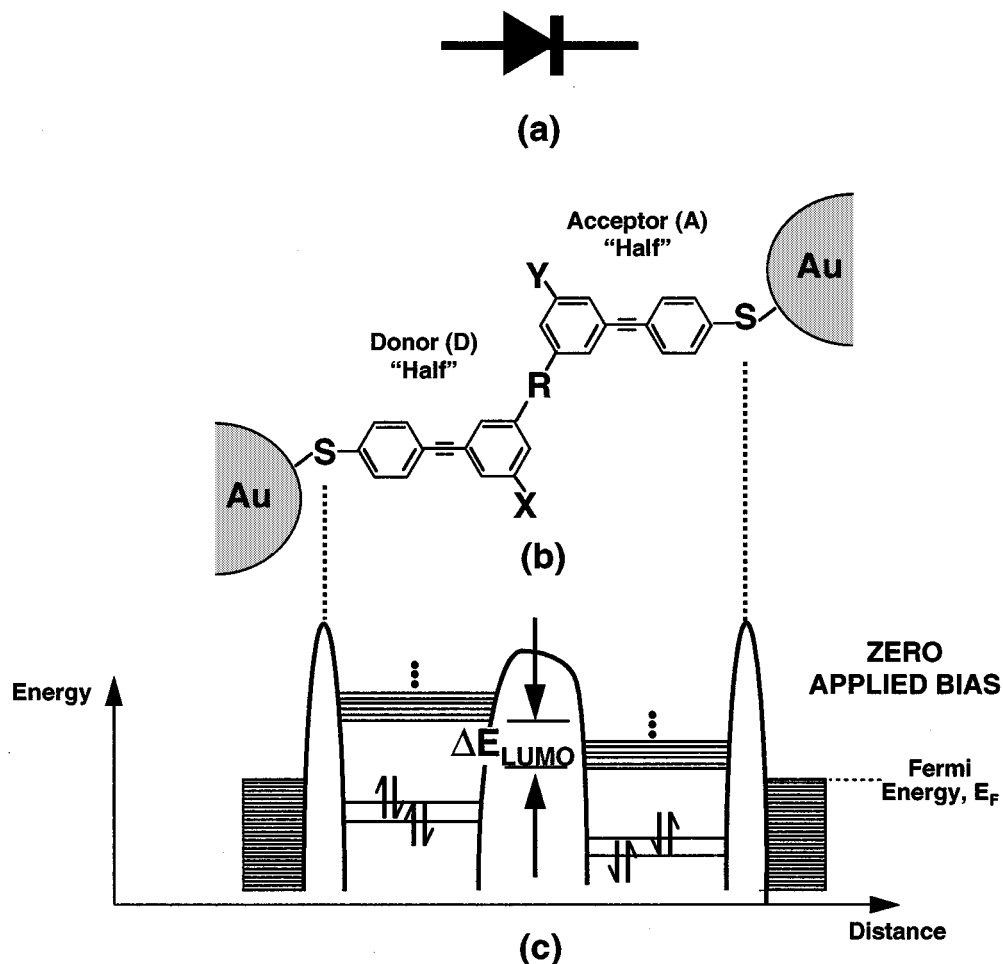


Fig. 8. Molecular structure and schematic of electron orbital energy levels for a proposed polyphenylene-based molecular rectifying diode switch.

operational principles as the A&R-type molecular rectifiers recently demonstrated [7], [9], but with structures that should be easier to combine chemically with single molecular polyphenylene-based wires to make molecular-scale electrical circuits. Specifically, rather than connect disaggregate switching molecules together with polyphenylene-based wires, we propose to make the molecular wires themselves into molecular electronic switches. This solves an important design problem, because it eliminates the need for incorporating other, much less conductive switching molecules into molecular circuits.

A. Proposed Polyphenylene-Based Designs for A&R-Type Rectifying Diodes

1) *Basic Structure:* Fig. 8 depicts schematically the molecular structure and the energy level structure of the authors' proposed variant of Aviram and Ratner's basic concept for a molecular rectifying diode. The unique feature of this variant is that it uses chemically doped polyphenylene-based molecular wires as the conductive backbone. In this paper, electron donating and electron withdrawing substituent groups chemically bound to a single molecule shall be termed "intramolecular dopants." This terminology

serves to emphasize the similarity in influence and function that these substituent groups have to dopant atoms which commonly are introduced as randomly distributed impurities in solid-state semiconductors in order to control their electrical properties. However, the modifier "intramolecular," which is applied in a manner consistent with its usage in other chemical contexts, also serves to distinguish the dopant substituents used here, which are precisely placed and bound in position on an individual molecule, from their analogs in solids.

Applying this terminology, the structure shown in Fig. 8 has two intramolecular dopant groups: the electron donating substituent group, X, and the electron withdrawing substituent group, Y. The first of these is an intramolecular analog of a n-type dopant in solid-state semiconductors and the second is an intramolecular analog of a p-type dopant. Additionally, the terminology "intramolecular" distinguishes the dopants employed in this paper from "extramolecular" dopants such as those applied in metal contacts to which otherwise undoped molecules are adsorbed. For example, in the work of Zhou *et al.* [7], a different type of molecular rectifier is produced via such extramolecular dopants.

In contrast, the characteristic general structure of an A&R-type monomolecular rectifying diode features an

electron donor subcomplex at one end (i.e., the donor “half” of the molecule) and an electron acceptor sub-complex at the other end (the acceptor “half”) [49]. The donor subcomplex consists of an electrically conductive molecular backbone with one or more electron donating intramolecular dopant substituents covalently bound to it. The acceptor subcomplex consists of a similar backbone with one or more electron withdrawing intramolecular dopant substituents covalently bound to it. These donor and acceptor subcomplexes are separated within the diode structure by a semi-insulating bridging group, to which they both are chemically bonded. Usually, this three-part “donor-acceptor complex” is envisioned or implemented as being in electrical contact with metal terminals at both ends.

Consistent with this concept, in Fig. 8(b) the polyphenylene-based A&R diode is shown to consist of an electron donor subcomplex (the Tour wire on the left containing the electron donating intramolecular dopant substituent X) that is separated by a semi-insulating group R from an electron acceptor sub-complex (the Tour wire on the right containing the electron withdrawing dopant substituent Y). Fig. 8(c) shows a schematic of the molecular orbital energy diagram associated with the polyphenylene-based A&R diode.

Observe that the insulating group R in the middle of the molecule is associated with a potential energy barrier. This group serves as an insulating bridge or barrier between the donor and acceptor “halves” of the diode. The barrier is intended to preserve the potential drop induced by the donor and acceptor substituents, X and Y, respectively, which serve in the role of chemically bonded intramolecular dopants. The barrier group prevents the differing electron densities in the substituted complexes on either side from coming to equilibrium, while it still permits added electrons under a voltage bias to tunnel through.

There are also barriers between the molecule and the gold (Au) contacts at either end due to the thiol linkages, as discussed above. These barriers serve to maintain a degree of electrical isolation between the different parts of the structure, sufficient to prevent the equilibration of the electron densities (and the associated one-electron energy levels) of the parts on either side. However, none of these barriers is so wide or high as to completely prevent electrons under a suitable voltage bias from tunneling through them.

The most likely candidates for R are aliphatic groups such as sigma-bonded methylene groups ($R = -CH_2-$) or dimethylene groups ($R = -CH_2CH_2-$). Their insulating properties are discussed above and have been demonstrated by Reed and Tour. For the polyphenylene-based rectifying diode designs used here, the aliphatic dimethylene group is selected as the central bridging group because it is the smallest nonconducting, aliphatic group that can serve as a narrow insulating tunnel barrier R, but still permit the aromatic rings on either side to be aligned easily in the same plane. Coplanarity of the donor-substituted and acceptor-substituted aromatic rings is desirable in order to enhance the extent of π -orbital conjugation between the rings and thereby increase the conductivity of the diodes in the preferred direction. The dimethy-

lene bridging barrier group also permits internal rotations wherein the donor- and acceptor-substituted benzene rings are moved to different planes but still remain parallel. This provides useful flexibility in circuit designs where it may be necessary for one molecular wire to cross over another without intersecting it. Further, as is shown below in Section IV-B, rotations of this sort do not necessarily change the energies of the key orbitals upon which the operation of a polyphenylene-based rectifying diode depends.

2) *Operational Principles for Polyphenylene-Based and Other A&R-Type Rectifying Diodes:* The principles of operation for these proposed polyphenylene-based, molecular rectifying diodes are similar to those of other A&R-type molecular rectifiers [49]. To understand, qualitatively, these principles of operation and how they dictate such a molecular structure, we must examine in detail the dependence of the molecule’s energy levels on its structure, and how the energy levels change when a voltage bias is applied across the molecule.

Fig. 8 shows the correspondence of the molecular structure to the molecular energy levels when there is no externally applied voltage bias. By contrast, Fig. 9 depicts schematically the operational principles of the polyphenylene-based molecular rectifier by showing how the energy levels change under an externally applied bias.

In Fig. 9 and in similar following figures, it is assumed and depicted implicitly that the voltage drop across a molecular diode is divided equally between its two “halves.” This may not be exactly true, but it is a useful simple approximation.

a) *Energy structure of the donor half of the polyphenylene-based molecular rectifier:* Observe in Fig. 8(c) that, to the left of the central barrier, on the side or half of the molecule associated with the electron donating dopant substituent group X, the valence energy levels are elevated in energy. This energy elevation affects all the molecular orbitals that are localized on the left-hand side of the molecule. This includes the highest occupied molecular orbital (HOMO), the lowest unoccupied molecular orbital (LUMO), and the associated low-energy unoccupied pi orbitals (collectively, the “LUMO’s”) on the left-hand, donor side of the molecule.

These effects are due to the influence of the electron donating substituent group X. Substituent groups with this characteristic behavior have been known for decades to organic chemists due to their effect on the stability of aromatic reactive intermediates [42], independent of any considerations having to do directly with molecular conductivity. The common electron donating substituents X are $-NH_2$, $-OH$, $-CH_3$, $-CH_2CH_3$, etc.

An electron donating group bonded to an aromatic ring tends to place more electron density upon the ring (or upon a group of neighboring conjugated aromatic rings). This increases the mutual repulsion among the electrons in the molecular orbitals associated with the (conjugated) ring structure. In the case of the conjugated ring structure to the left of the central barrier shown in Fig. 8(b), these additional repulsive interactions raise the total energy, as well as the component orbital energies, as suggested in Fig. 8(c).

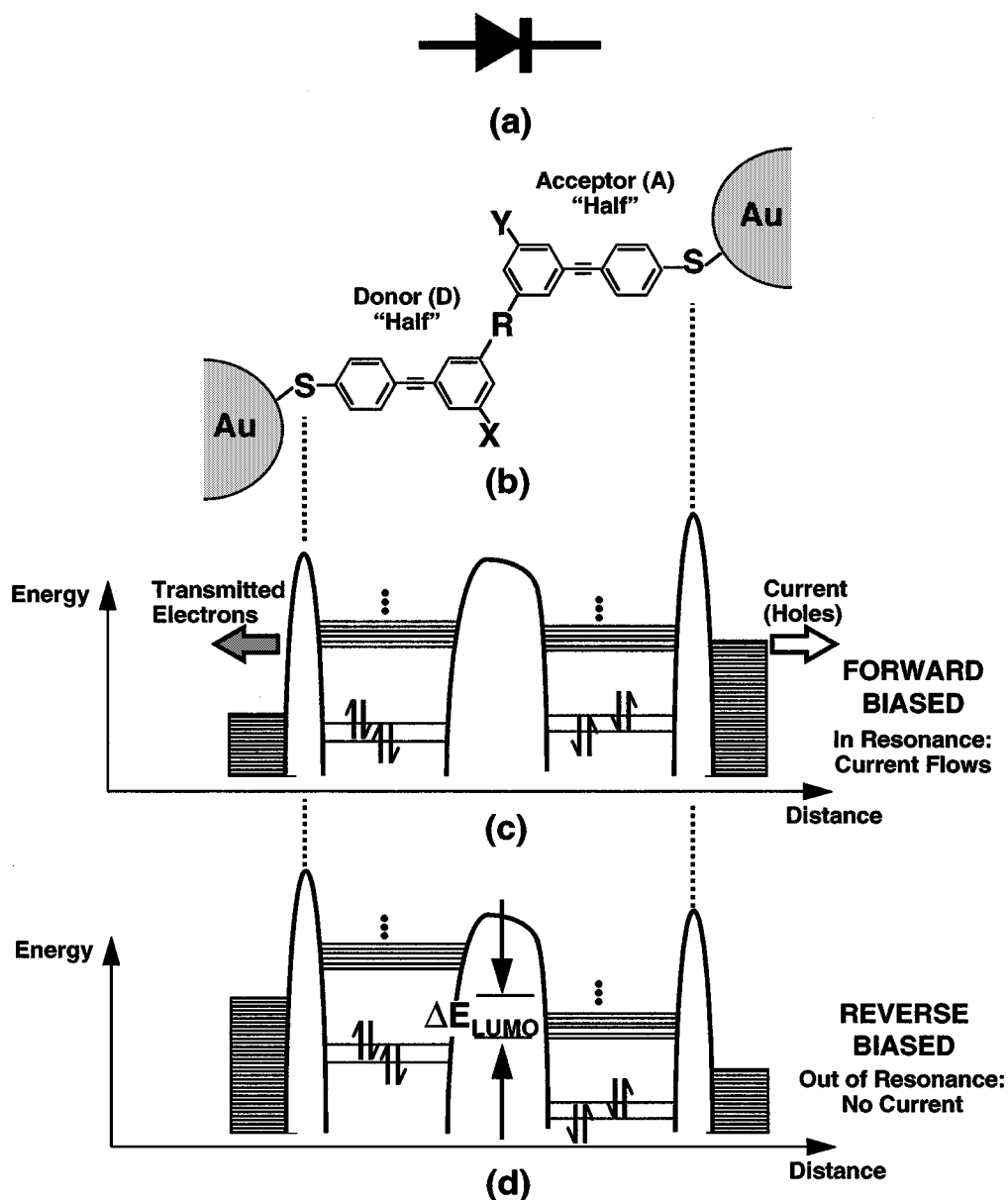


Fig. 9. Schematic describing operation of a proposed polyphenylene-based molecular rectifying diode switch under two opposite externally applied voltages.

b) Energy structure of the acceptor half of the polyphenylene-based molecular rectifier: Contrariwise, to the right of the central barrier, all the valence energy levels are lowered by the presence of an electron withdrawing dopant substituent group Y. This energy lowering affects all the molecular orbitals localized primarily on the right-hand side of the molecule. This includes the HOMO and the LUMO's that are localized on the right-hand side of the molecule.

As is the case for the donating group X discussed above, substituent groups with electron withdrawing characteristic behavior also have been well known for decades to organic chemists [42]. The common electron withdrawing substituents Y are $-\text{NO}_2$, $-\text{CN}$, $-\text{CHO}$, $-\text{COR}'$, etc., where R' is an aliphatic chain.

An electron withdrawing group bonded to a ring (or to several neighboring conjugated aromatic rings) tends to remove electron density from the ring, thereby reducing electron repulsion within the (conjugated) ring structure. These diminished repulsive interactions lower the total energy of the structure to the right of the central barrier, as well as its component orbital energies, as is shown in Fig. 8(c).

3) Forward-Bias Operation of the Polyphenylene-Based Molecular Rectifier: As shown in Fig. 8(c) and described above, even with no external applied bias, there is a dopant-induced difference in the relative energetic positions of the π -orbitals in the donor and acceptor halves of the molecule in Fig. 8(b). This energy-level difference is analyzed quantitatively in detail in Appendix I. Here, we observe simply that

the dopant-induced energy-level difference in the rectifying diode may be assessed in terms of the quantity

$$\Delta E_{\text{LUMO}} \equiv E_{\text{LUMO}}(\text{Donor}) - E_{\text{LUMO}}(\text{Acceptor}) \quad (1)$$

where $E_{\text{LUMO}}(\text{Donor})$ is the energy of the lowest unoccupied orbital localized on the donor side of the central barrier and $E_{\text{LUMO}}(\text{Acceptor})$ is the energy of the lowest unoccupied orbital localized on the acceptor side. Under most circumstances, the latter should be expected to be the LUMO for the entire molecule, as well. The energy difference ΔE_{LUMO} is depicted in Fig. 8(c).

This dopant-induced difference in the energy levels localized, respectively, on the donor and the acceptor portions of the molecule provides the foundation for the operation of the polyphenylene-based A&R-type molecular rectifying diode. This operation is illustrated schematically in Fig. 9.

Imagine first that a “forward” voltage bias is being placed upon the system in Fig. 9(b), as depicted in Fig. 9(c), with the higher voltage on the left-hand gold contact and the lower voltage on the right-hand contact. As shown, the process of applying the field shifts the electrons on the right-hand contact to higher energies and the electrons on the left-hand contact to lower energies, since the energy change for the electrons is of the opposite sign from the applied voltage. The energy differential induces the electrons in the occupied quantum levels of the high-energy right-hand contact to attempt to flow from right to left through the molecule to reach the lower energy left-hand contact.

Note that the very densely spaced occupied quantum levels in the valence band of each contact are represented by the closely spaced horizontal lines at the far left and far right of Figs. 8(c) and 9(c). The highest of these occupied levels, the Fermi level, in the metal contact has an energy known as the Fermi energy (E_F). Above this energy, there is also a very dense band of unoccupied energy levels which are not depicted in the figure. Applying a bias voltage tends to raise the Fermi level in the low voltage contact and lower the Fermi level in the other one.

For this right-to-left flow of electrons to occur under forward bias, the voltage bias must be sufficient to raise the Fermi energy of the electrons in the occupied levels of the external gold contact on the right at least as high as the energy of the LUMO π -orbital in the right-hand acceptor portion of the molecule. Then, the electrons can tunnel from the right contact into the empty LUMO's for the acceptor.

The electrons that have migrated from the right-hand contact into the acceptor LUMO's can tunnel once again to the left through the central insulating barrier to the unoccupied manifold of molecular orbitals in the donor half of the complex (which above a certain threshold applied voltage are sufficiently lowered in energy so that one or more of them matches an orbital in the unoccupied manifold in the acceptor half to the left). From this point, resonant transmission into the left-hand contact is assured, because the unoccupied manifold of the metal is very dense. This situation is depicted in Fig. 9(c), where the transmitted electrons are

shown flowing from the right to the left and the positively charged current is shown flowing from the left to the right.

In summary of the forward-bias mechanism, due to the application of a high voltage applied on the left contact and low voltage on the right contact: 1) the Fermi energy in the right contact exceeds the LUMO energy in the right-hand acceptor half of the molecule and 2) the LUMO's on the left-hand side of the molecule align with those on the right-hand side. This permits electrons to pass all the way through the molecule via resonant transmission.

Fortunately, in the forward bias case, only a relatively small voltage bias is required to raise the Fermi energy of the right-hand contact sufficiently to exceed the LUMO energy of the acceptor. This is because all the energy levels of the acceptor have been lowered beforehand by the presence of the intramolecular dopant group Y, as shown in Fig. 8(c). Also, in the forward bias case, it is very important that the applied potential tends to pull the higher energy unoccupied orbitals on the donor half of the diode down in energy toward the energies of the acceptor LUMO's, as illustrated in Fig. 9(c). This tendency of the forward bias to bring the donor LUMO's in coincidence with the acceptor LUMO's enhances electron tunneling from the acceptor to the donor through the central barrier of the molecule.

4) Reverse-Bias Operation of the Polyphenylene-Based Molecular Rectifier: In contrast, imagine now that a “reverse” voltage bias has been placed upon the system in Fig. 9(b), with the higher voltage on the right-hand gold contact and the lower voltage on the left-hand contact driving up the Fermi energy on the left and depressing it on the right.

In analogy to the forward bias case described above, for the electrons in the external left-hand contact to begin to flow from left to right through the molecule, the reverse voltage bias must be sufficient to raise the Fermi energy of the gold contact on the left so that it is at least as high as the energy of the LUMO π orbitals in the left-hand, donor portion of the molecule.

However, in the reverse bias case, the amount of voltage that must be applied is considerably greater than in the forward bias case in order to raise the Fermi energy of the contact sufficiently to exceed the LUMO energy of the adjoining portion of the molecule. This is because, as shown in Fig. 8(b), all the energy levels of the donor half have been raised by the presence of the substituent group X. Fig. 8(d) confirms that simply applying the same amount of voltage in the reverse direction as is used to induce a current in the forward direction is insufficient to allow electrons to tunnel from the left contact into the LUMO energy levels of the molecule.

Thus, more voltage must be applied in the reverse (right-to-left) direction than in the forward (left-to-right) direction in order to get electrons to flow through the molecule. This is the classic behavior of a rectifying diode, as represented by the schematic symbol shown in Fig. 9(a). Thus, this behavior and this symbol may be associated with the molecule.

Furthermore, the reverse bias tends to drive up the energy of the LUMO's on the donor portion of the molecule relative to the LUMO's on the acceptor to the right. As depicted in Fig. 9(d), this increases the separation of the lowest lying unoccupied orbitals on the two sides of the molecule to a value greater than the unbiased value ΔE_{LUMO} , rather than decreasing their energy separation. This makes it difficult at moderate bias voltages to bring the energy levels of the donor-half LUMO's in coincidence with the low-energy unoccupied manifold that is localized on the acceptor half to its right. Consequently, tunneling through the central barrier from left to right, from donor to acceptor, is impeded rather than enhanced by a reverse bias.

The discussion above suggests why it is highly likely that a doped polyphenylene-based wire of the general molecular structure shown in Figs. 8(b) and 9(b) should behave as an A&R-type molecular rectifying diode switch.

5) Additional Considerations—Nonresonant Electron Transport Under Reverse Bias: To ensure the effective performance of the doped polyphenylene molecular rectifiers discussed above, it is essential that charge transport under a forward bias be made as large as possible, while charge transport is kept as small as possible under reverse bias. Toward that latter goal, it is desirable to understand how current might flow in the reverse direction, in order to see how to prevent this. By considering analogies to the better known mechanisms that can permit charge to flow in larger, conventional solid-state diodes under a reverse bias, some qualitative insight may be gained into the possible ways that charge might flow under reverse bias in a molecular rectifying diode.

When solid-state p–n junction rectifying diodes are placed under a reverse bias, there is a small current, corresponding to a nearly constant baseline conductance, that occurs at all reverse voltages, even small ones. This reverse flow usually is several orders of magnitudes smaller than the large currents that flow when the rectifier is under a forward bias. The small reverse-bias “leakage current” arises due to a “drift” mechanism that is different from the diffusion of electrons that dominates the forward-bias electron flow [48].

Similarly, in molecular rectifiers, one can expect that there will be reverse leakage largely due to electron transport via “nonresonant” mechanisms. These are mechanisms different from the resonant transport that one desires to dominate electron flow in the forward direction—and to shut it off in the reverse direction. Nonresonant mechanisms can result, for example, from the coupling of the vibrational and electronic modes of the molecules (“vibronic” coupling). Vibronic coupling seems analogous, in certain ways, to the drift mechanism of solids. Other nonresonant transport mechanisms, such as electron hopping, also could contribute [20], [24], [25].

At sufficiently high reverse-bias voltages, above the “breakdown voltage,” very large currents will flow through solid-state p–n junction rectifiers. This breakdown corresponds to voltages so high that large numbers of electrons in the localized orbitals in the valence band of the n-doped solid on one side of the rectifier are given additional energy

greater than the central barrier (or “depletion region”) in the diode. In that case, electrons are ripped out of valence orbitals of atoms in the n-doped solid and injected in quantity into the delocalized orbitals of the conduction band on the p-doped side of the rectifier. This results in large currents in the reverse direction [48].

Likewise, in molecules, as is suggested by Fig. 8, a sufficiently large applied voltage bias in the reverse direction could raise the energies of electrons from the localized valence orbitals on the donor half of a rectifier so that they become greater than the maximum energy of the central barrier in the molecule. (This is the energy above which orbitals do not show characteristics that tend to localize the associated electron density primarily on one side of the barrier.) When valence π -electrons from the donor half of the molecule are promoted above this barrier energy, they may be injected into the unoccupied, delocalized conduction orbitals that lie above the energy barrier on the acceptor half of the molecular rectifier. Large currents should result. This would be the equivalent of breakdown for molecular rectifiers, and these devices must be operated at voltages below this threshold.

In view of the discussion above, qualitative design steps that seem likely to enhance the function of polyphenylene molecular rectifiers are those that would disfavor nonresonant transport in the reverse direction and/or raise the voltage at which reverse breakdown occurs. Disfavoring nonresonant transport requires, for example, ensuring that the structure of the diode is such that the vibrational modes of motion in the molecule are not excited by moderate voltages applied across the molecule in the reverse direction. This would reduce reverse transport by vibronic mechanisms.

The reverse breakdown voltage is raised by using central aliphatic insulating bridge structures and intramolecular dopants that tend to enhance localization of the π -type charge density on the opposite sides of this central insulator. This tends to keep high the central energy barrier shown in Fig. 8. One wishes to keep this energy barrier relatively high for valence electrons on the donor half of the molecule without severely impairing the flow of current under a forward bias. (Resonant tunneling transport through an energy barrier in the forward direction also is disfavored by a higher central barrier.)

This tendency toward charge localization on opposite sides of the central insulator in the molecular diode also should be assisted by using intramolecular dopant substituents that couple or bond particularly strongly with the π -orbitals of the aromatic rings and thereby make the value of ΔE_{LUMO} large. Requirements for this condition are explored in detail in the next section.

B. Results of Quantum Calculations for the Selection of Particular Polyphenylene-Based Rectifier Molecules

Detailed quantum mechanical calculations were performed [101] to characterize quantitatively the electrical properties of several molecular electronic rectifying diodes with a structure of the type shown in Figs. 8 and 9. In combination with the experimental conductivity demonstrations

for polyphenylene-based Tour wires, these calculations indicate that our proposed polyphenylene-based A&R diodes are likely to have the properties required to produce molecular rectification. The results of these calculations were used to select a particular polyphenylene-based molecule most likely to have strong rectifying properties.

First, in performing the calculations, the barrier group R in the middle of the structure was chosen to be a dimethylene group $-\text{CH}_2\text{CH}_2-$. As noted above, it is the shortest aliphatic insulating chain that would still permit the aromatic components on either side to occupy the same plane and, thereby, be able to maintain a relatively high conductivity through the molecule. One might expect, though, that the dimethylene group would reduce the conductivity of the wire by approximately the same factor of approximately 10^5 as do the two methylene groups in the molecular RTD (see Table 1 and Section II-A2 for details).

Second, the quantum calculations were used to determine the donor substituent group(s) X and the acceptor substituent group(s) Y that would yield a molecule with a relatively large intrinsic energy drop ΔE_{LUMO} across the barrier. Candidate molecules were considered that were doubly substituted in X and in Y, as well as molecules that only were singly substituted in those groups, as shown in Figs. 8 and 9.

The geometry of each such molecular diode structure was optimized, subject to certain constraints, via an energy minimization procedure prior to the use of the structure for the quantum calculation of the properties pertinent to its function as a diode switch. Except for the aforementioned constraints, the optimal geometries of the diode molecules usually would have been nonplanar. The geometry constraints we used forced the planes of the two aromatic benzene rings in the diode to be at least parallel, and in some cases forced the two rings into the same plane. This was done because, as will be seen below, it is envisioned that these diode rectifier molecules will be embedded in a larger molecular circuit structure, and that larger structure or its supporting medium would enforce or nearly enforce geometry constraints of the type just described.

Other details of the calculations are presented in Appendix I near the end of this article. The primary conclusion of the calculations is the choice of the dimethoxy-dicyano substituted polyphenylene-based rectifying diode, the structure for which is shown in Fig. 10. As indicated by the computational results for this structure, which appear in Table 2, the molecule has an intrinsic voltage drop from donor to acceptor of $\Delta E_{\text{LUMO}} = 1.98$ eV. This was nearly the largest value of ΔE_{LUMO} calculated for the various diode structures considered here, and, as indicated in Table 2, this value was particularly stable with respect to out-of-plane deformations of the molecule.

For example, the results in the second column of Table 2 correspond to an out-of-plane deformation in the molecule in Fig. 10 that places the dimethylene bridge that connects the aromatic rings at a full 90° angle out of the parallel planes of the two aromatic rings. This deformation results in an interplane separation of fully 1.46 \AA (or 0.146 nm). Nonetheless, as shown in Table 2, the key orbital energies associated

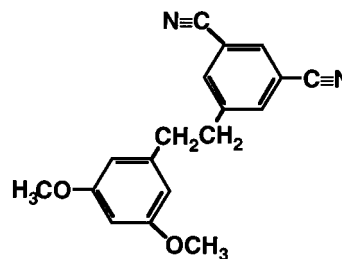


Fig. 10. Structure of proposed dimethoxy-dicyano polyphenylene-based rectifying diode for use in the design of molecular electronic diode–diode logic circuits.

with this nonplanar molecular conformation are very close to those tabulated in the first column of the table for the planar conformation.

Additional computational results, displayed in Table 3, showed that a dimethyl-dicyano substituted polyphenylene-based rectifying diode, the structure shown in Fig. 11, would be likely to have rectification properties comparable to that for the dimethoxy-dicyano molecule in Fig. 10. The calculations indicate that either molecule might serve as an effective rectifier, but it is the diode molecule in Fig. 10 that will be used to build the molecular circuits depicted in subsequent sections of this work.

V. NOVEL DESIGNS FOR DIODE-BASED MOLECULAR ELECTRONIC DIGITAL CIRCUITS

A. Novel Diode-Based Molecular Electronic Logic Gates

Based upon the foregoing development, in this section the authors propose what they believe to be among the first designs for nanometer-scale logic gates and among the first designs for nanometer-scale arithmetic functions based upon the conduction of electrical current through a single molecule.

Tour, Kozaki, and Seminario (TKS) [51] recently have proposed molecular-scale logic gates based upon a mechanism that involves perturbing the equilibrium electric charge distribution to change the electrostatic potential of a molecule. However, that work specifically and deliberately avoids employing nonequilibrium currents moving through a molecule under the influence of a strong externally imposed field or voltage. Therefore, the Tour group proposes logic structures significantly different than those proposed and discussed here.

Because of its reliance on the equilibrium (or near-equilibrium) charge distribution for computation rather than nonequilibrium electrical currents, the molecular-scale logic in the TKS proposal is more closely analogous to the micron-scale implementations [102]–[104] of the quantum cellular automata approach to computing suggested by Lent and Porod [18], [105] than it is to micron-scale conductive logic circuitry. The present work, on the other hand, is and is intended to be the molecular-scale analog of micron-scale conductive circuitry, with the exception that the circuits proposed in this paper explicitly take advantage of quantum effects, like tunneling, that would impair the operation of micron-scale circuits.

Table 2

Results of HF STO 3-21G Molecular Orbital Calculations to Determine ΔE_{LUMO} Between Donor and Acceptor Halves of the Dimethoxy-Dicyano Polyphenylene-Based Molecular Rectifying Diode Shown in Fig. 10

Results of Hartree-Fock 3-21G Molecular Orbital Calculations to Determine ΔE_{LUMO} for Dimethoxy-Dicyano Polyphenylene-Based Molecular Rectifying Diode				
	Two Di-Substituted Benzene Rings are <i>Co-Planar</i>		Two Di-Substituted Benzene Rings are <i>Non-Planar</i> , but Parallel	
Molecular Orbital	Orbital Energy	Localization D A	Orbital Energy	Localization D A
HOMO	-9.23 eV	X	-9.24 eV	X
LUMO	1.52	X	1.50	X
LUMO+1	2.17 ΔE_{LUMO}	X	2.12 ΔE_{LUMO}	X
LUMO+2	3.49	X	3.49	X
LUMO+3	3.69	X	3.67	X
ΔE_{LUMO}	1.97 eV		1.99 eV	
$\Delta E_{\text{LUMO}}(R=\infty)$	2.28 eV		2.28 eV	

Table 3

Results of HF STO 3-21G Molecular Orbital Calculations to Determine ΔE_{LUMO} Between Donor and Acceptor Halves of Dimethyl-Dicyano Polyphenylene-Based Molecular Rectifying Diode Shown in Fig. 11

Results of Hartree-Fock 3-21G Molecular Orbital Calculations to Determine ΔE_{LUMO} for Dimethyl-Dicyano Polyphenylene-Based Molecular Rectifying Diode				
	Two Di-Substituted Benzene Rings are <i>Co-Planar</i>		Two Di-Substituted Benzene Rings are <i>Non-Planar</i> , but Parallel	
Molecular Orbital	Orbital Energy	Localization D A	Orbital Energy	Localization D A
HOMO	-9.11 eV	X	-8.99 eV	X
LUMO	1.74	X	1.59	X
LUMO+1	2.36 ΔE_{LUMO}	X	2.22 ΔE_{LUMO}	X
LUMO+2	3.79	X	3.74	X
LUMO+3	3.945	X	3.80	X
ΔE_{LUMO}	2.05 eV		2.15 eV	
$\Delta E_{\text{LUMO}}(R=\infty)$	2.59 eV		2.59 eV	

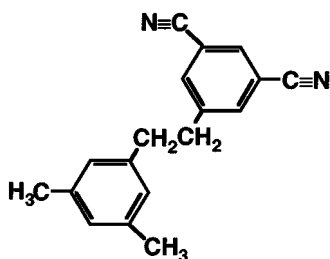


Fig. 11. Structure of proposed dimethyl-dicyano polyphenylene-based molecular rectifying diode for use in the design of molecular electronic diode-diode logic circuits.

As explained in the preceding sections, various conducting molecular-scale circuit components—wires and diode switches—have been demonstrated and/or simulated to function in a manner somewhat analogous to well-known solid-state electrical components. This suggests that assembling the molecular components in a circuit according to a schematic that normally is applied to a solid-state circuit would yield a molecular circuit that performs in a manner somewhat analogous to the corresponding solid-state, micron-scale digital logic circuits.

Thus, molecular diodes and molecular wires are used below in this way to design a functionally complete set of logic devices. This includes AND gates, OR gates, and XOR gates (or NOT gates) from which any more complex binary digital function may be designed and constructed, at least in principle. (To understand why an XOR gate is useful in making a complete set of logic gates, note that an XOR gate is readily adapted to produce a NOT gate, as is explained below.)

1) Molecular AND and OR Gates Using Diode-Diode Logic: Circuits for AND and OR digital logic gates based upon diodes, so-called “diode-diode” logic structures, have been known for decades. Schematic diagrams for these two circuits are shown, respectively, in Figs. 12(a) and 13(a) [106], [107]. The operation of these logic circuits is explained in Appendix II-A and B.

Part (b) of each of these figures shows a structure for a corresponding novel molecular implementation of each of these logic gates. It is noteworthy that these molecular logic gates each would measure only about 3 nm × 4 nm, which is approximately one million times smaller in area than the corresponding logic element fabricated on a semiconductor

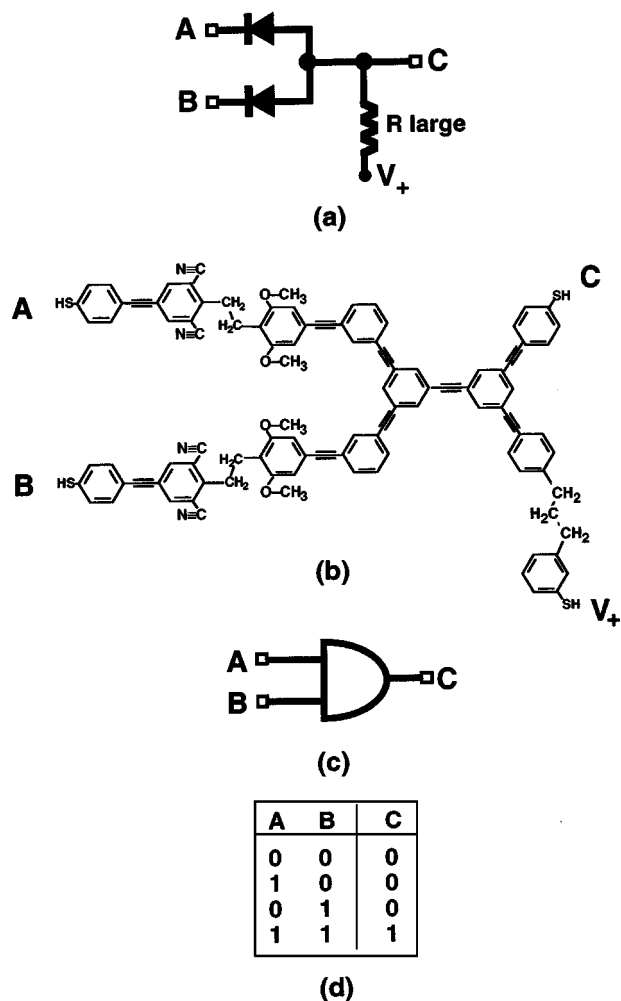


Fig. 12. Diode–diode-type molecular electronic AND gate incorporating polyphenylene-based molecular rectifying diodes embedded in Tour wires.

chip using transistor-based circuits. (See Appendix III for a detailed size comparison.)

In the molecular implementations of both logic gates, the doped polyphenylene-based rectifying diode structures proposed above and depicted schematically in Fig. 10 are connected together via conductive polyphenylene-based Tour wires, respecting the geometric constraints imposed by the chemical bonding behavior of organic molecules. Insulating aliphatic chains, as described in connection with Fig. 1(e), are used for the purely resistive elements of the circuit. In particular, the three-methylene chains at the lower right of the molecular structure diagrams for both the AND gate and the OR gate correspond to the large resistances R specified in the schematics immediately above them in Figs. 12 and 13, respectively. As is explained further in Appendix II, these large resistances serve to reduce power dissipation and to maintain a distinct output voltage signal at C when the inputs at A and B cause the diodes in either logic gate to be forward biased so that a current flows through them.

The primary structural difference between the AND gate in Fig. 12(b) and the OR gate in Fig. 13(b) is that the orientation

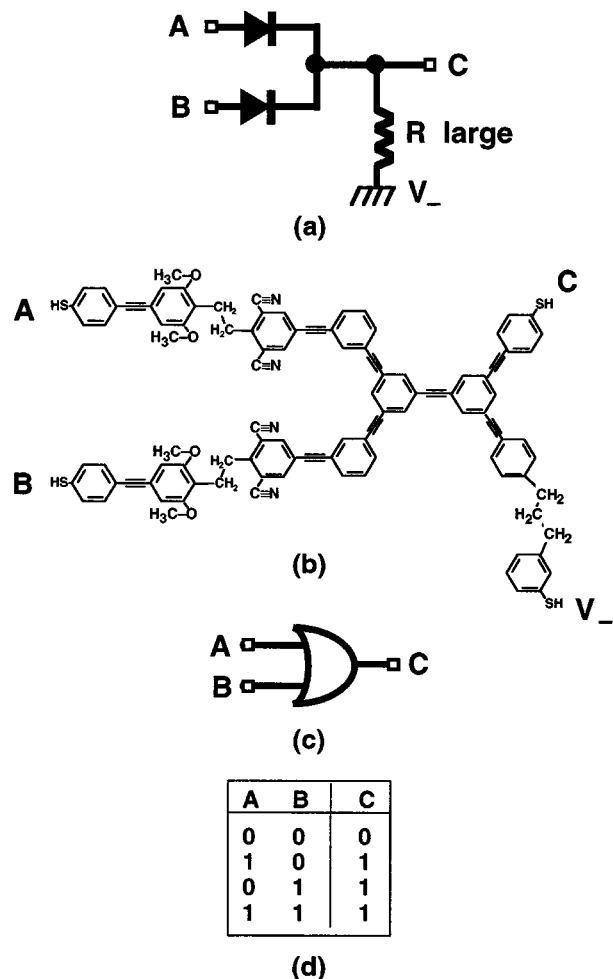


Fig. 13. Diode–diode-type molecular electronic OR gate incorporating polyphenylene-based molecular rectifying diodes embedded in Tour wires.

of the molecular diodes is reversed. Figs. 12(d) and 13(d) show the truth tables of the inputs and outputs for each gate.

Similar diode–diode logic gates might be built from molecules like that shown in Fig. 4(a), which recently were demonstrated by Metzger as having the properties of rectifying diodes. Metzger's experiment was conducted using a Langmuir–Blodgett film of such molecules, as sketched in part (b) of the same figure. Metzger *et al.* are attempting to demonstrate an AND gate and an OR gate based upon the present authors' suggestion of diode–diode logic [108], as shown schematically in Figs. 12(a) and 13(a) [106], [107].

2) *Molecular XOR Gate Using Molecular RTD's and Molecular Rectifying Diodes:* AND gates and OR gates alone are not sufficient to permit the design of more complex digital functions. A NOT gate is required to complete the diode-based family of logic gates. However, rectifying diodes alone are not sufficient to build a NOT gate [107]. To make a NOT gate with diodes, and thereby make it possible to build any higher function, we also must employ resonant tunneling diodes in the logic circuits.

a) *Structure for the Molecular XOR Gate:* A schematic diagram for an diode-based XOR gate is shown in Fig. 14(a).

This circuit schematic is due to Mathews and Sollner of the Massachusetts Institute of Technology (MIT) Lincoln Laboratory, who employed it for the purpose of developing diode-based solid-state logic circuits [109]. In the circuit schematic, the device symbol that resembles an “N” or a “Z” lying on its side represents an RTD.

Our proposed molecular implementation of this diode-based XOR circuit is shown in Fig. 14(b). The structure, which would have dimensions of approximately 5 nm × 5 nm, is built using one of the Reed–Tour molecular RTD’s and two of the polyphenylene-based molecular rectifying diodes proposed above. All three of these switching devices are built utilizing a backbone of polyphenylene-based Tour wires. The molecular circuit for the XOR gate is similar to that for the OR gate shown in Fig. 13(b), except for the insertion of the molecular RTD.

This extra inserted element makes the output from the XOR gate different from the OR gate in the case that both inputs are binary 1’s. The truth table for the XOR circuit is shown in Fig. 14(c).

b) Overview of the Operation of the Molecular XOR Gate: Stated simply, the diode-based XOR gate operates like the diode-based OR gate except in the case that both of the XOR gate’s inputs A and B are “1”—i.e., high voltages at both inputs. Those inputs put the operating point of the RTD into the valley region of the I – V curve shown schematically in Fig. 7(b). This shuts off the current flowing through the RTD and makes the voltage low or 0 at the output C of the XOR gate. The detailed principles of operation for the XOR gate are explained in Appendix II-C of this paper.

The addition of the molecular XOR gate to the set including the molecular AND and OR gates produces a functionally complete set, which can be made logically equivalent to the complete set AND, OR, and NOT. This is because an XOR gate can be adapted readily to produce a NOT gate simply by fixing one of the input terminals of the XOR gate to binary 1, as may be seen from the truth table in Fig. 14(c). However, an XOR gate is better than just a simple NOT gate, because the XOR makes it possible to construct some higher functions in a particularly simple manner, as is shown below.

B. Molecular Electronic Half Adder

Given the complete set of molecular logic gates introduced above and displayed in Figs. 12–14, the well-established principles of combinational logic [110] suggest designs that bond together several molecular logic gates to make larger molecular structures that implement still higher binary digital functions. For example, by combining the structures for the molecular AND gate and the molecular XOR gate given in Figs. 12 and 14, respectively, one may build a structure for a molecular electronic half adder, as shown in Fig. 15.

The well-known combinational logic circuit for a binary half adder is shown in Fig. 15(a) [110]. The novel design for the molecular structure corresponding to that combinational logic diagram is displayed in Fig. 15(c). It arises from the substitution of the molecular structures proposed above for the component AND and XOR gates, the use of a framework of Tour wires, and an accounting for the geometry and steric

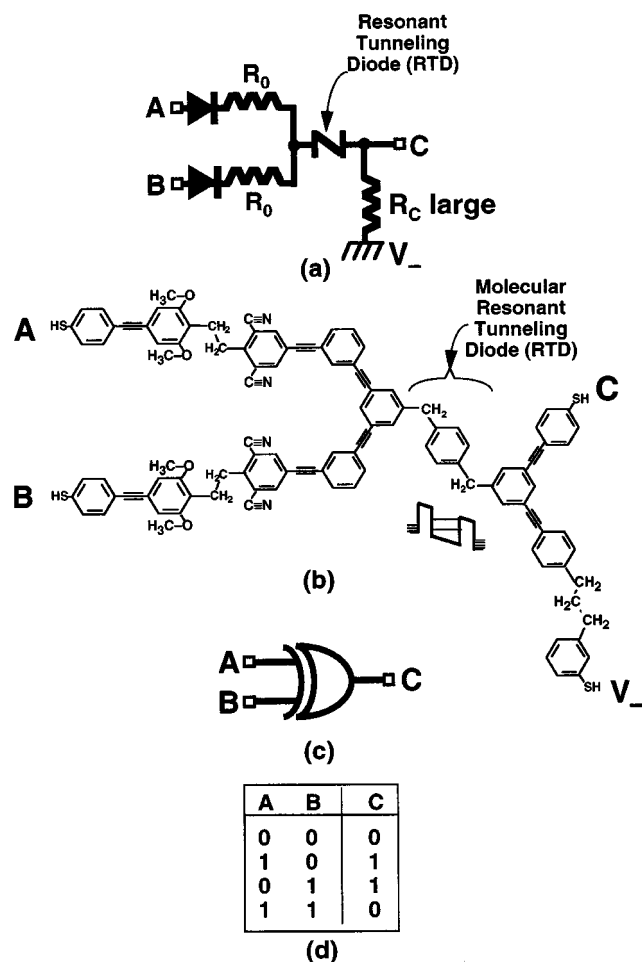


Fig. 14. Diode-based molecular electronic XOR gate incorporating molecular rectifying diodes and a molecular resonant tunneling diode.

constraints imposed by the bonding and shapes of the organic molecules. The resulting structure should have dimensions of about 10 nm × 10 nm, and it should behave in accordance with the truth tables shown in Fig. 15(b). That is, the structure in Fig. 15(c) is a molecule that should add two binary numbers electronically when the currents and voltages representing the addends are passed through it.

In Fig. 15(c), A and B represent the 1-bit binary inputs to the adder, while S and C represent the 1-bit outputs, the sum and the carry bits, respectively. Currents introduced into the half adder structure via either of the input leads A or B on the left are divided to pass into both of the function’s component molecular logic gates.

As is suggested by Fig. 15(b), the logic operation performed by the XOR gate forms the sum of two bits and outputs it at lead S , with the “excluded” XOR operation on a 1 input to the adder at A and 1 input at B representing the arithmetic binary sum $1 + 1 = 0$. Simultaneously, the AND gate component of the half adder can form the carry bit from the same two input 1 bits, and it provides this result as an output at C .

The Tour-type molecular wire that constitutes the adder’s input lead B branches in the plane of the molecule immediately to the right of B to connect to the lower input lead of the

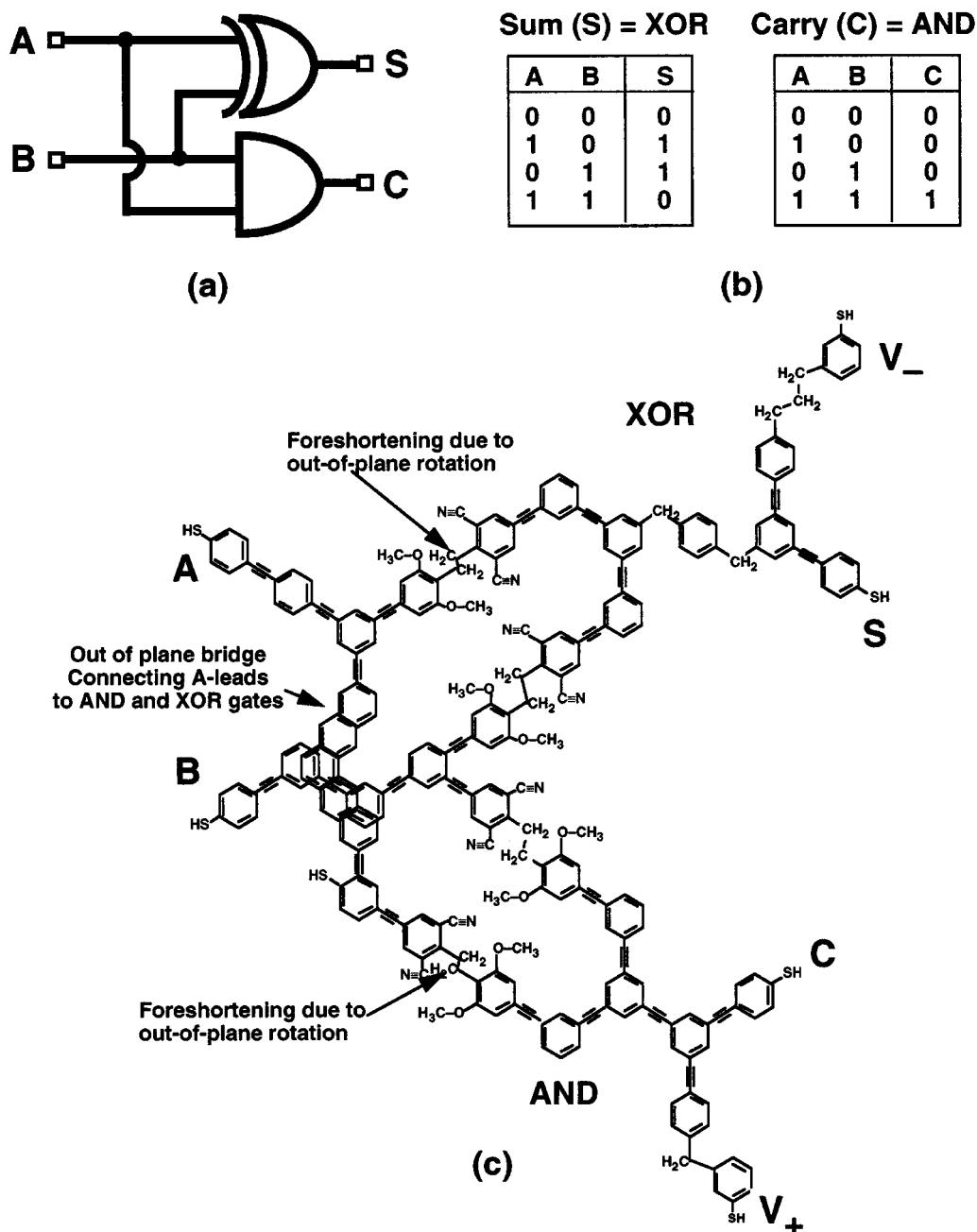


Fig. 15. Design for a molecular electronic half adder built from two diode-based molecular logic gates.

XOR gate and the upper input lead of the AND gate. The input signal current through lead *B* would be split accordingly between the two component gates, just as is suggested by the more schematic combinational logic diagram in Fig. 15(a).

The other input signal, which passes through the molecular half adder's lead *A*, similarly would be split between both the AND gate and the XOR gate. The Tour wire that begins on the left at *A* in Fig. 15(c) connects directly to the upper lead of the XOR gate in the plane of the molecule. However, the out-of-plane, linked-ring, arc-like aromatic molecular structure is then necessary to pass over the in-plane molecular wire for lead *B* and then connect lead *A* to the lower lead

of the AND gate. This out-of-plane molecular connector corresponds to the arc in the schematic in Fig. 15(a), which also is used to pass over input lead *B*.

Thus, the very small input through each molecular input lead is immediately split and therefore, halved. This should not be a major problem, though, for small diode-based molecular circuits, such as the half-adder. For one thing, the half-adder molecule also recombines the split signals at the right of the structure, so signal loss should not be overwhelming. Some amount of signal strength almost certainly would be dissipated, though, into the ground structure labeled V_- at the top right of

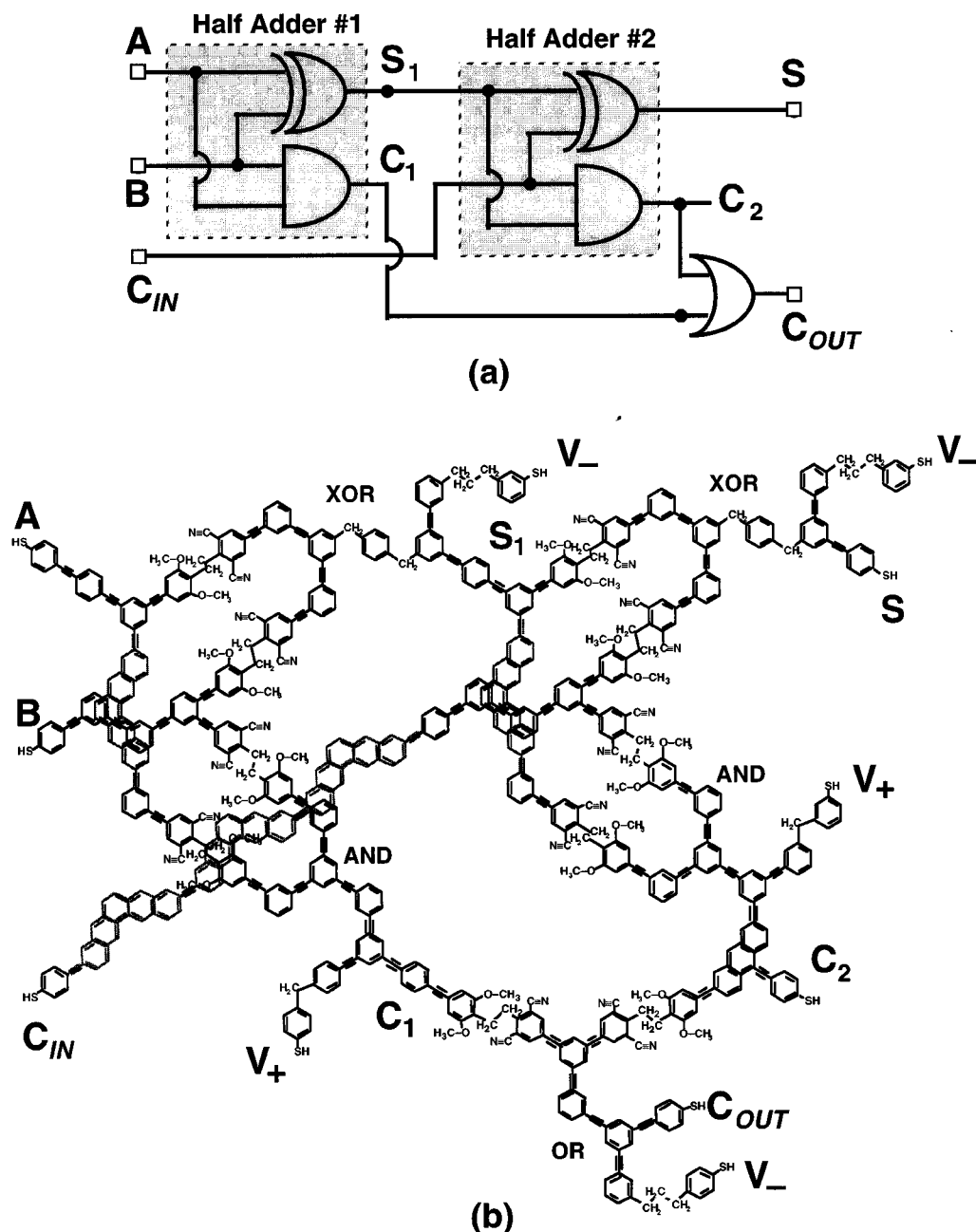


Fig. 16. Design for a molecular electronic full adder built from two diode-based molecular half adders and a diode-based molecular OR gate.

Fig. 15(c). The three-methylene aliphatic chain shown embedded in the output lead to the ground is intended to form a resistor that will make this dissipation small.

Still, in the absence of three-terminal molecular electronic devices (i.e., molecular transistors) to effect signal restoration, branched diode-based molecular electronic circuits probably will have to remain small in order to function with a satisfactory signal-to-noise ratio. This point is suggested by Fig. 16 and in the next section, where a larger molecular circuit structure, a molecular electronic full adder, is shown and discussed.

C. Molecular Electronic Full Adder

Extending the combinational design process begun above yields designs for molecular electronic structures that perform still higher functions. Combinational logic incorporating two half adders like that shown in the preceding section, plus an OR gate is sufficient to produce the molecular electronic full adder shown in Fig. 16. Fig. 16(a) shows the well-known combinational logic schematic for a full adder based upon two half adders [110], while Fig. 16(b) shows the novel design proposed here for the corresponding molecule based upon molecular electronic diodes. This full

adder molecule would have dimensions of approximately $25\text{ nm} \times 25\text{ nm}$.

The full adder circuit adds the carry bit C_{IN} from a previous addition to the one-bit sum S_1 of the addition of two new bits A and B . The three inputs C_{IN} , A , and B are shown at the left of Fig. 16(a) and (b). The results shown at the right of both figures are the 1-bit sum S , a carry bit C_2 associated with that sum, as well as a third bit C_{OUT} that is result of the logical OR operation used to combine carry bits C_1 and C_2 from each of the two half-additions.

To interpret in detail the function of the two diode-based molecular half adder circuits and the diode-based molecular OR gate when they are combined to make the full adder circuit, one needs to be conscious of the relatively high resistance of molecular diodes, even when they are forward biased or “on.” Otherwise, the explanation of the function of the full adder in Fig. 16(b) follows directly from the discussion in the preceding section of its major subcomponent, the half adder, although some patience is required to absorb all the details.

Even a glance, however, at the molecular structure proposed in Fig. 16(b) to perform this full addition reveals the rapid growth in the size and complexity of the molecular structure that is required just to perform relatively simple arithmetic on numbers that contain only a very few bits. The implications of this observation are discussed further below in Section VI-A5.

VI. DISCUSSION

The approach to conductive molecular electronic digital circuit design in this work makes use of and builds upon designs developed for and widely employed in familiar macroscopic and micron-scale electronic digital systems. Above, it also is illustrated how familiar, well-tested combinational principles might be employed to build up specific larger digital circuits from the smaller logic modules. Thus, an approach to larger scale computer architectures that employs such combinational principles is implicit in the explicit designs and molecular structures displayed and explained above in the small modular circuits for logic gates and functions.

It follows that this work raises a number of issues at both: a) the design level and b) the architectural level. Issues at both levels are considered separately below.

A. Further Design Challenges for Molecular Electronic Circuits

Several issues that complicate the design of monomolecular conductive logic circuitry are: 1) the problem of combining devices on the molecular scale without altering their individual electrical responses as a result of quantum mechanical effects and other close-range interactions; 2) the several different mechanisms that can produce conductance through the molecule; 3) the nonlinear I - V behavior of individual molecular devices; 4) the dissipation of electron energy into vibrational and other modes of motion in the molecule; 5) the difficulty of achieving gain in extended circuits; and 6) the limitations on the operating speed of a molec-

ular electronic computer. The discussion above of proposed logic circuits neglected these details in order to focus on the primary point of this paper: building elementary molecular electronic logic circuits may require simply assembling a few previously demonstrated individual devices. However, to implement the resultant designs proposed in this paper may require special attention to the specific issues enumerated above.

1) *Combining Individual Devices:* To simplify the initial design of molecular-scale logic functions, we have proposed that existing individual elementary devices—molecular switches and wires—might be bonded together to create circuits with more complex functionality, much in the same way as is done in conventional solid-state circuits. Solid-state circuit design exploits the fact that the electrical properties of individual devices do not change significantly when they are linked together in a complex circuit. Thus, the behavior of the whole macroscopic or micron-scale circuit is defined simply by the combination of the electrical properties of the isolated individual components used in the circuit.

Unlike bulk solid-state electronics, however, when small sections of molecular-scale wires and switches are combined into larger molecular circuits, these molecular components probably will not behave in circuits in the same way they do in isolation. Instead, strong coulombic effects at short range and quantum wave interference among the electrons in all the components will alter the characteristic properties of each device. The potential impact of such quantum effects was suggested above in Section III. Quantum wave interference manifests itself most obviously in the fact that the number of one-particle quantum levels in the combined molecular circuit is the sum of the number of levels from the two or more separate molecular devices. This change is likely to increase the relatively sparse density of states around the molecular Fermi level—especially in the low-lying conduction manifold of molecular orbitals. There is a similar summing of one-particle states when two solid-state circuit elements are combined, but the density of states is already so large relative to the number of electrons that the impact is not likely to be as noticeable as one might expect in a conductive molecular assembly.

However, the simple summation of the number of levels contributed by each device does not fully characterize the combined circuit either. When the energy levels from each device mix, the magnitude of the coupling between the levels will determine whether or not the electron density associated with particular orbitals remains localized primarily in one region of the entire molecule. Also, redistribution of the electron densities in the molecule can alter the Fermi level relative to the center of the HOMO–LUMO bandgap. This is somewhat analogous to the redistribution of electrons in p–n-doped semiconductor junctions.

Recently published theoretical work by Magoga and Joachim [96], [97] and by Yaliraki *et al.* [98], [99] emphasizes the possibility of strong influences upon the overall function of a molecular electronic circuit due to the mutual quantum interference of nearby devices. This is being explored elsewhere analytically by one of the present authors

[94]. In addition, modeling software presently is being developed to take account of quantum mechanical issues in order to predict the responses of entire molecular electronic circuits [95].

2) *Mechanisms of Conductance*: Electrons can flow through molecules by several possible mechanisms, as discussed in great detail by Ratner and others [21]–[27]. Different mechanisms with different current versus voltage responses may dominate in larger molecular structures than in smaller ones. More than one type of mechanism may be manifested in extended structures.

In the simplest monomolecular electronic systems, the electron transport mechanisms of interest are those governing the flow of electrons through a molecular wire attached at both ends to a metal electrode. Experiments to date suggest that transmission of electrons in polyphenylene-based molecular wires can occur via a resonance pathway—i.e., coherent transport through a small number of one-particle states aligned in energy [5], [6], [12]. For very short molecules between electrodes, the transport mechanism more readily observed is electron tunneling from one metal electrode to another modulated by the molecular orbitals available on the molecule.

This nonresonant “superexchange” mechanism has the advantage that dissipation is low, but the rate of transport falls off exponentially with distance as in standard tunneling [111]. Hence, the molecule does not behave like the familiar ohmic wire (i.e., one governed by Ohm’s Law). This is because the transported electrons reside primarily in the continuum orbitals of the two metal contacts. In superexchange, these orbitals do not mix directly (in first order of perturbation theory) with the orbitals of the molecule. The molecule only influences the electron transport indirectly (in second order). For conductance to occur by this mechanism, the Fermi level of the metal contact must fall between the energies of the HOMO and LUMO of the molecule [24], [25].

In the absence of resonant transport, conductance in extended molecular systems must be based on incoherent mechanisms, with the electrons hopping across the molecule along a chain of localized orbitals. This incoherent electron transport, which has been both predicted and observed, much improves the distance dependence of the conductance [20]. The resistance in an ohmic-type wire with incoherent transport increases only linearly as the wire gets longer, so that electron transport falls off only linearly with the inverse of the length. Further, in long, nonrigid molecules, inelastic electron scattering off the nuclear framework of the molecule can inhibit coherent transport. Such scattering could be a factor in long polyphenylene-based systems with inserted, flexible alkyl chain potential barriers. That would make it desirable to find ways to enhance the incoherent transport mechanisms.

In large polyphenylene-based molecular circuits, both mechanisms of conductance discussed above may be important. In the active regions of the circuit such as the diodes, experiments indicate that it should be possible to take advantage of coherent resonant transport. However,

between switching devices, molecular structures may have to be optimized to ensure that the electrons can move via incoherent transport.

3) *Nonlinear I – V Behavior*: In bulk solid-state electronics, the current-voltage (I – V) behavior of wires and resistors varies linearly according to Ohm’s Law, $V = IR$. As an initial approximation, this rule has been used in the design of the proposed circuits presented here. Actually, though, the I – V behavior of a molecular wire is observed and calculated to be nonlinear [27], [28]. Still, for small variations in the voltage, Ohm’s Law is likely to be a good approximation. The I – V behavior for molecular electronic circuits operating by incoherent transport ought to be nearly linear (ohmic). However, novel devices may also take advantage of the nonlinearity inherent to small molecules, allowing new architectures for computation that have no meaningful analogs in bulk-effect solid-state electronics.

4) *Energy Dissipation*: Energy dissipation will diminish the effectiveness of electron transport and signal transmission through a molecular structure. Also, dissipation results in heating that could have a particularly negative cumulative impact in an ultra-dense molecular electronic system with many closely spaced wires, switches, gates, and functions. As electrons move through a molecule, some of their energy can be transferred or dissipated to the motions of other electrons and to the motions of the nuclei in the molecule, such as the internal molecular vibrations and rotations. The amount of energy transferred is dependent on how strongly the electronic energy levels of the molecule couple (or interact) with the vibrational modes of the molecule. The molecular motion can, in turn, relax by dissipating energy or heat to the substrate or other surroundings.

The amount of energy dissipation in the structure is closely tied to the mechanism of conductance. For example, in the superexchange mechanism discussed above, where electrons are not directly coupled to the wire itself, the dissipation within the molecule should be small, since the electrons are not thought to interact strongly enough with the molecule to transfer much energy. In larger molecules where incoherent transport mechanisms dominate and the electrons are localized in orbitals on the molecule itself, dissipation of energy to the molecular framework should be significantly larger.

The loss of energy to the lattice vibrations and the surroundings decreases the signal strength and, in the extreme, could break bonds in the structure, destroying the device. Since it is likely that extended molecular circuits will utilize at least some incoherent transport mechanisms, it will be necessary to implement circuit designs with robust structures or a built-in means of transferring the molecular motion out of the circuit molecule itself.

5) *Necessity for Gain in Molecular Electronic Circuits*: Generation of the design for the molecular electronic full adder shown in Fig. 16(b) is a useful exercise revealing the size of molecular structures that will be required to perform useful computation. Such large molecular structures made from narrow wires and devices with relatively high resistances will likely require some form of power

gain to achieve signal restoration and to compensate for the dissipative losses in the signal.

In solid-state logic, it is possible to achieve power gain using only diodes. Rectifying diodes cannot achieve this. However, RTD's organized in a circuit known as a Goto pair may be used for this purpose [112]–[114]. This also might be an option for molecular-scale electronic circuits. If so, molecular diode switches like those described and employed in this work might be sufficient to build complex molecular electronic computer logic, without the absolute requirement for molecular transistors to permit operation of the extended circuitry. In the near term, this might have some particular practical advantages. Presently it is much easier to make electrical contact with two-terminal molecular switches than with molecular switches having three or more terminals.

In conventional, solid-state digital electronics it is more common, of course, to achieve power gain and signal restoration by employing three-terminal devices, i.e., transistors. This is because it is much easier to accomplish these goals with transistors. Transistorized solid-state circuits tend to be less sensitive and contain fewer switching devices than diode–diode circuits. This seems likely to be the case for molecular-scale electronic circuits, too.

Thus, it will be important to develop three-terminal molecular devices with power gain, i.e., a molecular electronic transistor. It will be important, also, to refine methods for making electrical contact with large numbers of densely spaced three-terminal molecular devices. Such advances would make it possible to achieve signal isolation, maintain a large signal-to-noise ratio and achieve fan-out in molecular circuits. In addition, solid-state logic gates based upon three-terminal devices usually can achieve much more reliable “latching” than can diode-based logic [115], [116].

Several groups of investigators have suggested how such molecular electronic transistors can be made with hybrid structures in which molecules are adsorbed to solids [64], [117], [118]. However, few, if any, of the molecular-scale switches proposed elsewhere involve purely molecular structures.

Building upon the principles and structures introduced in this paper, a subsequent paper will show molecular structures for a three-terminal molecular electronic amplifying switch, as well as designs for logic gates and functions based upon this molecular-scale three-terminal device [119]. Nonetheless, the authors anticipate that molecular diode switches—molecular two-terminal devices—and diode-based logic are likely to be important components of future densely-integrated molecular electronic digital circuits, demanding many fewer interconnects than three-terminal devices.

6) Potentially Slow Speeds: The speed at which operations can be performed by a molecular electronic circuit is closely related to the issue of energy dissipation in the system. Strong dissipative couplings could decrease the signal-to-noise ratio dramatically. Such reduction in signal strength would require a greater total charge flow to ensure the appropriate reading of a bit, thereby requiring more time.

Moreover, an examination of Table 1 shows that the currents measured in electrons per second that pass through each molecule, while amazingly large, nonetheless limit the speed of signal transmission to a range between approximately 10 kHz and 1 GHz. These upper limits assume that only one electron per bit is required to transmit a signal reliably. Obviously, if more than one electron were required per bit of signal, as would certainly be the case in the presence of dissipation and noise, the number of electrons per bit necessarily would rise, and the speed of the computer would decrease. If as many as 10 or 100 electrons were required to transmit a single bit, as is possible, molecular computer circuits like those described in this paper could be no faster than conventional microelectronic computers that presently operate in the several hundred megahertz range. From the current-based arguments alone, molecular electronic computers might even be much slower.

Also, it is likely that extended molecular circuits including internal molecular interconnections and external metal contacts will have a significant capacitance. The corresponding *RC* time constants for the components of the molecular circuit could be large and that would also slow the speed at which the system could be clocked.

On the other hand, the synthesis of a very small (micron-scale to millimeter-scale) and very dense ($\sim 10\,000$ devices/ μm^2) molecular electronic computer ought to be possible, in principle. Such machines might even be made three-dimensional to increase the density and to shorten interdevice communication delay. At that scale and density, such molecular electronic computers may not need to be very fast to be extremely useful.

The human brain is a massively parallel computer capable of performing 100 million MIPS (million instructions per second) [120], [121]. For comparison, a Pentium chip only performs at approximately 750 MIPS. Thus, it could require more than 100 000 Pentium chips wired in parallel in order to achieve the number of instructions per second carried out by the human brain. Many molecular electronic processors wired in parallel, each with only the computational power of a Pentium, would offer greater computational power per unit volume than is possible with the present state-of-the-art parallel processing. The area of a Pentium processor is approximately 1 cm^2 . Using the same scaling ratio estimated for the molecular half-adder in Appendix III (1 million times smaller in area or 1000 times smaller linearly), a molecular electronic equivalent of a Pentium would measure approximately $10\text{ }\mu\text{m} \times 10\text{ }\mu\text{m}$. Although each micron-scale molecular electronic processor might operate more slowly, in only a two-dimensional layout, 100 000 molecular electronic Pentium-equivalent circuits would require only one tenth of the space required by an existing Pentium. Very small and relatively slow, but powerful, distributed computing could be realized using molecular circuitry.

The design challenges discussed above will require serious consideration in implementing the logic structures proposed here or variants of them. Overcoming these challenges is likely to require further innovations.

Present architectural approaches for using small molecules to make electronic digital logic structures fall into two broad categories:

- 1) those that rely on small electrical currents to transfer and to process information;
- 2) those that rely on the deformation of the molecular electronic charge density to transfer and process information.

Examples of the latter category include both the TKS approach [51] discussed in Section V-A, as well as other possible molecular implementations of quantum cellular automata [18], [105]. The present work obviously falls in the former category that relies on electrical currents.

In either architectural approach, however, one must overcome a formidable array of architectural issues. Among the most important of these are the following.

- 1) Designing logic gates, functions, and extended circuitry using molecules.
- 2) Making reliable, uniform electrical contacts with molecules.
- 3) For current-based architectures: minimizing resistance in narrow molecular wires; for charge-based architectures: avoiding trapping in metastable states.
- 4) Interconnect issues: geometric and dynamic. As discussed above, the dynamic interconnect problem involves the slowdown of circuits due to high capacitances in tiny junctions, while the geometric problem involves the problem of laying out the many, many closely spaced junctions required for dense logic in a manner such that they do not conflict.
- 5) Assembly strategies for extended systems of smaller molecular logic units.
- 6) Fault tolerance: evolving strategies for mitigating effects of errors and structural imperfections.
- 7) Dissipation: reducing heating in extended ultra-dense circuitry or charge receptacles and also the cooling of such tiny systems.

In the preceding sections of this paper, only architectural issue 1) has been addressed in detail. However, the approach proposed here for designing diode-based electronic logic gates, functions, and extended circuitry using molecules also may assist in reducing the number of interconnects required, one of the problems specified in issue 4) above.

Elements of an approach to addressing issue number 5) are outlined below in Sections VII-B and VII-C. Investigators elsewhere also are working toward addressing at least issues 2), 5), and 6) for molecular-scale computer circuitry [43], [44], [122], [123]. In subsequent papers, the present authors and their collaborators will discuss strategies for addressing some of the other architectural issues listed above, systematically working toward the design and implementation of electronic digital computers integrated on the molecular scale.

VII. SUMMARY AND CONCLUSION

A. The Next Logical Step in Molecular Electronics

This paper outlines an architectural approach for building molecular electronic digital logic structures. Designs for a complete set of molecular electronic logic gates and molecular adders are given. These molecular electronic digital circuit designs only require simple arrangements of a few molecular electronic devices—switches and wires—variants of which already have been demonstrated individually by other investigators. Thus, it is likely that some of these molecular circuits can be fabricated and tested experimentally soon as the next logical step in the development of molecular electronics.

B. Environment and Interface for Molecular Electronic Circuits

In order to test and to operate such molecular circuits it will be necessary to provide an electrically benign environment for them, to support them structurally, and to make contact with them electrically. However, judging from the molecular electronics experiments to date, circuits based upon conductive polyphenylene and carbon nanotube molecules should not need to be held in a vacuum or cooled to cryogenic temperatures in order to operate. They should operate in open air at room temperature.

Generally speaking, though, it would be desirable to support the molecular circuits above a relatively nonconductive dielectric layer. This layer would be penetrated only by the conductive structures that will serve as their contacts, or else their conductive contacts also would lie upon and be supported by this layer.

Supporting molecular electronic systems on very thin, nonconductive layers would offer the obvious advantage that it would be likely to reduce the occurrence of electrical noise and errors in the system. In addition, this method of support might make it possible to stack the very thin layers of molecular circuitry to produce an ordered three-dimensional electronic computer processor or memory.

Several approaches to making contact with molecular circuits supported above a dielectric layer are suggested by previous experimental work with molecular-scale electronic devices, as discussed below.

1) *Grid of Metal Nanowires:* Williams, Kuekes, Heath, and their collaborators at Hewlett-Packard Corporation in Palo Alto, CA, and at the University of California, Los Angeles, have demonstrated a method for assembling closely spaced parallel lines of conductive metal wires, each of which is only approximately 1 nm wide [124]. They envision that these can be used to make a grid of addressable contacts for molecular devices by pressing together two layers of perpendicular nanowires, with an insulating molecular monolayer or pad at each of the points of intersection [125].

The different terminal ends of a molecular device or molecular circuit would be adsorbed via their molecular alligator clips (e.g., the -SH group) to different nanowires that bound each square cell in the grid. Since four nanowires bound each cell, which could be as small as only 5 nm

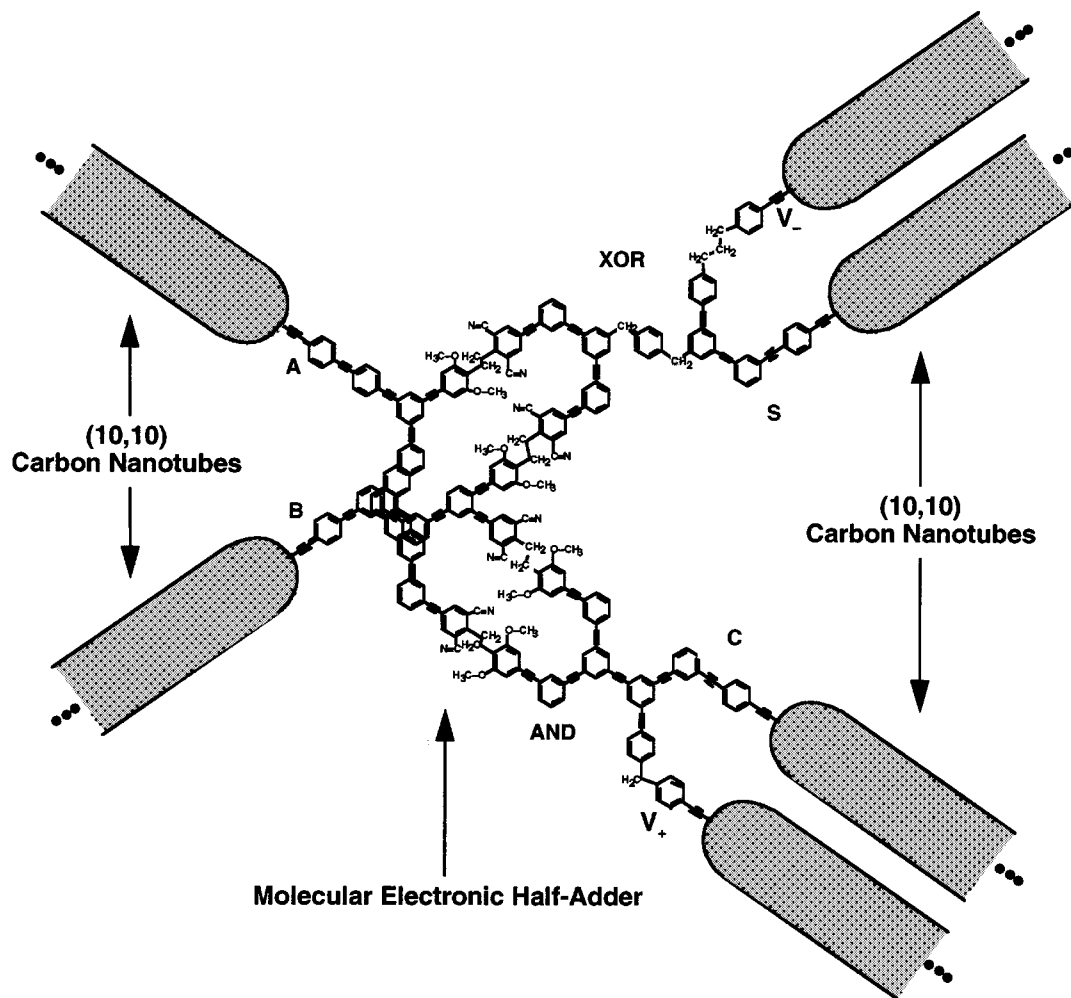


Fig. 17. Conceptual diagram of a molecular electronic circuit in which carbon nanotube molecules are employed to make electrical contact with and support a polyphenylene-based molecular electronic half adder.

across, a number molecular devices and circuits with up to four terminal ends might be supported, contacted electrically, and addressed in such an extended, grid-like, conductive nanostructure.

2) *Molecular Electronic "Breadboard"*: In this approach a regularly spaced array of nanofabricated or self-assembled, conductive metal "posts" would simultaneously make electrical contact with the molecular circuits and provide support for them. If the posts were made of gold, then the thiol molecular alligator clips (SH groups) on the terminal ends of the molecular circuit structures would bind to the posts. The posts might be self-assembled quantum dots or metal nanocrystallites. An interesting approach for using gold nanocrystallites to make an array of conductive posts has been pioneered by an interdisciplinary group at Purdue University [3].

In the Purdue work, the posts were tightly spaced over a conductive substrate, but refinements of the Purdue work might allow a less dense regular array of such structures to be self-assembled over the conductive nanopatterned substrate. The pattern on the substrate would allow the posts to be selectively addressed—turned on and off. A nonconduc-

tive molecular monolayer might be self-assembled over the exposed regions of the substrate between the posts. Finally, the molecular circuits could be "arranged" on top of the dielectric layer and connected to the conductive posts where they penetrated above the dielectric layer.

3) *Carbon Nanotubes*: While carbon nanotubes are not very reactive on their sidewalls, it is relatively easy to substitute other organic molecules on their open or closed ends. Thus, it might be possible to use these very conductive, nanometer-scale structures as wires and contacts to address the terminals of molecular electronic devices that are made out of smaller molecules. For example, one might use several carbon nanotubes arranged on an insulating substrate to address and to support a polyphenylene-based molecular electronic adder, of the type described above in Section V-B. A possible nanostructure of this type is sketched in Fig. 17.

Such a molecular circuit structure would have the advantage that it uses each type of molecule in a role for which it is most suited. Small, finely articulated structures are made out of aromatic organic molecules, which are more reactive than carbon nanotubes. Current is carried over long distances

by carbon nanotubes, which are more conductive than small, polyphenylene-based molecules.

In a similar spirit, if controlled sidewall substitution of nanotubes were to become easier and more routine, it might even be possible to affix small conductive molecules to a grid-like carbon nanotube contact structure analogous to the grid of metal nanowires envisioned above.

4) *Nanopore*: Nanopores, such as have been fabricated by Reed and his collaborators [7], also are an option for supporting and making contact with molecular electronic devices and circuits. In such a nanopore, the conductive contacts are at the top and the bottom of the pore, which means that the molecules are arranged vertically, rather than tiled horizontally on a substrate. This increases the potential packing density of molecular devices in a horizontal layer, but only two-terminal devices can be attached to and addressed by the two contacts of an individual nanopore.

It might be possible, though, to effect “hybrid” molecular-solid diode-diode logic circuits by building electrically connected ultradense circuits and systems of nanopores that contain molecular diode switches. Such circuitry might even be embedded on top of microelectronic devices in order to build, for example, a dense, low-power preprocessor or cache memory right on top of a microelectronic processor.

C. Circuits One Million Times Denser Than Microelectronics

As discussed in Section VI and immediately above, much remains to be learned about the mechanisms of conductance for small molecular wires, as well as about the means for manipulating, bonding, and ordering them in extended circuit-like structures [37]. However, when such molecular electronic digital logic circuits are fabricated and tested, they are likely to be on the order of one million times smaller in area than the corresponding conventional silicon semiconductor logic circuits. For example, the OR gate displayed in Fig. 13 is only about $3\text{ nm} \times 4\text{ nm}$ or, conservatively stated, it is on the order of 10 nm on a side. As detailed in Appendix III, this may be compared with the same type of logic gate made from micron-scale solid-state silicon semiconductor transistorized logic. A microelectronic OR gate occupies (approximately) a square on the order of $10\text{ }\mu\text{m}$ or $10\,000\text{ nm}$ on a side. The size advantages of the molecular electronic logic circuits laid out in the preceding section therefore are on the order of a factor of 1000 in linear dimensions and a factor of 1 000 000 in area. On that small scale, they constitute a lower limit on the miniaturization of conductive electronic logic. For this reason, at least, intensive study and experiments upon such logic designs are essential.

1) *Gate and Function-Level Integration to Produce Molecular-Scale Electronic Computers*: Using one of the interface strategies enumerated and discussed in Section VII-B, small monomolecular logic gates and functions like those described in Section V, Figs. 12–15, might someday be linked together to build complex extended molecular-scale electronic computer circuitry. This could be described as molecular gate-level and molecular function-level integration. Even working in only two dimensions,

given the small, approximately $10\text{ nm} \times 10\text{ nm}$ size of those molecular building blocks, it can be estimated that as many as 10 000 logic gates would fit in an area of only one square micron. Thus, molecular integration at this level might fit the circuitry for an entire computer in the area that now is occupied on a microchip by only one micron-scale, solid-state transistor.

2) *Device-Level Integration for More Rapid Prototyping of Molecular-Scale Electronic Logic*: Alternatively, with only a little sacrifice in size and density, one might use interface strategies like those discussed in Section VII-B to connect together several separate molecular diode switches in accordance with the diode-diode logic schematics shown above. This molecular device-level integration might afford a strategy for the more rapid fabrication and testing of prototype molecular diode-diode logic gates, without having to take on immediately the challenge of synthesizing them in their most compact and most densely integrated, monomolecular structure. Only two or three molecular diode switches need be connected together in this way to demonstrate a molecular-scale electronic logic gate. Thus, molecular electronic integration of this sort is just a small step further along a path that already is being traveled successfully by some experimentalists [14].

D. Future Prospects

The physical characteristics of the molecular electronic devices and logic structures considered in detail in this work suggest future applications and trends in advanced computer electronics as it evolves toward integration on the molecular scale.

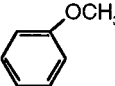
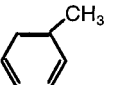

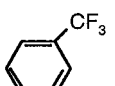
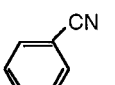
1) *Key Advantages and Key Applications for Proposed Molecular Electronic Logic*: Because of their extremely small size, molecular electronic digital logic structures, such as those suggested here, might permit a great increase in the density of digital electronics, well beyond the limits of conventional silicon-based circuitry. In that case, such ultrahigh-density molecular circuitry could be useful in increasing the power of conventionally sized computer chips, a few centimeters on a side. This could make available a whole new class of desktop supercomputers and open new vistas for computationally intensive applications.

However, ultrahigh-density molecular circuitry might have an even greater impact by making it possible to shrink dramatically the area and volume occupied by a computer with moderate computational power comparable to a conventional Intel Pentium chip or an even older, simpler microprocessor chip. A whole new domain of applications might be foreseen for such a Pentium on a pinhead. Such computers necessarily would draw less electrical power than conventional computers of comparable computational capability, and they would open the possibility of much smaller, lighter and smarter portable devices. They might even be used as controllers—“brains”—for microsensors and the millimeter-scale robots that are just now coming into development [126].

2) *Matter as Software*: The small molecular logic gates for which designs are proposed in this work, and other sim-

Table 4

HOMO and LUMO Energies Determined from Molecular Orbital Theory Calculations for Benzene and Benzene Rings Monosubstituted with Donor and Acceptor Substituent Groups

	Mono-substituted Benzene	Structure	Experimental Ionization Potential (IP)*	Results of SCF Molec Orb. Calc'ns**			
				STO 3-21G Basis		STO 6-31G Basis†	
				E _{HOMO}	E _{LUMO}	E _{HOMO}	E _{LUMO}
<div style="display: flex; align-items: center;"> <div style="writing-mode: vertical-rl; transform: rotate(180deg);">Increasing IP</div> <div style="margin-left: 10px;"> <div style="writing-mode: vertical-rl; transform: rotate(180deg);">Donor Substituents (X)</div> <div style="writing-mode: vertical-rl; transform: rotate(180deg);">Acceptor Substituents (Y)</div> </div> </div>	Methoxybenzene C ₆ H ₅ -OCH ₃		8.20 eV	-8.93 eV	3.86 eV	-8.75 eV	3.85 eV
	Methylbenzene C ₆ H ₅ -CH ₃		8.83 eV	-8.88 eV	4.15 eV	-8.69 eV	4.09 eV
	Benzene C ₆ H ₆		9.24 eV	-9.20 eV	4.02 eV	-8.98 eV	4.00 eV
	Trifluoromethylbenzene C ₆ H ₅ -CF ₃		9.69 eV	-9.98 eV	2.73 eV	-9.69 eV	2.87 eV
	Benzonitrile C ₆ H ₅ -CN		9.73 eV	-9.71 eV	2.33 eV	-9.58 eV	2.27 eV

* Source of experimental ionization potentials: NIST Chemistry Webbook [129] located on the Internet World Wide Web at: <http://webbook.nist.gov/chemistry/>.

** SCF molecular orbital calculations performed using the commercial MacSpartan Plus, version 1.1, quantum chemistry computer simulation program [101,128].

† For most properties, calculations using larger STO 6-31G Gaussian basis set would be anticipated to be more accurate than calculations using smaller STO 3-21G basis set.

ilar structures, embody the potential for a kind of molecular “macro” language. Each molecular logic gate might be bonded to a slightly larger, nonconductive, supportive molecular “handle” to permit the molecules to be manipulated and assembled quickly and easily, as needed, in any desired extended circuit structure or “program.” Entire complex programs still could be embodied in molecular-scale structures much smaller and just as flexible as any material structure in which conventional microcomputers store a single bit of information. Thus, matter—modular molecular logic structures—might become the basic nanoscopic elements of future software, eroding once and for all the technological and the economic distinctions between computer hardware and computer software [127].

APPENDIX I

AB INITIO QUANTUM CALCULATIONS OF RECTIFYING PROPERTIES FOR POLYPHENYLENE-BASED MOLECULAR RECTIFIERS

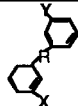
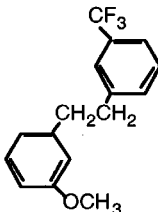
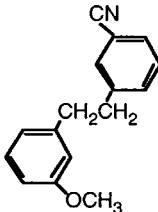
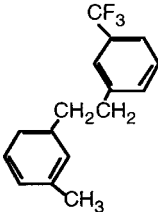
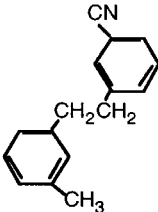
To characterize the likely electrical properties of the proposed polyphenylene-based molecular electronic rectifying diodes, we have conducted *ab initio* quantum mechanical molecular orbital calculations [101]. As described below, these calculations were integral to the selection of the most favorable polyphenylene-based structure to employ as a rectifying diode in molecular electronic digital circuits.

Rectifying diode behavior has not yet been demonstrated experimentally for molecules of the structure shown in Fig. 8(b). However, the likelihood that such a structure will function as a molecular rectifier is suggested by the rectifying diode behavior that was demonstrated using a monolayer of many Tour-type molecular wires adsorbed at either end to two different thin metal layers in the experiment conducted by Reed’s group at Yale University [7]. In addition, we have conducted molecular orbital calculations and assembled related experimental data for molecular structures of the type shown in Fig. 8(b). These calculations, as detailed below, suggest that these single molecules should have the electronic structure and the behavior characteristic of an A&R-type rectifying diode, as shown in Figs. 8(c), 9(c) and (d). In combination with the experimental conductivity demonstrations for polyphenylene-based Tour wires, these calculations indicate that our proposed polyphenylene-based A&R diodes are likely to have the properties required to produce molecular rectification.

Displayed in Tables 4–6 of this Appendix and in Tables 2 and 3 of the main text are the results of our theoretical calculations to estimate the electrical properties of the proposed polyphenylene-based A&R-type rectifying diodes. The calculations are premised on the notion that the energy gap ΔE_{LUMO} determines the static, asymmetric energy step along the length of an A&R-type rectifying diode switch of the general structure shown in Fig. 8(b). Consequently, the

Table 5

Orbital Energies and LUMO Energy Differences Calculated via 3-21 G SCF Molecular Orbital Theory [101], [128] for Archetypal Polyphenylene-Based Diodes Assembled from Singly Substituted Benzene Components Separated by an Insulating Dimethylene Group

Acceptor Substituents (Y)					
Donor Substituents (X)		Trifluoromethyl-Benzene C ₆ H ₅ -CF ₃ E _{LUMO} =7.15 eV		Benzonitrile C ₆ H ₅ -CN E _{LUMO} =6.40 eV	
	Methoxy-benzene C ₆ H ₅ -OCH ₃ E _{LUMO} =7.90 eV				
	Molecular Orbital	Orbital Energy	Localization D A	Orbital Energy	Localization D A
	HOMO	-8.59 eV	X	-8.98 eV	X
	LUMO	3.03		2.38	X
	LUMO+1	3.42		3.24	X
	LUMO+2	3.83	X	3.71	X
	LUMO+3	4.21	X	3.91	X
	ΔE _{LUMO}	0.80 eV		1.33 eV	
	ΔE _{LUMO} (R=∞)	0.75 eV		1.50 eV	
Donor Substituents (X)	Methyl-benzene C ₆ H ₅ -CH ₃ E _{LUMO} =8.73 eV				
	Molecular Orbital	Orbital Energy	Localization D A	Orbital Energy	Localization D A
	HOMO	-8.82 eV	X	-8.87 eV	X
	LUMO	3.02		2.42	X
	LUMO+1	3.42		3.31	X
	LUMO+2	3.83	X	3.79	X
	ΔE _{LUMO}	0.81 eV		1.37 eV	
	ΔE _{LUMO} (R=∞)	1.58 eV		2.33 eV	

energy gap ΔE_{LUMO} measures the general effectiveness of the molecule as an A&R diode. As depicted in Fig. 8, the quantity ΔE_{LUMO} is the difference in energy between the LUMO's localized separately on the aromatic donor and acceptor halves of the molecule. In Fig. 8(b), the aromatic donor and acceptor halves are located, respectively, on the left and right sides of the central aliphatic insulating barrier group R. (Such aliphatic barrier groups are discussed in Section I-A2.)

The calculations applied the *ab initio* Hartree-Fock self-consistent field (SCF) molecular orbital method [40], [41] as implemented in the MacSpartan Plus 1.1 commercial quantum chemistry simulation program [128]. In performing these calculations, we had assistance from D. Moore, our collaborator in the MITRE Nanosystems Group. The calculations proceeded in several stages, as described below.

A. Calculations Upon Isolated Benzene Rings Monosubstituted with Donor and Acceptor Substituents

First, as displayed in Table 4, we determined computationally the one-electron energies of the HOMO and the LUMO molecular orbitals for benzene and for benzene rings that had been singly substituted with the one of the two donor substituents $X = -OCH_3$, $-CH_3$ or with one of the two acceptor substituents $Y = -CF_3$, $-CN$. The molecular orbital energies were determined using the commonly applied STO 3-21G Gaussian atomic basis set and also in more time-consuming calculations with the larger STO 6-31G Gaussian atomic basis set. The second set of calculations with the larger basis set was used to assess whether the smaller basis set would be sufficient for an estimate of the LUMO energies which would be relatively insensitive to the choice of basis set. In this connection, we observed from the values listed in

Table 6
HOMO and LUMO Energies Determined from Molecular Orbital Theory Calculations for Benzene and Benzene Rings Disubstituted with Donor and Acceptor Substituent Groups

	Mono-substituted Benzene	Structure	Experimental Ionization Potential (IP)*	SCF MO Calc's**	
				STO 3-21G Basis	
Donor Substituents (X)	1,3-Dimethoxybenzene $C_6H_5(OCH_3)_2$		8.16 eV	E_{HOMO} -8.93 eV	E_{LUMO} 3.79 eV
	1,3-Dimethylbenzene $C_6H_5-(CH_3)_2$		8.55 eV	-8.66 eV	4.10 eV
	Benzene C_6H_6		9.24 eV	-9.20 eV	4.02 eV
Acceptor Substituents (Y)	1,3-Dicyanobenzene $C_6H_3-(CN)_2$		10.40 eV	-10.32 eV	1.51 eV

* Source of experimental ionization potentials: NIST Chemistry Webbook[129] located on the Internet World Wide Web at: <http://webbook.nist.gov/chemistry/>
** SCF molecular orbital calculations performed using the commercial MacSpartan Plus, version 1.1, quantum chemistry computer simulation program [101,128].

Table 4 that the calculations with the larger basis set yielded LUMO energies that were very nearly the same as those with the smaller STO 3-21G basis set.

In general, though, Hartree–Fock calculations, such as we have performed here, do not give an accurate estimate of the value of the LUMO energy for a single atom or molecule. Such calculations usually give values that are too high for the difference between the energies of the HOMO and LUMO orbitals. This is because Hartree–Fock calculations do not accurately reflect the relaxation energy associated with the other electrons due to an electron that is added to the neutral species in the LUMO orbital. However, we apply the Hartree–Fock method here as a simple way to determine the trend in the value of ΔE_{LUMO} , assuming a constant error in the relaxation energy across a sequence of calculations.

As also may be observed from Table 4, in applying Koopmans' Theorem [40], [41]

$$E_{HOMO} = -I \quad (2)$$

the smaller STO 3-21G basis set provided HOMO energies E_{HOMO} that generally agreed well with the experimental [129] molecular ionization potentials I . Thus, we determined that we could rely upon the smaller STO 3-21G basis set for the estimation of the HOMO and LUMO energies. We employ it for all subsequent calculations.

The calculated LUMO energies given in Table 4 for the electron-acceptor-substituted aromatic rings are lower than the LUMO energies for the donor substituted rings. This is expected from the notion that the electron-acceptor substituents ($Y = -CF_3, -CN$) should reduce the electron density on the ring slightly and thereby lower the positive energy contribution due to the repulsive interaction between electrons on the ring. On the contrary, electron-donor substituents

($X = -OCH_3, -CH_3$) should tend to raise the LUMO energies, as is observed for the methyl substituted benzene in Table 4, by enhancing the electron density on the ring slightly and thereby increasing the positive repulsive energies among the electrons on the ring.

To conclude the first part of the theoretical calculations, the STO 3-21G Hartree–Fock orbital energy estimates for E_{LUMO} in Table 4 were used to approximate crudely the relative magnitudes of the anticipated potential drops ΔE_{LUMO} across the polyphenylene-based diodes. This was done by taking the difference

$$\Delta E_{LUMO}(R = \infty) = E_{LUMO}(C_6H_5-X) - E_{LUMO}(C_6H_5-Y) \quad (3)$$

between $E_{LUMO}(C_6H_5-X)$ determined for an isolated benzene monosubstituted with donor substituent X and the LUMO energy $E_{LUMO}(C_6H_5-Y)$ for an isolated benzene monosubstituted with acceptor substituent Y.

These approximations $\Delta E_{LUMO}(R = \infty)$ are displayed in Table 5 for the four possible donor and acceptor pairs. The values of $\Delta E_{LUMO}(R = \infty)$ range from 0.75 to 2.33 electron volts (eV). Of these, the pairings of the methyl-substituted benzene donor molecules with acceptor molecules yielded the largest two values of $\Delta E_{LUMO}(R = \infty)$. Further, the cyano-substituted acceptor molecule (benzonitrile) produced a larger approximate potential drop than the trifluoromethyl-substituted acceptor molecule when each was paired with the methyl-substituted benzene donor.

In actuality, we would expect these LUMO energy differences or potential drops across the molecule all to be somewhat smaller than is estimated by the values of $\Delta E_{LUMO}(R = \infty)$, which yield an estimate based upon the isolated donor and acceptor components of the diode structure. Some equilibration of the electron density across the central insulating barrier, with a corresponding reduction in the chemical potential difference, should be expected when the aromatic donor and acceptor halves of the molecule each are bound chemically to the same central insulating group R. Also, if these diodes were embedded in molecular wires, the other large undoped molecular components would reduce ΔE_{LUMO} still further.

B. Calculations Upon Bonded Polyphenylene-Based Donor-Acceptor Complexes Built from Monosubstituted Aromatic Rings

To estimate more accurately the trend in the potential drops across the several proposed molecular rectifying diodes, in the second part of the theoretical analysis, STO 3-21G *ab initio* Hartree–Fock self-consistent field molecular orbital calculations were performed upon several chemically bonded polyphenylene-based donor–acceptor complexes. These four complexes, illustrated in Table 5, were built from pairs of the monosubstituted benzene rings shown in Table 4. A donor-benzene ring and an acceptor-benzene ring are chemically bonded to the opposite ends of an insulating central dimethylene barrier group (i.e., $R = -CH_2CH_2-$).

The results of the *ab initio* calculations upon the complete donor-acceptor complexes bonded to either side of the dimethylene bridge are displayed in Table 5. For each of the four molecules, values are given for the uppermost molecular orbital energy in the occupied manifold (i.e., E_{HOMO}) and for the lower several orbitals in the unoccupied orbital manifold (E_{LUMO} , $E_{\text{LUMO}+1}$, $E_{\text{LUMO}+2}$, etc.). Here, we use the notation $E_{\text{LUMO}+k}$ to specify the energy of the k th unoccupied orbital above the LUMO, taking the orbitals in order of increasing orbital energy.

Observe in Table 5 that for each of the orbitals listed for each molecule, we specify with an “X” in the appropriate column of Table 5 whether the orbital is calculated to be localized primarily on the donor (D) side of the molecule or on the acceptor (A) side of the molecule. Note that the LUMO orbital always is localized on the acceptor side of the molecule.

It follows, consistent with the definition in (1), that the potential drop ΔE_{LUMO} across each polyphenylene-based diode structure is determined in Table 5 by subtracting E_{LUMO} from the lowest value $E_{\text{LUMO}+k}$ for an unoccupied orbital localized on the opposite (donor) side of the molecule from the LUMO, i.e.,

$$\begin{aligned}\Delta E_{\text{LUMO}} &\equiv E_{\text{LUMO}}(\text{Donor}) - E_{\text{LUMO}}(\text{Acceptor}) \\ &= E_{\text{LUMO}+k}(\text{Donor LUMO}) - E_{\text{LUMO}}. \quad (4)\end{aligned}$$

In this way, it is determined that the largest potential drop $\Delta E_{\text{LUMO}} = 1.37$ eV is produced by the pairing of the methyl-substituted benzene donor molecule with cyano-substituted benzene acceptor molecule. However, contrary to our expectations from the tabulated values of $\Delta E_{\text{LUMO}}(R = \infty)$, there is nearly as large a potential drop $\Delta E_{\text{LUMO}} = 1.33$ eV for the diode produced by the pairing of the methoxy-substituted benzene donor molecule with cyano-substituted benzene acceptor molecule.

Moreover, in view of its large value for ΔE_{LUMO} , closer examination of the results calculated for methoxybenzene-cyanobenzene complex reveals that it is likely to be preferable to the methylbenzene-cyanobenzene complex for use as a rectifying diode switch. This is because the localization of the unoccupied orbitals is more pronounced in the methoxybenzene-cyanobenzene complex. Specifically, it is observed that the methoxy-substituted complexes described in Table 5 have four unoccupied orbitals (LUMO, LUMO+1, LUMO+2, and LUMO+3) for which strong localization on one or the other side of the molecule is seen. For the methyl-substituted complexes, however, there are only three strongly localized orbitals in the unoccupied manifold—LUMO+3 and higher orbitals are calculated to be delocalized across the entire molecule [101]. This is shown in Table 5.

A larger number of localized unoccupied orbitals in the “conduction band” of the diode is a significant advantage because it provides additional channels for efficient resonant transport through the central barrier of the switching structure. A structure with fewer such unoccupied orbitals operates efficiently over a narrower range of voltages. (See [24]

and Section VI-A above for a more detailed discussion of the mechanisms of electron transport through molecular wires and switches.)

C. Calculations Upon Bonded Polyphenylene-Based Donor-Acceptor Complexes Built from Disubstituted Aromatic Rings

The methoxybenzene-cyanobenzene donor-acceptor complex and the methylbenzene-cyanobenzene complexes built from monosubstituted aromatic rings do exhibit significant intrinsic internal potential drops, as was anticipated. However in each case the magnitude of the drop is less than 1.5 eV, as indicated by the calculated values of ΔE_{LUMO} . Larger permanent potential drops might be desirable to ensure robust operation under a range voltages in molecular electronic circuits.

To attempt to increase the intrinsic internal potential drop across the molecular diodes (i.e., to restore the amount of the value of ΔE_{LUMO} “lost” due to equilibration of electron densities across the central barrier upon binding to it), one might use two donor substituents and two acceptor substituents on the respective aromatic component halves of the diode molecule, instead of just one each. This is the strategy adopted in this paper.

Thus, as shown in Table 6, along with Tables 2 and 3, in the third and final phase of the computational analysis of the polyphenylene-based rectifying diodes we repeat for disubstituted donor-acceptor complexes calculations analogous to those that are reported in Tables 4 and 5 for complexes built from only monosubstituted benzenes. For the central insulator, we continue to employ a dimethylene bridging group.

Specifically, these further calculations analyze a dimethoxybenzene-dicyanobenzene donor-acceptor complex and a dimethylbenzene-dicyanobenzene complex. The structure for these molecules are shown in Figs. 10 and 11 in the main body of this paper. As shown in Tables 2 and 3, both of these doubly disubstituted molecular structures are calculated to have similar large values of ΔE_{LUMO} . This is a favorable indication of the likelihood that each doubly disubstituted molecule is a good molecular rectifier. The computed values of ΔE_{LUMO} for the doubly disubstituted rectifier molecules shown in Tables 2 and 3 exhibit significant increases of approximately 50% (or 0.7 eV) relative to the proposed monosubstituted diodes depicted in Table 5.

Additionally, both of the doubly disubstituted diodes described by the data in Tables 2 and 3 have four unoccupied orbitals localized on either the donor or the acceptor half of the molecule. Thus, each of these diode molecules has channels for robust resonant electron transport across it.

One difference, though, between the dimethoxy and the dimethyl diodes, however, is that the dimethoxy diode may be slightly less sensitive to rotations out of the plane. This can be inferred from the data near the bottom of Tables 2 and 3, where we note that ΔE_{LUMO} changed by only 0.02 eV for an out-of-plane rotation of the dimethoxy substituted diode, but it changed by 0.1 eV for the out-of-plane rotation of the dimethyl substituted diode.

Low sensitivity to such out-of-plane rotations is desirable, since they prove to be necessary in some of the designs proposed below for molecular electronic digital circuits. Thus, in the designs below we choose to use the dimethoxy-dicyano-substituted diode structure shown in Fig. 10 in preference to the dimethyl-dicyano substituted diode shown in Fig. 11.

Nonetheless, the calculations here indicate that both of the doubly disubstituted molecular structures depicted in Figs. 10 and 11 should perform well as molecular rectifying diodes in such circuits. Both of these proposed diode structures have a large intrinsic internal potential drop of approximately 2.0 eV, and both have an unoccupied manifold with two unoccupied orbitals localized on either side of the central barrier to ensure robust efficient electron transport in the preferred direction under a forward bias.

APPENDIX II EXPLANATION OF DIODE-DIODE LOGIC

The development of molecular electronic logic circuits described in the body of this work depends heavily upon the schematics and operational principles for diode-based circuits developed originally for implementation on much larger scales. Thus, for completeness, in this Appendix we explain in detail the operation of the diode-diode AND, OR, and XOR gates. In formulating these explanations, we had assistance from K. Wegener, our collaborator in the MITRE Nanosystems Group.

A. Operation of the Diode-Based AND Gate

A diode-based molecular AND gate is described above in Fig. 12 and Section V-A1. Diode-based logic also is described in detail elsewhere [106], [107], but a brief explanation of the operational principles for the diode-based AND gate is presented here.

A rectifying diode is a two-terminal switch that can be “on” or “off” depending on the applied voltage. A diode is said to be forward biased when the voltage difference across the diode is greater than or equal to zero. As shown in Fig. 3(b), an ideal diode is “on” when it is forward biased, i.e., current flows. The diode is switched “off” when it is reverse biased, i.e., no current flows. Thus, the ideal rectifying diode is a simple switch that is either open or closed depending on the bias applied. (Note that the circuits described in this appendix behave in the same manner when real diodes are used, but for a simple qualitative explanation, the rectifying diodes are assumed here to be ideal.)

Fig. 18 shows how a diode can be utilized in simple circuits to give a particular output voltage, V_C . The direction the diode is positioned relative to the input is the same as would be the case for the AND gate. The voltage across the diode is the difference between the voltages at nodes A and C with respect to ground (taken to be zero volts). There are two relevant examples to examine how a rectifying diode behaves under a voltage bias.

In Example 1 shown in Fig. 18(a), the potential at A with respect to ground is V_0 . The potential at C is V_0 less the

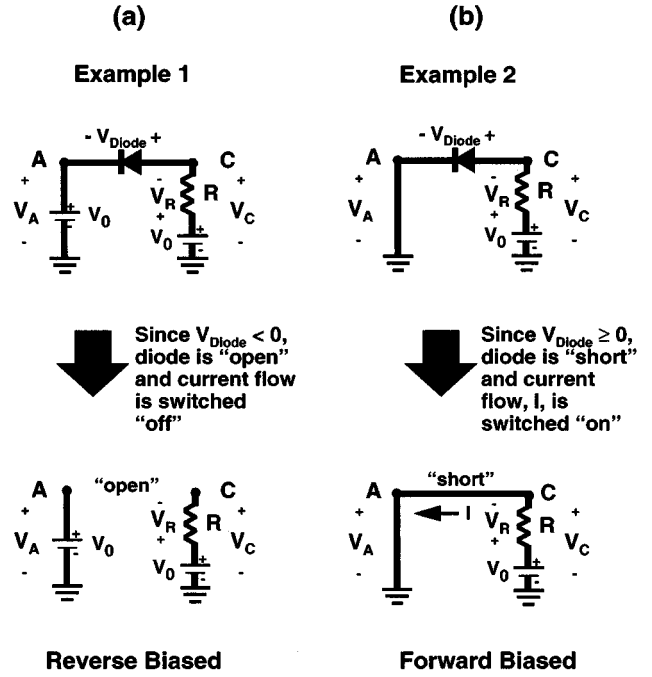


Fig. 18. Two modes of operation for ideal rectifying diodes in the component circuits for a diode-based AND gate.

voltage drop across the resistor, V_R . Thus, the voltage across the diode is

$$V_{\text{Diode}} = V_C - V_A = (V_0 - V_R) - V_0 = -V_R.$$

Assuming $V_R > 0$, the voltage across the diode is less than zero. If the bias is less than zero, the diode must be reversed biased or switched “open.” There is no current flow in the system. The potential at C corresponds to the measured output, V_C

$$V_C = V_0 - V_R = V_0 - IR = V_0.$$

That is, because the diode is reverse biased or “open,” it prevents the current I from flowing, and the potential or output at C is V_0 , which corresponds to a “high” voltage or a binary bit “1.”

In the circuit Example 2, shown in Fig. 18(b), the potential at A with respect to ground is set at 0 V. Now, the voltage across the diode is

$$V_{\text{Diode}} = V_C - V_A = (V_0 - V_R) - 0 = V_0 - V_R.$$

This voltage is greater than or equal to zero, implying that there is a forward bias (assuming $V_0 \geq V_R$). A forward biased ideal diode behaves like a closed switch, allowing current to flow in the circuit. The direction of the current is illustrated in the lower portion of Fig. 18(b). The potential at C with respect to ground is $V_C = V_A = 0$. In other words, the potential at C is zero volts because it is connected directly to ground through the forward biased diode. Thus, the output is a “low” voltage or a binary “0.”

The more complex circuit of an AND logic gate is implemented with diode logic simply by connecting in parallel two

of the elementary diode circuits described above. This parallel circuit layout is depicted in Fig. 19. Note that V_A and V_B can be set independently to “on” (i.e., “1”) or “off” (i.e., “0”) via two-way switches. This allows the different combinations of binary inputs to be represented.

There are three possible pairs of binary inputs to the circuit as shown in Fig. 19. In Case 1, both inputs are switched to low voltage or “off.” Then, both inputs represent the binary number “0.” Following the same operational principles described above for the simple circuit in Example 2, Fig. 18(b), both V_A and V_B are less than V_C so both diodes A and B are forward biased. Thus, current flows and the potential at C drops to 0 as expected for the output of the entire AND gate circuit, i.e., 0 AND 0 = 0.

In Case 2, Fig. 19(b), either input A or input B is set to “off” and the other to “on.” The potential applied in the “on” setting corresponds to a binary “1” input. Since one of the two inputs is set to “off,” there is a forward biased diode in the circuit allowing current to flow. Therefore, the potential at C is zero volts, corresponding to an output of “0” for the entire circuit, e.g., 0 AND 1 = 0, as expected.

In Case 3, Fig. 19(c), where both A and B are switched to “on,” the inputs are both “1.” As described above for Example 1, Fig. 18(a), when V_A is greater than V_C , the diode is reverse biased. The diode behaves just like an open switch that prevents current from flowing. When both diodes are reversed biased, there is no pathway for current to flow—i.e., $I = 0$. The potential at C is V_0 or a binary 1. Thus, of the three possible sets of inputs, only this combination of inputs yields an output of a binary “1,” matching the correct output for an AND gate, namely 1 AND 1 = 1.

Using considerations related to those above, it is also possible to determine that the resistance R should be large in the AND gate when it is implemented using nonideal diodes. For example, when either or both diodes are forward biased and the output voltage of the AND gate is supposed to be approximately zero or LOW, representing a binary 0, a large value of R ensures that the voltage from the power source (not the input signal) is dropped across this resistor, rather than across the diode. Therefore, the voltage at the output is kept relatively small, following the analysis above. Then, if more AND gates were attached to the output, the equivalent resistance of those circuits and the diode is smaller, and the majority of the voltage still is dropped across the resistor R . This serves to increase fanout, which is the number of circuits that can be connected to the output. A value of R at least one order of magnitude greater than the nonzero resistance of the nonideal diodes in the circuit is essential for this purpose.

The appropriate magnitude of resistance R for the resistor in the AND gate also can be determined by examining the expected power dissipation from the diode-based AND gate. Power is defined as

$$P = IV = V^2/R = I^2R.$$

When either A or B or both are “off” and $I > 0$, the power dissipated is V_0^2/R W. For the case where both A and B are “on” and no current flows, then the power dissipated is 0 W.

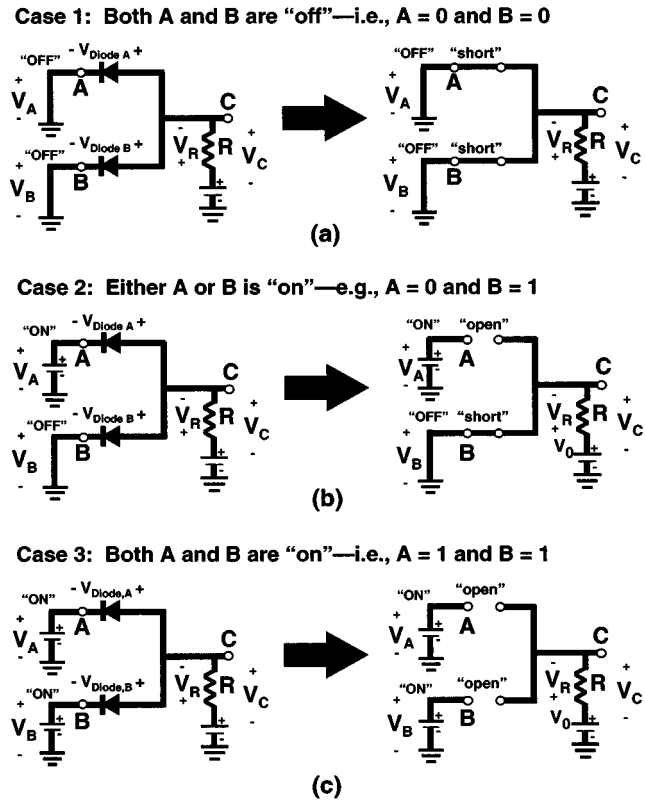


Fig. 19. Three cases for operation of a diode-based AND gate.

A large resistance R makes P small. That is, when R is large, V_0 will supply less current since I is inversely proportional to R by Ohm’s Law for a given V_0 —e.g., $I = V_0/R$.

B. Operation of the Diode-Based OR Gate

A diode-based molecular OR gate is described above in Fig. 13 and Section V-A1. Diode-based logic has been discussed previously elsewhere [106], [107], but a brief explanation of the operational principles for the diode-based OR gate is presented here.

The OR gate consists of two simple diode circuits wired in parallel much like the AND gate described above. For the OR gate, the simple circuit differs from the one used to make the AND gate in the direction the diode is positioned relative to the input signals, as seen in Fig. 20. Thus, in order for the diode to be forward biased in the example circuits, the difference between the potentials at nodes A and C with respect to ground must be greater than or equal to zero. (Note that this is reversed from the required bias direction for the simple circuits that compose the AND gate described above.)

In Example 1 of Fig. 20(a), the potential at A is V_0 , while the potential at C is V_R . If the initial assumption is that the diode is forward biased, then current would be flowing from A to C . Since the diode is ideal, there is no voltage drop across the diode itself and the potential measured at C with respect to ground is equal to the potential measured at A so $V_C = V_A = V_0$. In other words, the assumption of a forward bias on the diode was correct and the output at C would be on or a binary 1.

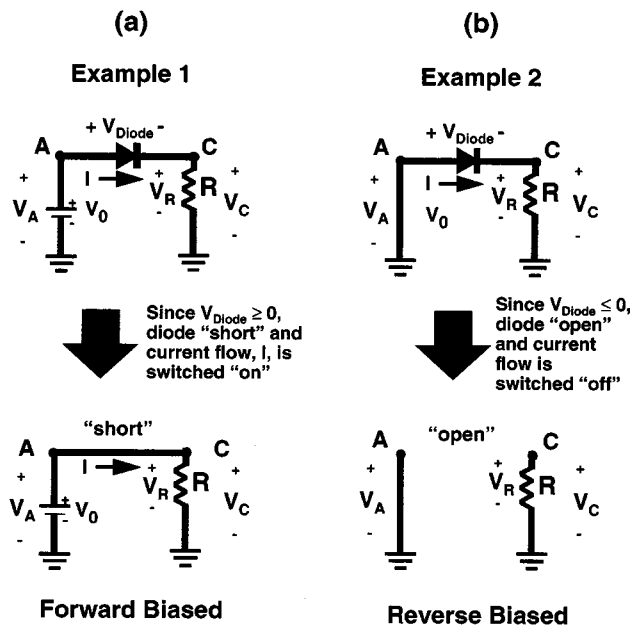


Fig. 20. Two modes of operation for ideal rectifying diodes in the component circuits for a diode-based OR gate.

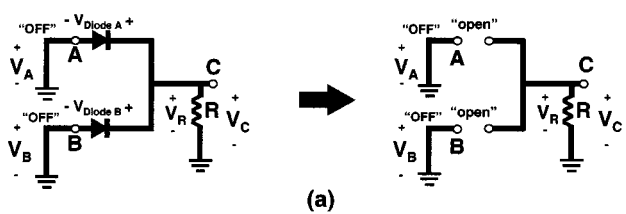
In Example 2 of Fig. 20(b), the potential at A with respect to ground is 0 V. If the initial assumption is that there is current flowing, then the voltage drop across the resistor by Ohm's Law would be $V_R = IR$. This implies that the potential difference between A and C across the diode would be $-V_R$ (i.e., a negative voltage). This is a reverse biased condition for the diode, so the initial assumption that current was flowing was incorrect. The reverse biased diode acts as an open circuit. The potential measured at C with respect to ground is $V_C = IR$, but since $I = 0$, $V_C = 0$. Therefore, the output is "off" or a binary "0".

The OR logic gate is implemented with diode logic simply by connecting in parallel two of the elementary diode circuits described in Fig. 20. This parallel circuit layout is depicted in Fig. 21 with the three possible input cases. Note that V_A and V_B can be set independently to "on" (i.e., "1") or "off" (i.e., "0") via two-way switches. This allows the different combinations of inputs to be represented.

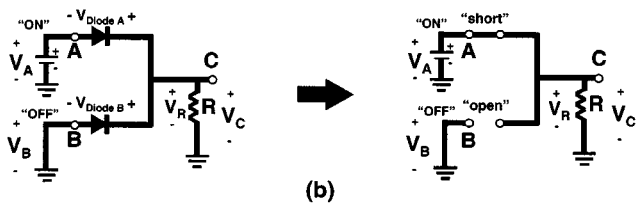
There are three possible pairs of binary inputs to the circuit as shown in Fig. 21. In Case 1, both inputs A and B are switched to a "low" voltage or "off." These inputs both represent the binary number "0." Following the same operational principles described above for the simple circuit in Example 2, Fig. 20(b), both diodes A and B are reverse biased. Since both diodes act like "open" switches and no current flows, the potential at C is "0" as expected for the output of the entire OR gate circuit, i.e., $0 \text{ OR } 0 = 0$.

In Case 2, Fig. 21(b), either input A or input B is set to "off" and the other to "on." The potential applied in the "on" setting corresponds to a binary number "1" input. Since one of the two inputs is set to "on," there is a forward biased diode in the circuit allowing current to flow as described above in Example 1 in Fig. 20(a). Since there is no voltage drop

Case 1: Both A and B are "off"—i.e., $A = 0$ and $B = 0$



Case 2: Either A or B is "on"—e.g., $A = 0$ and $B = 1$



Case 3: Both A and B are "on"—i.e., $A = 1$ and $B = 1$

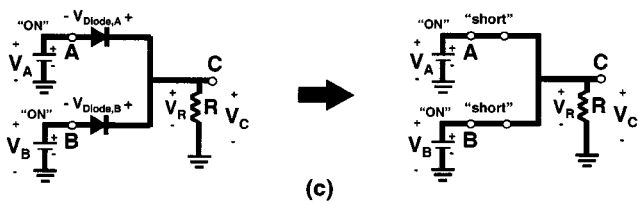


Fig. 21. Three cases for operation of a diode-based OR gate.

across the ideal diode, the potential at C is $V_C = V_A = V_0$, corresponding to an output of a binary "1" as expected for the OR function, e.g., in Fig. 21(b), $1 \text{ OR } 0 = 1$.

In Case 3, Fig. 21(c), where both A and B are switched to "on," the inputs are both "1." As described above for Example 1, Fig. 20(a), when V_A is greater than V_C , the diode is forward biased. The diode behaves just like a wire that allows current to flow. When both diodes are forward biased, there is a pathway for current to flow. Since there is no voltage drop across the ideal diode, the potential at C is $V_C = V_A = V_0$ or a binary "1". The output of the circuit is "on" when either A or B or both are "on" as expected for the entire circuit—e.g., in Fig. 21(c), $1 \text{ OR } 1 = 1$.

Using considerations related to those above, it is also possible to determine that the resistance R should be large in the OR gate when it is implemented using nonideal diodes. For example, when either or both diodes are forward biased and the output voltage of the OR gate is supposed to be approximately V_0 or HIGH, representing a binary "1", a large value of R ensures that the voltage from the input signal (not the power source) is dropped across this resistor rather than across the diode. Therefore, the voltage at the output is kept relatively large, following the analysis above. Then, if more OR gates were attached to the output, the equivalent resistance of those circuits and the diode is smaller, and the majority of the voltage still is dropped across the resistor R . This serves to increase fanout, which is the number of circuits that can be connected to the output. A value of R at least one order of magnitude greater than the nonzero resistance of the nonideal diodes in the circuit is essential for this purpose.

The appropriate magnitude of resistance R for the resistor in the OR gate can be determined by examining the expected power dissipation from the diode-based OR gate. Power is defined as

$$P = IV = V^2/R = I^2 R.$$

For the case where both A and B are “off” and no current flows, then the power dissipated is 0 W. When either A or B or both are “on,” the power dissipated is V_0^2/R W. A large resistance R means the input signal V_0 will supply less current since I and R are inversely proportional by Ohm’s Law for a given V_0 , i.e., $I = V_0/R$. Therefore, to minimize power loss, R should be relatively large.

C. Operation of the Diode-Based XOR Gate

A diode-based molecular XOR gate is described above in Fig. 14 and in Section V-A2. This molecular electronic logic gate is based upon a novel schematic due to Mathews and Sollner [109]. The principles of operation for this novel circuit deserve some explanation [116], [130].

The first key idea is that the known total voltage drop V_T that is applied across the XOR gate is the sum of the effective voltage drop V_{IN} across the input resistances that are associated with the rectifying diodes at the left in Fig. 14(a) and (b), plus the voltage drop V_{RTD} across the RTD to the right in those figures, i.e.,

$$V_T = V_{IN} + V_{RTD}. \quad (5)$$

This relation is depicted in the circuit schematic in Fig. 22(a), which shows the XOR gate as it might have current and voltage provided to it in a larger circuit. From (5), the voltage drop across the RTD may be written

$$V_{RTD} = V_T - V_{IN}. \quad (6)$$

A second key idea is that the effective resistance of the part of the logic gate containing the rectifying diodes differs depending upon whether one or both of the two identical parallel inputs is “on” If only one of the inputs is “on” (e.g., A is 1 and B is 0), the effective resistance of the left-hand, input portion of the XOR gate shown in Fig. 14 or in Fig. 22(a) is R_0 . However, if both of the inputs are “on” (e.g., A is 1 and B is 1), the aggregate effective resistance of the left-hand, input portion of the gate is only $R_0/2$.

Thus, if a (variable) current I is passed through only one input to the gate, then the voltage drop across the input resistance is $V_{IN} = IR_0$. However, if the total current I is split evenly between the two inputs A and B , then the voltage drop across the input resistances is $V_{IN} = IR_0/2$. It follows from these ideas and from (6) that there are two possible operating equations for the gate. Depending upon the inputs, these two equations are approximately

$$V_{RTD} = V_T - IR_0, \quad \text{if only one input is "1"} \quad (7a)$$

$$V_{RTD} = V_T - IR_0/2 \quad \text{if both inputs are "1".} \quad (7b)$$

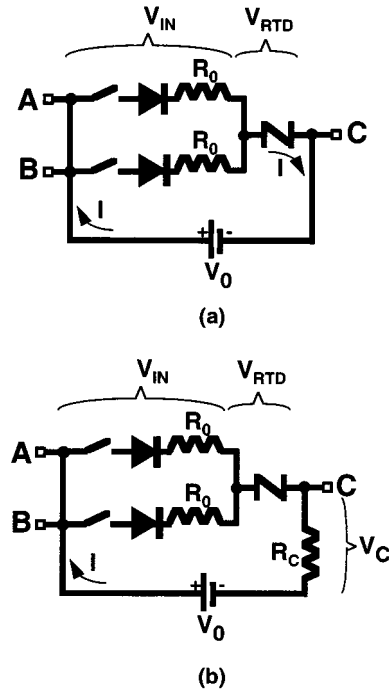


Fig. 22. Circuit schematics explaining the operation of the molecular electronic XOR gate.

By solving these two equations for the variable operating current through the XOR circuit, we derive approximate equations for the two possible operating lines for the circuit, which often are termed the “load lines” for the RTD in the XOR gate

$$I = (V_{RTD} - V_T)(-1/R_0) \quad \text{one input is "1"} \quad (8a)$$

$$I = (V_{RTD} - V_T)(-2/R_0) \quad \text{both inputs are "1".} \quad (8b)$$

These two straight lines, which have different slopes, but the same intercept on the V -axis, both are depicted in the I versus V plot for the RTD that appears in Fig. 7(b). In Fig. 7(b), it may be noted that these two approximate operating lines for the circuit have two different points of intersection with the curved operating line for the RTD.

Which of these two common “operating points” applies plainly depends upon the inputs to the gate. In the case that only one input is “1,” (7a) yields the less steep load line and the operating point on the peak of the RTD operating curve, where the RTD is on and the output voltage of the gate is therefore a “1.”

However, in the case that both inputs to the XOR gate are “1,” (7b) and the steeper load line applies. The corresponding operating point is in the “valley” of the RTD operating curve, where the RTD is “off.” Thus, the output of the XOR gate is likewise off or “0” for two “1’s” on input. This result, which is opposite from that produced by the same inputs in the ordinary or inclusive OR gate, is a consequence of the valley current shut off that is manifested by the RTD past its first peak on the I - V curve.

Thus far, the analysis has ignored other resistances in the circuit that also would affect its operation—especially the resistance R_C at the lower right of the circuit associated with the measured output voltage. However, by adjusting the value of R_0 , other resistances such as R_C may be inserted into the circuit, as illustrated in Fig. 22(b), without affecting the essential current response of the circuit, which is, in summary:

- 1) having only the A input set to “1” or only the B input set to “1,” but not both, yields V_{RTD} as a low voltage, while it produces a relatively high value for the current I ;
- 2) both A and B set to “1” yields a relatively high value of V_{RTD} , but a low output current.

Thus, the low current in the latter case ensures that the measured output voltage drop $V_C = IR_C$ in the latter case with both inputs as “1” will be lower than in the former case with only one input as “1.” Of course, this is precisely the output voltage response desired for an XOR gate.

A final observation about the analysis above in Appendix I concerns our implicit and explicit use of the use of Ohm’s Law, $V = IR$, thereby assuming both constant resistances R for the molecular circuit elements and a linear relationship between the voltage V and the current I . In fact, neither of these assumptions is exactly true for molecular wires [1], [28]. However, over narrow ranges of values for the current these assumptions are likely to be nearly true. The current through a molecular wire still rises monotonically and nearly linearly as the voltage is swept through a narrow range. Thus, the sense of the preceding analysis is likely to be true, although the details may require adjustment when such a circuit actually is constructed and its current–voltage behavior is measured.

APPENDIX III

SIZE ESTIMATE FOR CMOS HALF ADDER AND SCALING ESTIMATE FOR A MOLECULAR ADDER

A. Motivation

It is of interest to have a quantitative estimate of the degree of scaling that might be provided by molecular electronic circuits such as the approximately $3 \text{ nm} \times 4 \text{ nm}$ molecular logic gates and the approximately $10 \text{ nm} \times 10 \text{ nm}$ adder function for which designs are given in the body of this work. Ideally, we would compare these dimensions with those for the analogous functions on commercial CMOS logic circuits. Data on the actual measurements of structures on commercial computer chips often are regarded as proprietary information, though. Thus, such data have proven to be difficult to obtain.

However, D. Naegle of Sun Microsystems, Inc., in Palo Alto, CA, has very graciously performed for us an approximate calculation of the sizes for the microelectronic implementations of the analogous logic functions when they are fabricated using conventional CMOS technology, assuming 250 nm or $0.25 \mu\text{m}$ lithographic linewidths. His estimate, including his detailed reasoning, appears immediately below.

B. Naegle’s Estimate of the Sizes for CMOS Logic Structures

The 1998 edition of the *IBM ASIC SA-12 Databook* [131] can be used to compute cell sizes of two-input AND, OR, and XOR gates for their smallest implementation (lowest drive) by an IBM $0.25 \mu\text{m}$ SA-12 process.

The areas of the individual logic gates are not available directly in the format adopted by the *Databook*. Instead of quoting an area for each of the active devices by itself, the number of “cells” that the collection of subcomponent devices occupies is quoted. This appears to account for some amount of the interconnect structure that is needed to wire together devices within the gate. For example, quoting from p. 20 of the *Databook*:

Cell Units = Area of [gate name], in number of cell units. A cell unit is $2 \text{ Metal-2} \times 16 \text{ Metal-1}$ wiring channels for non-IO cells. . . . Each wiring channel is $1.26 \mu\text{m}$ wide.

On that basis, assuming that both the metal 1 and the metal 2 wiring channels have a width of $1.26 \mu\text{m}$, a cell unit is

$$2 \times 16 \times (1.26 \mu\text{m})^2 = 50.8032 \mu\text{m}^2.$$

This evaluation of the area of a cell permits the tabulation of the areas in μm^2 of the CMOS AND, OR, and XOR gates from the data given for the areas of these gates in cells. The tabulation is as follows:

2-input AND (p. 274):	2 cells = $101.6064 \mu\text{m}^2$
2-input OR (p. 291):	2 cells = $101.6064 \mu\text{m}^2$
2-input XOR (p. 296):	4 cells = $203.2128 \mu\text{m}^2$.

For completeness, I also tabulate the estimated areas for NAND, NOR, and Invert logic functions, as follows:

2-input NAND (p. 281):	2 cells = $101.6064 \mu\text{m}^2$
2-input NOR (p. 286):	2 cells = $101.6064 \mu\text{m}^2$
Inverter (p. 279):	1 cell = $50.8032 \mu\text{m}^2$.

The pages quoted above are from the *Databook* [130].

The lack of a difference in area for AND and NAND gates in the results above is somewhat troubling if one hopes to understand in detail the areas involved in implementing these cells. The unit cell described above clearly is too coarse a measure of area to get a very accurate idea of the actual sizes of the gates. Nevertheless, this is the best area a designer can achieve in the SA-12 standard cell library. It may be expected that these numbers are not off by more than a factor of two or three. That is, a custom layout by hand of the equivalent standard cells probably would not be smaller than one half or one third the quoted size, especially if you take into account the size of the p-well for the n-channel transistors.

C. Conclusion

From Naegle’s calculation, the approximately $100 \mu\text{m}^2$ area of the silicon CMOS microelectronic logic gates would

be about 6 to 8 million times greater in area than the approximately 12 nm^2 molecular AND, OR, and XOR gates for which designs are proposed in the body of this paper. Allowing for the approximate nature of the calculation above, this implies a scale-down factor of approximately 10^6 or 10^7 for the molecules.

A circuit for a half adder function, be it solid state or molecular, consists of at least two logic gates of the types listed above. Thus, on the basis of Naegle's results, it would appear likely that the 100 nm^2 molecular electronic half adder would be at least one million to 10 million times smaller in area than a conventional silicon CMOS half adder.

ACKNOWLEDGMENT

For their invaluable material assistance to this work in so generously sharing their ideas and their unpublished research results with us, the authors wish to express particular thanks to Prof. M. Reed of Yale University and Prof. J. Tour of Rice University, Dr. G. Sollner and Dr. R. H. Mathews of MIT-Lincoln Lab, as well as to Dr. A. Seabaugh of Notre Dame University and J. Soreff of the IBM Corporation, East Fishkill, NY. Several of our colleagues reviewed an earlier, September 1998 draft version of this paper and made very helpful comments and suggestions. These have been incorporated into this final version and have improved it greatly. We are grateful to those reviewers, who are as follows: D. Allara, Penn State University; D. Goldhaber-Gordon, Harvard University; R. Lytel and D. Naegle, Sun Microsystems, Inc.; P. MacDougall, Middle Tennessee State University; R. Merkle, Xerox Palo Alto Research Center; M. Ratner, Northwestern University; J. Seminario, University of South Carolina; W. Tolles, Miniaturization Science and Technology; J. Tour, Rice University; G. Whitesides, Harvard University; plus T. Bollinger, G. Tseng, and A. Wissner-Gross, The MITRE Corporation. Additional thanks in this regard are due to the referees of this final version of the paper. D. Naegle of Sun Microsystems, Inc., graciously contributed the analysis and estimate of the size of a silicon CMOS half adder, which appears in Appendix III. The authors wish to express their appreciation for his generous contribution of that effort. Thanks are due, as well, to many of our other colleagues and collaborators in the nanoelectronics community for their positive comments and their encouragement of the investigations upon which this paper is based. Dr. G. Pomrenke, Dr. B. Gnade, and Dr. W. Warren of the Defense Advanced Research Projects Agency have been especially generous in this way, and we are grateful. In addition, we are grateful to the other members of the MITRE Nanosystems Group, especially G. Tseng, D. Moore, K. Wegener, and K. H. Hanson Wong, for their collaboration in the nanoelectronics research investigations which supported or led up to the one upon which this paper is based. We also are indebted to many other colleagues at MITRE for their longstanding support of this research, notably D. Lehman, S. Huffman, E. Palo, C. Cook, W. Hutzler, and K. Pullen.

REFERENCES

- [1] M. A. Reed, C. Zhou, C. J. Muller, T. P. Burgin, and J. M. Tour, "Conductance of a molecular junction," *Science*, vol. 278, pp. 252–254, 1997.
- [2] L. A. Bumm *et al.*, "Are single molecular wires conducting?," *Science*, vol. 271, pp. 1705–1707, 1996.
- [3] R. P. Andres *et al.*, "'Coulomb staircase' at room temperature in a self-assembled molecular nanostructure," *Science*, vol. 272, pp. 1323–1325, 1996.
- [4] S. J. Tans *et al.*, "Individual single-wall carbon nanotubes as quantum wires," *Nature*, vol. 386, pp. 474–477, 1997.
- [5] M. A. Reed, "Electrical properties of molecular devices," presented at the 1997 DARPA ULTRA Program Review Conference, Santa Fe, NM, Oct. 26–31, 1997. This presentation discussed the experimental measurement of a molecular RTD. We thank Professor Reed for providing us with a copy of his presentation materials, especially the experimental I-V curve for the molecular RTD, well in advance of its publication in a journal. See also [6].
- [6] M. A. Reed, "Molecular-scale electronics," *Proc. IEEE*, vol. 87, pp. 652–658, Apr. 1999.
- [7] C. Zhou, M. R. Deshpande, M. A. Reed, and J. M. Tour, "Nanoscale metal/self-assembled monolayer/metal heterostructures," *Appl. Phys. Lett.*, vol. 71, pp. 611–613, 1997.
- [8] C. Zhou, "Atomic and molecular wires," Ph.D. dissertation, Yale University, 1999. See especially the results of experimental measurements on the conductances of polyphenylenic molecular wires that are presented in Chapter 5 of this work. We very much thank Prof. M. Reed of Yale University and Dr. C.-W. Zhou for their generosity in sharing a draft version of this dissertation with us, prior to its publication.
- [9] R. M. Metzger *et al.*, "Unimolecular electrical rectification in hexadecylquinolinium tricyanoquinodimethanide," *J. Amer. Chem. Soc.*, vol. 119, pp. 10455–10466, 1997.
- [10] A. Dhirani, R. Zehner, P.-H. Lin, L. R. Sita, and P. Guyot-Sionnest, "Self-assembled molecular rectifiers," *J. Chem. Phys.*, vol. 106, pp. 5249–5253, 1997.
- [11] L. Ottaviano *et al.*, "Rectifying behavior of silicon-phthalocyanine junctions investigated with scanning tunneling microscopy/spectroscopy," *J. Vac. Sci. Technol. A*, vol. 15, pp. 1014–1019, 1997.
- [12] M. A. Reed, "Progress in molecular-scale devices and circuits," in *Proc. 57th Annu. IEEE Device Research Conf.*, Santa Barbara, CA, June 28–30, 1999. This presentation contained information about an intramolecularly doped polyphenylene-based molecular RTD which exhibited an extremely large switching transition, a 1000:1 peak-to-valley current ratio, with an approximately 1 nanoamp peak current at 60 degrees Kelvin, under an approximately 2 volt bias. The molecular structure was synthesized by Prof. J. Tour of Rice University and tested by Prof. Reed and his collaborators at Yale University. We thank Profs. Reed and Tour for sharing these recent results with us in advance of their publication in a journal. See also [13].
- [13] J. Chen, M. A. Reed, A. M. Rawlett, and J. M. Tour, "Large on-off ratios and negative differential resistance in a molecular electronic device," *Science*, vol. 286, pp. 1550–1552, 1999.
- [14] Z. Yao, H. W. C. Postma, L. Balents, and C. Dekker, "Carbon nanotube intramolecular junctions," *Nature*, vol. 402, pp. 273–276, 1999.
- [15] C. Zhou, C. J. Muller, M. A. Reed, T. P. Burgin, and J. M. Tour, "Mesoscopic phenomena studied with mechanically controllable break junctions at room temperature," in *Molecular Electronics*, J. Jortner and M. Ratner, Eds. London, U.K.: Blackwell, 1997.
- [16] J. C. Ellenbogen, "A brief overview of nanoelectronic devices," in *Proc. 1998 Government Microelectronics Conf. (GOMAC98)*, Arlington, VA, Mar. 13–16, 1998. This paper provides a brief summary of previous research in nanoelectronics that led to the present effort to design molecular circuitry that operates in a manner analogous to microelectronic and solid-state nanoelectronic circuitry. [Online]. Available WWW: http://www.mitre.org/technology/nanotech/GOMAC98_article.html.
- [17] D. Goldhaber-Gordon, M. S. Montemero, J. C. Love, G. J. Opiteck, and J. C. Ellenbogen, "Overview of nanoelectronic devices," *Proc. IEEE*, vol. 85, pp. 521–540, 1997. See also references cited in the extensive bibliography in this work. [Online]. Available WWW: http://www.mitre.org/technology/nanotech/IEEE_article.html.

- [18] M. S. Montemerlo, J. C. Love, G. J. Opiteck, D. J. Goldhaber-Gordon, and J. C. Ellenbogen, "Technologies and designs for electronic nanocomputers," MITRE Rep. 96W000044, The MITRE Corporation, McLean, VA, July 1996. [Online] Available WWW: http://www.mitre.org/technology/nanotech/review_article.html.
- [19] (1996–2000) "The Nanoelectronics and Nanocomputing Home Page". The MITRE Corporation, McLean, VA. [Online] Available WWW: <http://www.mitre.org/technology/nanotech>. This large WWW site provides [16]–[18] and [127] as downloadable documents.
- [20] W. B. Davis, W. A. Svec, M. A. Ratner, and M. R. Wasielewski, "Molecular-wire behaviour in p-phenylenevinylene oligomers," *Nature*, vol. 396, pp. 60–63, 1998.
- [21] V. Mujica, M. Kemp, and M. A. Ratner, "Electron conduction in molecular wires. I. A scattering formalism," *J. Chem. Phys.*, vol. 101, pp. 6849–6855, 1994.
- [22] —, "Electron conduction in molecular wires II: Application to scanning tunneling microscopy," *J. Chem. Phys.*, vol. 101, pp. 6856–6864, 1994.
- [23] V. Mujica, M. Kemp, A. Roitberg, and M. Ratner, "Current–voltage characteristics of molecular wires: Eigenvalue staircase, Coulomb blockade, and rectification," *J. Chem. Phys.*, vol. 104, pp. 7296–7305, 1996.
- [24] M. A. Ratner and J. Jortner, "Molecular electronics: Some directions," in *Molecular Electronics*, J. Jortner and M. Ratner, Eds. London, U.K.: Blackwell, 1997, pp. 5–72. See also references cited therein.
- [25] M. A. Ratner *et al.*, "Molecular wires: Charge transport, mechanisms, and control," *Ann. NY Acad. Sci. (Special Issue on Molecular Electronics: Science and Technology)*, vol. 852, pp. 22–37, 1998.
- [26] M. P. Samanta, W. Tian, S. Datta, J. I. Henderson, and C. P. Kubiak, "Electronic conduction through organic molecules," *Phys. Rev. B*, vol. 53, pp. 7626–7629, 1996.
- [27] S. Datta, *Electron Transport in Mesoscopic Systems*. Cambridge, U.K.: Cambridge Univ. Press, 1995.
- [28] S. Datta *et al.*, "Current–voltage characteristics of self-assembled monolayers by scanning-tunneling microscopy," *Phys. Rev. Lett.*, vol. 79, pp. 2530–2533, 1997. This important theory paper points out that the actual conductance of molecular wires may be much higher than the measured conductance in some experiments.
- [29] D. A. Muller *et al.*, "The electronic structure at the atomic scale of ultrathin gate oxides," *Nature*, vol. 399, pp. 758–761, 1999.
- [30] P. A. Packan, "Pushing the limits," *Science*, vol. 285, pp. 2079–2081, 1999.
- [31] J. R. Reimers and N. S. Hush, "Electron transfer and energy transfer through bridged systems III," *J. Photochem. Photobiol. A*, vol. 82, pp. 31–46, 1994.
- [32] L. E. Hall, J. R. Reimers, N. S. Hush, and K. Silverbrook, "Formalism, analytical model, and *a priori* Green's function-based calculations of the current-voltage characteristics of molecular wires," *J. Chem. Phys.*, to be published. See also references cited therein.
- [33] E. G. Emberly and G. Kirczenow, "Electrical conduction through a molecule," *Ann. N.Y. Acad. Sci.*, vol. 852, pp. 54–67, 1998.
- [34] —, "Theoretical study of electrical conduction through a molecule connected to metallic nanocontacts," *Phys. Rev. B*, vol. 58, pp. 10911–10920, 1998. A preprint of this article also is available as paper number 9807290 in the condensed matter section of the Los Alamos National Laboratory e-print archive on the WWW: xxx.lanl.gov.
- [35] —, "Electrical conductance of molecular wires," *Nanotechnol.*, vol. 10, pp. 285–291, 1999. A preprint of this article also is available as paper number 9908392 in the condensed matter section of the Los Alamos National Laboratory e-print archive on the WWW: xxx.lanl.gov.
- [36] S. T. Pantelides, M. DiVentra, and N. D. Lang, "Ab initio simulation of molecular devices," presented at the 1999 DARPA Molecular Electronics (Moletronics) Program Review Conference, Ashburn, VA, July 8–9, 1999. This presentation discussed highly detailed quantum mechanical calculations of the conductance of polyphenylene-based molecular wires, and it compared these theoretical results to experimental data. A manuscript is in preparation.
- [37] G. M. Whitesides, private communication, Oct.–Jan. 1998–1999. We thank Prof. G. Whitesides of Harvard University for valuable and stimulating discussions on this point.
- [38] J. S. Schumm, D. L. Pearson, and J. M. Tour, "Iterative divergent/convergent approach to linear conjugated oligomers by successive doubling of the molecular length: A rapid route to a 128 Å-long potential molecular wire," *Angew. Chem. Int. Ed. Engl.*, vol. 33, pp. 1360–1363, 1994.
- [39] J. M. Tour, R. Wu, and J. S. Schumm, "Extended orthogonally fused conducting oligomers for molecular electronic devices," *J. Am. Chem. Soc.*, vol. 113, pp. 7064–7066, 1991.
- [40] P. W. Atkins, *Quanta: A Handbook of Concepts*, 2nd ed. Oxford, U.K.: Oxford, 1992. This excellent guide to the basic terms and ideas of molecular quantum mechanics would be of particular assistance to those readers less familiar with this essential background subject matter.
- [41] —, *Molecular Quantum Mechanics*, 3rd ed. Oxford, U.K.: Oxford, 1997.
- [42] R. T. Morrison and R. N. Boyd, *Organic Chemistry*, 2nd ed. Boston, MA: Allyn & Bacon, 1966. Note: the authors actually used in their investigations the out-of-print 1966 edition of this standard text. However, a newer edition, presently in print, contains similar information. See [133].
- [43] M. A. Reed, private communication, Oct. 1997.
- [44] J. M. Tour, private communication, Dec. 1998. Prof. Tour at Rice University in Houston, TX, and his collaborators are exploring innovative strategies toward easing the problem of making contact with electrically conductive small molecules, as well as new strategies for assembling extended circuitry composed of such small molecules.
- [45] —, "Chemical synthesis of molecular electronic devices," presented at the 1997 DARPA ULTRA Review Conference, Santa Fe, NM, Oct. 26–31, 1997. This presentation discussed the synthesis of a molecular RTD, as well as the strategy for inserting acetylenic linkages between aromatic rings in polyphenylene-based molecular wires to reduce the steric interference between the hydrogen atoms bonded to adjacent aromatic phenyl groups in the molecular wire.
- [46] P. S. Weiss *et al.*, "Probing electronic properties of conjugated and saturated molecules in self-assembled monolayers," *Ann. NY Acad. Sci. (Special Issue on Molecular Electronics: Science and Technology)*, vol. 852, pp. 145–168, 1998.
- [47] M. Riordan and L. Hodgeson, *Crystal Fire: The Birth of the Information Age*. New York: Norton, 1997.
- [48] L. Edwards-Shea, *The Essence of Solid-State Electronics*. Hertfordshire, U.K.: Prentice-Hall, 1996.
- [49] A. Aviram and M. A. Ratner, "Molecular rectifiers," *Chem. Phys. Lett.*, vol. 29, pp. 277–283, 1974.
- [50] A. S. Martin, J. R. Samles, and G. J. Ashwell, "Molecular rectifier," *Phys. Rev. Lett.*, vol. 70, pp. 218–221, 1993.
- [51] J. M. Tour, M. Kozaki, and J. M. Seminario, "Molecular scale electronics: A synthetic/computational approach to digital computing," *J. Amer. Chem. Soc.*, vol. 120, pp. 8486–8493, 1998.
- [52] J. M. Seminario, A. G. Zacharias, and J. M. Tour, "Molecular alligator clips for single molecule electronics. Studies of group 16 and isonitriles interfaced with Au contacts," *J. Amer. Chem. Soc.*, vol. 121, pp. 411–416, 1998.
- [53] D. K. Ferry, *Quantum Mechanics: An Introduction for Device Physicists and Electrical Engineers*. London, U.K.: IOP, 1995.
- [54] B. I. Yakobson and R. E. Smalley, "Fullerene nanotubes: C(1,000,000) and beyond," *Amer. Scientist*, vol. 85, pp. 324–337, 1997. See also references therein.
- [55] S. J. Tans, "Electron transport through single molecular wires," Ph.D. dissertation, Delft Tech. Univ., Delft, The Netherlands, 1998. See also the references cited therein, which give an excellent background on the fundamentals of the structure and electronic properties of carbon nanotubes or "buckytubes." This remarkable thesis is available in a version published by Delft University Press, Delft, The Netherlands, 1998.
- [56] J. W. G. Wildöer, L. C. Venema, A. G. Rinzler, R. E. Smalley, and C. Dekker, "Electronic structure of atomically resolved carbon nanotubes," *Nature*, vol. 391, pp. 59–62, 1998.
- [57] T. W. Odom, J.-L. Huang, P. Kim, and C. M. Lieber, "Atomic structure and electronic properties of single-walled carbon nanotubes," *Nature*, vol. 391, pp. 62–64, 1998.
- [58] M. Bockrath *et al.*, "Single-electron transport in ropes of carbon nanotubes," *Science*, vol. 275, pp. 1922–1925, 1997.
- [59] H. Dai, E. W. Wong, and C. M. Lieber, "Probing electrical transport in nanomaterials: Conductivity of individual carbon nanotubes," *Science*, vol. 272, pp. 523–526, 1996.

- [60] H. Yorikawa and S. Muramatsu, "Electronic properties of semi-conducting graphitic microtubules," *Phys. Rev. B*, vol. 50, pp. 12203–12206, 1994.
- [61] C. T. White, D. H. Robertson, and J. W. Mintmire, "Helical and rotational symmetries of nanoscale graphitic tubules," *Phys. Rev. B*, vol. 47, pp. 5485–5488, 1993.
- [62] R. Saito, M. Fujita, G. Dresselhaus, and M. S. Dresselhaus, "Electronic structure of chiral graphene tubules," *Appl. Phys. Lett.*, vol. 60, pp. 2204–2206, 1992.
- [63] P. G. Collins *et al.*, "Nanotube nanodevice," *Science*, vol. 278, pp. 100–104, 1997. Evidence for inherent nanotube rectifiers.
- [64] S. J. Tans, A. R. M. Verschueren, and C. Dekker, "Single nanotube-molecule transistor at room temperature," *Nature*, vol. 393, pp. 49–51, 1998.
- [65] J. Chen *et al.*, "Solution properties of single-walled carbon nanotubes," *Science*, vol. 282, pp. 95–98, 1998.
- [66] M. A. Hamon *et al.*, "Dissolution of single-walled carbon nanotubes," *Adv. Materials*, vol. 11, pp. 834–840, 1999.
- [67] E. T. Mickelson *et al.*, "Fluorination of single-wall carbon nanotubes," *Chem. Phys. Lett.*, vol. 296, pp. 188–194, 1998.
- [68] E. T. Mickelson *et al.*, "Solvation of fluorinated single-wall carbon nanotubes in alcohol solvents," *J. Phys. Chem. B*, vol. 103, pp. 4318–4322, 1999.
- [69] P. Boul *et al.*, "Reversible sidewall functionalization of buckytubes," *Chem. Phys. Lett.*, vol. 310, pp. 367–372, 1999.
- [70] K. S. Kelly *et al.*, "Insight into the mechanism of sidewall functionalization of single-walled nanotubes: An STM study," *Chem. Phys. Lett.*, vol. 313, pp. 445–450, 1999.
- [71] J. Li, C. Papadopoulos, and J. Xu, "Growing Y-junction carbon nanotubes," *Nature*, vol. 402, pp. 253–254, 1999.
- [72] Z. P. Huang *et al.*, "Growth of highly oriented carbon nanotubes by plasma-enhanced hot filament chemical vapor deposition," *Appl. Phys. Lett.*, vol. 73, pp. 3845–3847, 1998.
- [73] Z. F. Ren *et al.*, "Synthesis of large arrays of well-aligned carbon nanotubes on glass," *Science*, vol. 282, pp. 1105–1107, 1998.
- [74] Z. F. Ren *et al.*, "Growth of a single freestanding multiwall carbon nanotube on each nanonickel dot," *Appl. Phys. Lett.*, vol. 75, pp. 1086–1088, 1999.
- [75] G. E. Scuseria, "Negative curvature and hyperfullerenes," *Chem. Phys. Lett.*, vol. 195, pp. 534–536, 1992.
- [76] L. Chico, V. H. Crespi, L. X. Benedict, S. G. Louie, and M. L. Cohen, "Pure carbon nanoscale devices: Nanotube heterojunctions," *Phys. Rev. Lett.*, vol. 76, pp. 971–974, 1996.
- [77] M. Menon and D. Srivastava, "Carbon nanotube 'T junctions': Nanoscale metal-semiconductor-metal contact devices," *Phys. Rev. Lett.*, vol. 79, pp. 4453–4456, 1997.
- [78] —, "Carbon nanotube based molecular electronic devices," *J. Materials Res.*, vol. 13, pp. 2357–2361, 1998.
- [79] M. S. Smith, M. H. Schleier-Smith, G. Y. Tseng, and J. C. Ellenbogen, "Architectures for molecular electronic computers. 4. Designs for digital logic structures constructed from carbon nanotubes," The MITRE Corporation, McLean, VA, Rep. MP 99W0000165, to be published.
- [80] J. Kong, A. Cassell, and H. Dai, "Chemical vapor deposition of methane for single-walled carbon nanotubes," *Chem. Phys. Lett.*, vol. 292, p. 567, 1998.
- [81] J. Kong, H. T. Soh, A. Cassell, C. F. Quate, and H. Dai, "Synthesis of single single-walled carbon nanotubes on patterned silicon wafers," *Nature*, vol. 395, pp. 878–881, 1998.
- [82] H. Dai, N. Franklin, and J. Han, "Exploiting the properties of carbon nanotubes for nanolithography," *Appl. Phys. Lett.*, vol. 73, pp. 1508–1510, 1998.
- [83] S. Fan *et al.*, "Self-oriented regular arrays of carbon nanotubes and their functional devices," *Science*, vol. 283, pp. 512–514, 1999.
- [84] B. H. Robinson and N. Seeman, "The design of a biochip: A self-assembling molecular-scale memory device," *Protein Eng.*, vol. 1, pp. 295–300, 1987.
- [85] E. K. Wilson, "DNA conductance convergence?," *Chem. Eng. News*, pp. 43–48, 1999.
- [86] E. Meggers, M. E. Michel-Beyerle, and B. Giese, "Sequence dependent long-range hole transport in DNA," *J. Amer. Chem. Soc.*, vol. 120, pp. 12950–12955, 1998.
- [87] P. T. Henderson, D. Jones, G. Hampikian, Y. Kan, and G. B. Schuster, "Long-distance charge transport in duplex DNA: The phonon-assisted polaron-like hopping mechanism," *Proc. Nat. Acad. Sci.*, vol. 96, pp. 8353–8358, 1999.
- [88] J. Jortner, M. Bixon, T. Langenbacher, and M. E. Michele-Beyerle, "Charge transfer and transport in DNA," *Proc. Nat. Acad. Sci. USA*, vol. 95, pp. 12759–12765, 1998.
- [89] Y. A. Berlin, A. L. Burin, and M. A. Ratner, "On the long-range charge transfer in DNA," *J. Phys. Chem. B*, to be published. The authors thank Prof. M. Ratner for providing them with a preprint of this unpublished manuscript.
- [90] D. Porath, A. Bezryadin, S. de Vries, and C. Dekker, "Direct measurement of electrical transport through DNA molecules," *Nature*, vol. 403, pp. 635–638, 2000. The authors thank D. Porath and Prof. C. Dekker for providing them with a preprint of this paper well in advance of its publication.
- [91] L. R. Milgrom, *The Colours of Life: An Introduction to the Chemistry of Porphyrins and Related Compounds*. Oxford, U.K.: Oxford, 1997.
- [92] D. F. Bocian, W. G. Kuhr, and J. S. Lindsey, "Porphyrin-based molecular memories," manuscript in preparation.
- [93] G. Y. Tseng and J. C. Ellenbogen, "Architectures for molecular electronic computers. 3. Design for a memory cell built from molecular electronic devices," The MITRE Corporation, McLean, VA, Rep. MP 99W0000138, 1999, to be published.
- [94] M. S. Ullagaddi, K. Wegener, and J. C. Ellenbogen, "Molecular electronic circuit analysis. 1. Analysis of a molecular XOR gate," manuscript in preparation.
- [95] A computer software program tentatively named "MolSPICE" is being developed at The MITRE Corporation in McLean, VA. Using a library of characteristics previously determined for isolated molecular wires and molecular electronic switches, the software calculates the electrical behavior of conductive molecular-scale circuits that incorporate these components. In performing this function, the MolSPICE program acts in a manner that is analogous to the more familiar SPICE circuit modeling software that is commonly applied for microelectronic circuits. However, the modeling algorithms for MolSPICE necessarily are different in order to account for the explicitly quantum mechanical nature of the molecular-scale circuits.
- [96] M. Magoga and C. Joachim, "Minimal attenuation for tunneling through a molecular wire," *Phys. Rev. B*, vol. 57, pp. 1820–1821, 1998.
- [97] —, "Conductance of molecular wires connected or bonded in parallel," *Phys. Rev. B*, vol. 59, pp. 16011–16021, 1999.
- [98] S. N. Yaliraki and M. A. Ratner, "Molecule-interface coupling effects on electronic transport in molecular wires," *J. Chem. Phys.*, vol. 109, pp. 5036–5043, 1998.
- [99] S. N. Yaliraki, A. E. Roitberg, C. Gonzalez, V. Mujica, and M. A. Ratner, "The injecting energy at molecule/metal interfaces: Implications for conductance of molecular junctions from an *ab initio* molecular description," *J. Chem. Phys.*, vol. 111, pp. 6997–7002, 1999.
- [100] The authors thank the referees for their helpful comments in regard to this point in the discussion and for pointing out additional relevant references in the literature.
- [101] D. C. Moore and J. C. Ellenbogen, "Architectures for molecular electronic computers: Quantum mechanical calculations of the electrical properties of molecular electronic switches," manuscript in preparation. The authors thank D. C. Moore of the MITRE Nanosystems Group for his assistance in refining and extending their early quantitative estimates of the properties of rectifying diodes.
- [102] A. O. Orlov, I. Amlani, G. H. Bernstein, C. S. Lent, and G. L. Snider, "Realization of a functional cell for quantum-dot cellular automata," *Science*, vol. 277, pp. 928–930, 1997.
- [103] I. Amlani, A. O. Orlov, G. L. Snider, C. S. Lent, and G. H. Bernstein, "Demonstration of a six-dot quantum cellular automata system," *Appl. Phys. Lett.*, vol. 72, pp. 2179–2181, 1998.
- [104] I. Amlani *et al.*, "Digital logic gate using quantum-dot cellular automata," *Science*, vol. 284, pp. 289–291, 1999.
- [105] C. S. Lent, P. D. Tougaw, W. Porod, and G. H. Bernstein, "Quantum cellular automata," *Nanotechnol.*, vol. 4, pp. 49–57, 1993.
- [106] G. Epstein, *Multiple-Valued Logic Design: An Introduction*. Bristol, U.K.: Inst. Physics, 1993. See especially ch. 2 of this work for a discussion of diode-diode logic gates.
- [107] R. C. Jaeger, *Microelectronic Circuit Design*. New York: McGraw-Hill, 1997.
- [108] R. M. Metzger, private communication, Mar. 1998.

- [109] R. H. Mathews and T. C. L. G. Sollner, MIT Lincoln Lab., Cambridge, MA. The authors thank Dr. G. Sollner for providing them in October 1997 with a copy of the unpublished circuit schematic shown in Fig. 14(a). The schematic describes an XOR gate that incorporates only rectifying diodes and resonant tunneling diodes, but no transistors. The MIT Lincoln Laboratory team led by Dr. Sollner had been using this circuit as part of a strategy to implement diode-based logic in solid semiconductors. The authors of the present paper are responsible for the novel use of this schematic circuit to generate a molecular electronic XOR gate.
- [110] A. E. A. Almaini, *Electronic Logic Systems*, 2nd ed. Hertfordshire, U.K.: Prentice-Hall, 1989. See especially ch. 6 on "Arithmetic Logic Circuits" for a description of the principles of combinational logic that are required to generate a half adder and a full adder using AND, OR, and XOR gates.
- [111] M. A. Ratner, private communication, June 1999.
- [112] J. Soreff, private communication, Nov. 1999. The authors thank J. Soreff of IBM in East Fishkill, NY, for pointing out to them the possibility of achieving power gain in molecular circuits without three-terminal devices, using resonant tunneling diodes and Goto pairs. Also, the authors are grateful to Dr. G. Sollner of the MIT Lincoln Lab and Dr. H. C. Liu of the Physics Division of the National Research Council of Canada for additional discussions on this point. See, in addition, the two references listed immediately below this one.
- [113] W. F. Chow, "Tunnel diode logic circuits," in *Tunnel Diode and Semiconductor Circuits*, J. M. Carroll, Ed. New York: McGraw-Hill, 1963, pp. 101–105.
- [114] H. C. Liu and T. C. L. G. Sollner, "High-frequency resonant-tunneling devices," in *Semiconductors and Semimetals*, R. A. Kiehl and T. C. L. G. Sollner, Eds. Boston, MA: Academic, 1994, vol. 41, pp. 359–418.
- [115] A. C. Seabaugh, private communication, Oct.–Nov. 1997.
- [116] T. C. L. G. Sollner, private communication, Mar. 1998. The authors thank Dr. Gerry Sollner for a valuable suggestion that permitted them to perform the analysis presented in Appendix II-C of the operation of the diode-based XOR gate circuit that is displayed in Fig. 14.
- [117] M. A. Reed, "Conductance of molecular junctions," presented at the 1998 DARPA Molecular Electronics Workshop, Reston, VA, Feb. 2–3, 1998. This presentation proposed a novel hybrid molecular-solid state transistor.
- [118] ———, "Sub-nanoscale electronic systems and devices," U.S. Patent 475,341, Dec. 12, 1995.
- [119] J. C. Ellenbogen, "Architectures for molecular electronic computers: 2. Logic structures using molecular electronic FETs," manuscript in preparation.
- [120] H. Moravec. (1998) When will computer hardware match the human brain? *J. Transhumanism* [Online] Available WWW: <http://www.transhumanist.com/volume1/moravec.htm>.
- [121] R. C. Merkle. (1989) Energy limits to the computational power of the human brain. Xerox Palo Alto Research Center, Palo Alto, CA. [Online] Available WWW: <http://www.merkle.com/brainlimits.html>.
- [122] D. Naegle, private communication, July 1998. D. Naegle of Sun Microsystems, Inc., is designing new strategies for the efficient assembly of extended molecular electronic circuits.
- [123] J. R. Heath, P. J. Kuekes, G. S. Snider, and R. S. Williams, "A defect-tolerant computer architecture: Opportunities for nanotechnology," *Science*, vol. 280, pp. 1716–1721, 1998. This paper discusses a strategy that might be applied for addressing architectural issue number 6 listed in Section VI-B.
- [124] J. Markoff. (1999) Computer scientists are poised for revolution on a tiny scale. *New York Times* [Online] Available WWW: <http://www.nytimes.com/library/tech/99/11/biztech/articles/01nano.html>.
- [125] R. S. Williams and P. J. Kuekes, private communication, Oct. 1999. The authors thank S. Williams and P. Kuekes for relating and explaining their unpublished experimental work involving atom wires and their associated architectural concepts.
- [126] K. Wegener, D. Routenberg, and J. C. Ellenbogen, "Molecular electronic digital control circuits for a millimeter-scale walking robot," manuscript in preparation.
- [127] J. C. Ellenbogen, "Matter as software," presented at the Software Engineering and Economics Conference, McLean, VA, Apr. 2–3, 1997. Also published as MITRE Rep. MP 98W00000084. [Online] Available WWW: http://www.mitre.org/technology/nanotech/SWEE97_article.html.
- [128] *MacSpartan Plus1.1*, Wavefunction, Inc., Irvine, CA.
- [129] (1998–2000) NIST Chemistry Webbook. National Institute of Standards and Technology, Bethesda, MD. [Online] Available WWW: <http://webbook.nist.gov/chemistry/>. This WWW site provides a voluminous source of atomic and molecular ionization potentials, as well as other chemical data.
- [130] D. V. Bugg, *Circuits, Amplifiers, and Gates*. Bristol, U.K.: Inst. Physics, 1991. The authors found the early chapters of this work useful in considering the effect upon a small circuit of a nonlinear device, such as resonant tunneling diode.
- [131] *IBM ASIC-12 Databook*, International Business Machines Corp., 1998.
- [132] J. C. Ellenbogen, "Advances toward molecular-scale electronic digital logic circuits: A review and prospectus," in *Proc. 9th Great Lakes Symp. VLSI*, Ypsilanti, MI, Mar. 4–6, 1999. To appear in proceedings that will be published by the IEEE Computer Society.
- [133] R. T. Morrison and R. N. Boyd, *Organic Chemistry*, 6th ed. New York: Prentice-Hall, 1992.



James C. Ellenbogen received the Ph.D. degree in chemical physics from the University of Georgia in 1977.

He is Principal Scientist in the Nanosystems Group at The MITRE Corporation, McLean, VA, and Principal Investigator of MITRE's Nanosystems Modeling and Nanoelectronic Computers Research Project. He is the author of a number of technical papers on the modeling, simulation, and testing of military systems, on the theory of command and control, and on

diverse topics in computer science, physics, and chemistry. He taught at several universities before joining MITRE in 1984. Since 1993, he has devoted his energies to furthering the science and technology for designing and developing electronic computers integrated on the nanometer scale. In that effort, he has collaborated in the development of unique designs for nanoelectronic devices and co-authored several widely cited technical articles on nanoelectronics.



J. Christopher Love received the B.S. degree (with Highest Distinction) in chemistry from the University of Virginia in 1999. He is presently pursuing the Ph.D. degree in chemistry at Harvard University, Cambridge, MA.

He began his research into ultradense nanometer-scale computers at the MITRE Corporation, McLean, VA, in 1994. He is a coauthor of two earlier review articles about nanoelectronics, the 1996 MITRE report "Technologies and Designs for Electronic Nanocomputers" and

"Overview of Nanoelectronic Devices," published in the PROCEEDINGS OF THE IEEE in April 1997.

As an undergraduate in 1998–1999, Mr. Love was a Barry M. Goldwater National Scholarship winner, and he is the recipient of a National Defense Science and Engineering Graduate Research Fellowship to support his education toward an advanced degree.